

1 **Title: The genomic history and global expansion of domestic donkeys**

2 **Authors:** Evelyn T. Todd¹, Laure Tonasso-Calvière¹, Lorelei Chauvey¹, Stéphanie Schiavinato¹,
3 Antoine Fages¹, Andaine Seguin-Orlando¹, Pierre Clavel¹, Naveed Khan^{1,2}, Lucía Perez
4 Pardal^{3,4}, Laura Patterson Rosa⁵, Pablo Librado¹, Harald Ringbauer⁶, Marta Verdugo⁷, John
5 Southon⁸, Jean-Marc Aury⁹, Aude Perdereau⁹, Emmanuelle Vila¹⁰, Matilde Marzullo¹¹, Ornella
6 Prato¹¹, Umberto Tecchiati¹¹, Giovanna Bagnasco Gianni¹¹, Antonio Tagliacozzo¹², Vincenzo
7 Tinè¹³, Francesca Alhaique¹², João Luís Cardoso^{14,15}, Maria João Valente¹⁶, Miguel Telles
8 Antunes¹⁷, Laurent Frantz^{18,19}, Beth Shapiro^{20,21}, Daniel G. Bradley⁷, Nicolas Boulbes²², Armelle
9 Gardeisen²³, Liora Kolska Horwitz²⁴, Aliye Öztan²⁵, Benjamin S. Arbuckle²⁶, Vedat Onar²⁷,
10 Benoît Clavel²⁸, Sébastien Lepetz²⁸, Ali Akbar Vahdati²⁹, Hossein Davoudi³⁰, Azadeh
11 Mohaseb^{28,30}, Marjan Mashkour^{28,30,31}, Olivier Bouchez³², Cécile Donnadiéu³², Patrick Wincker⁹,
12 Samantha A. Brooks³³, Albano Beja-Pereira^{3,4,34,35}, Dong-Dong Wu^{36,37}, Ludovic Orlando^{1*}.

13 **Affiliations:**

14 ¹Centre d'Anthropobiologie et de Génomique de Toulouse, Université Paul Sabatier;
15 Toulouse 31000, France.

16 ²Department of Biotechnology, Abdul Wali Khan University; Mardan 23200, Pakistan.

17 ³CIBIO, Centro de Investigação em Biodiversidade e Recursos Genéticos, InBIO Laboratório
18 Associado, Campus de Vairão, Universidade do Porto; Vairão 4485-661, Portugal.

19 ⁴BIOPOLIS Program in Genomics, Biodiversity and Land Planning, Campus de Vairão,
20 Universidade do Porto; Vairão 4485-661, Portugal.

21

22 ⁵Department of Animal Science, Sul Ross State University, US-90, Alpine, TX 79830,
23 United States.

24 ⁶Department of Archaeogenetics, Max Planck Institute for Evolutionary Anthropology;
25 Leipzig 04103, Germany.

26 ⁷Smurfit Institute of Genetics, Trinity College Dublin; Dublin D02 PN40, Ireland.

27 ⁸Earth System Science Department, University of California; Irvine, CA 92697, United
28 States.

29 ⁹ Genoscope, Institut de biologie François Jacob, CEA, Université d'Evry, Université Paris-
30 Saclay ; Evry 91042, France.

31 ¹⁰Laboratoire Archéorient, Université Lyon 2; Lyon 69007, France.

32 ¹¹Dipartimento di Beni Culturali e Ambientali, Università degli Studi di Milano; Milan
33 20122, Italy.

34 ¹²Bioarchaeology Service, Museo delle Civiltà; Rome 00144, Italy.

35 ¹³Soprintendenza archeologia belle arti e paesaggio per le province di Verona, Rovigo e
36 Vicenza; Verona 37121, Italy.

37 ¹⁴ICArEHB, Campus de Gambelas, University of Algarve; Faro 8005-139, Portugal.

38 ¹⁵Universidade Aberta ; Lisbon 1269-001, Portugal.

39 ¹⁶Faculdade de Ciências Humanas e Sociais, Centro de Estudos de Arqueologia, Artes e
40 Ciências do Património, Universidade do Algarve ; Faro 8000-117, Portugal.

41 ¹⁷Centre for Research on Science and Geological Engineering, Universidade NOVA de
42 Lisboa; Lisbon 1099-085, Portugal.

43 ¹⁸Palaeogenomics Group, Department of Veterinary Sciences, Ludwig Maximilian
44 University; Munich, 80539, Germany.

45 ¹⁹School of Biological and Behavioural Sciences, Queen Mary University of London;
46 London E1 4DQ, United Kingdom.

47 ²⁰Department of Ecology and Evolutionary Biology, University of California; Santa Cruz,
48 CA 95064, United States.

49 ²¹Howard Hughes Medical Institute, University of California; Santa Cruz CA 95064, United
50 States.

51 ²²Institut de Paléontologie Humaine, Fondation Albert Ier, Paris / UMR 7194 HNHP,
52 MNHN-CNRS-UPVD / EPCC Centre Européen de Recherche Préhistorique, Tautavel
53 66720, France.

54 ²³Archéologie des Sociétés Méditerranéennes, Université Paul Valéry - Site Saint-Charles 2 ;
55 Montpellier 34090, France.

56 ²⁴National Natural History Collections, Edmond J. Safra Campus, Givat Ram, The Hebrew
57 University; Jerusalem 9190401, Israel.

58 ²⁵Archaeology Department, Ankara University; Ankara, 06100, Turkey.

59 ²⁶Department of Anthropology, University of North Carolina at Chapel Hill; Chapel Hill, NC
60 27599, USA.

61 ²⁷Osteoarchaeology Practice and Research Center and Department of Anatomy, Faculty of
62 Veterinary Medicine, Istanbul University-Cerrahpaşa; Istanbul 34320, Turkey.

63 ²⁸Archéozoologie, Archéobotanique, Sociétés, Pratiques et Environnements, Muséum National
64 d'Histoire Naturelle; Paris 75005, France.

65 ²⁹ Provincial Office of the Iranian Center for Cultural Heritage, Handicrafts and Tourism
66 Organisation, North Khorassan, Bojnord, Iran.

67 ³⁰Archaeozoology section, Bioarchaeology Laboratory of the Central Laboratory, University of
68 Tehran; Tehran CP1417634934, Iran.

69 ³¹Department of Osteology, National Museum of Iran; Tehran 1136918111, Iran.

70 ³²GeT-PlaGe - Génome et Transcriptome - Plateforme Génomique, GET - Plateforme Génome &
71 Transcriptome, Institut National de Recherche pour l'Agriculture, l'Alimentation et
72 l'Environnement; Castaneet-Tolosan Cedex 31326, France.

73 ³³Department of Animal Science, UF Genetics Institute, University of Florida; Gainesville, FL
74 32610, United States.

75 ³⁴DGAOT, Faculty of Sciences, Universidade do Porto; Porto 4169-007, Portugal.

76 ³⁵Sustainable Agrifood Production Research Centre (GreenUPorto), Universidade do Porto;
77 Vairão 4485-646, Portugal.

78 ³⁶State Key Laboratory of Genetic Resources and Evolution, Kunming Institute of Zoology,
79 Chinese Academy of Sciences; Kunming, 650201, China.

80 ³⁷Kunming Natural History Museum of Zoology, Kunming Institute of Zoology, Chinese
81 Academy of Sciences; Kunming, Yunnan, 650223, China.

82 * Ludovic Orlando, ludovic.orlando@univ-tlse3.fr

83 **Abstract:** Donkeys transformed human history as essential beasts of burden for long-distance
84 movement, especially across semi-arid and upland environments. They remain understudied
85 despite globally expanding and providing key support to low-to-middle income communities. To
86 elucidate their domestication history, we constructed a comprehensive genome panel of 207
87 modern and 31 ancient donkeys, including 15 wild equids. We found strong phylogeographic
88 structure in modern donkeys supporting a single domestication in Africa ~5,000 BCE, followed
89 by further expansions in this continent and Eurasia, ultimately returning back into Africa. We
90 uncover a new genetic lineage in the Levant ~200 BCE, which contributed increasing ancestry
91 towards Asia. Donkey management involved inbreeding and the production of giant bloodlines
92 at a time when mules were essential to the Roman economy and military.

93 **One-Sentence Summary:** Ancient and modern genomes elucidate the origins, spread and
94 management practices underlying donkey domestication.

95

96 **Main Text:**

97 Domestic donkeys (*Equus asinus*) have facilitated the movement of goods and people for
98 millennia, enabling trade and transport across a broad spectrum of landscapes (1). Despite their
99 importance to ancient pastoral societies, little is known about the deep history of donkeys and the
100 impact of human management on their genomes. This is most likely due to their undervalued
101 status and loss of utility in modern industrialized societies. Donkeys are, however, extraordinary
102 working animals and remain essential for developing communities, especially in semi-arid
103 environments (2). Understanding their genetic makeup is not only key to assess their contribution
104 to human history but also to improving their local management in the future.

105 The current archaeological record of early donkeys is limited (1, 3), which makes their domestic
106 origins and spread through the world contentious. The reduced body size of zooarchaeological
107 ass remains in Egypt at El Omari (4,800–4,500 BCE) and Maadi (4,000–3,500 BCE) have been
108 interpreted as early evidence of domestication (4-7). Carvings on the Libyan palette, found in
109 Abydos, Egypt (3,200-3,000BCE), depict lines of walking asses, cattle, and sheep, also
110 suggesting a domestication context (8, 9). Together with contemporary remains from the same
111 region that show morphological evidence for load carrying (10), these findings suggest that
112 donkeys could have been first domesticated within a range extending from the northeastern
113 Sahara, the Nile Valley, the Atbara River, the Red Sea Hills, to Eritrea. In this model, donkeys
114 were domesticated by pastoralists to assist with mobility around 5,500-4,500 BCE due to the
115 large-scale aridification of the Sahara (1). Independent evidence based on patterns of
116 mitochondrial (11, 12) and nuclear sequence variation (13) also point to African origins of the
117 donkey, due to their closer proximity to African wild asses (*Equus africanus* spp.), than to Asian
118 wild asses (*Equus hemionus* spp.).

119 However, candidate regions outside of Africa are also proposed as alternative domestication
120 centers. In Ash Shuman (Yemen), for example, ass remains of disputed domestic status predate
121 those from Egypt by 2,000 years (~6,500 BCE) (14). Likewise, textual, iconographic and
122 zooarchaeological material indicate a possible additional center in Mesopotamia during the 4th
123 and 3rd millennia BCE (15-19), a context in which first-generation hybrids of donkeys and Syrian
124 onagers have been identified genetically (20). Segregation of mitochondrial variation in two
125 main clades may also support a dual domestication process, for which the Nubian wild ass
126 (*Equus africanus africanus*) is securely identified as the progenitor of Clade I (11, 12). As for the
127 ancestor of Clade II, it could either be the extinct Atlas wild ass (*Equus africanus atlanticus*),
128 endemic to northern Africa, or another undescribed subspecies that potentially ranged outside of
129 Africa. Whether a single, maternally inherited marker captures the whole complexity of
130 underlying ancestries can, however, be questioned, following recent results from other animals
131 (e.g., horses (21)). Furthermore, previous analyses of nuclear genetic variation in African and
132 non-African donkeys have failed to disentangle their origins (13, 22). Overall, this lack of
133 consensus between genetic and archaeological data means that the geographic and temporal
134 origin of donkeys and whether they were domesticated more than once remains uncertain. The
135 global spread of donkeys is also unclear as their worldwide patterns of genomic diversity lacks
136 extensive characterization.

137 **Modern donkeys originated in Africa and spread into Eurasia**

138 To address these issues, we sequenced 49 modern donkey genomes from underrepresented
139 regions, and combined these with 158 publicly available to capture worldwide diversity (13, 23-
140 25) (Fig. 1A, Table S1). We constructed a fine-scale recombination map from genomes
141 encompassing all phylogenetic groups, which we used to phase 13,013,551 variants (Table S3,

142 S4). Principal Component Analysis (PCA; (26)) revealed strong geographical sub-structuring,
143 with donkeys from Africa, Europe, and Asia forming distinct genetic clusters (Fig. 1B, S1, S2).

144 A Treemix phylogenetic reconstruction, grouping modern donkeys according to sampling
145 locations (27), confirms the earliest split between African (Clade A) and mostly non-African
146 donkeys (Clade B) (Fig. 1C). Further structure within Clade A separates donkeys from the Horn
147 of Africa (Ethiopia and Somalia) plus Kenya, from those from western Africa (Ghana,
148 Mauritania, Nigeria, and Senegal). Within Clade B, we find another major divergence between
149 European and Asian donkeys, with east-to-west affinities in Europe from the Balkans (Croatia
150 and Macedonia) to Iberia, Denmark, and Ireland. Conversely, Asian subpopulations show west-
151 to-east sub-structuring from Iran and Central Asia to China and Mongolia. Combined, these
152 findings suggest expansions from a central source into both continents.

153 In Clade B, some of the most basal donkeys are from the southern Arabian Peninsula (Oman and
154 Yemen), whereas the single donkey from Saudi Arabia analyzed here shows European affinities
155 indicative of a secondary translocation. Similarly, the Pega donkey from Brazil is nested within
156 Iberia, mirroring the colonization history of the Americas. Clade B also includes donkeys from
157 Nubia (Egypt and Sudan) showing affinities to the Levant (Syria) and Anatolia (Turkey), as well
158 as donkeys from Maghreb (Tunisia), with closer genetic proximity to European subpopulations.
159 This suggests gene flow into Africa from donkeys native to Anatolia and the Levant, but not to
160 the Arabian Peninsula. Overall, this phylogenetic reconstruction is compatible with both models
161 of donkey domestication: a unique origin in Africa followed by dispersals out and back, or dual
162 origins in Africa and the southern Arabian Peninsula.

163 The unique origin model posits a demographic expansion in Africa first, and subsequent waves
164 into Europe and Asia. In contrast, dual origins would result in an earlier split of demographic
165 trajectories between African and Eurasian subpopulations, given their deep phylogenetic
166 divergence. To test these, we first performed demographic modelling using SMC++ (28), which
167 revealed the first expansion around 5,200 BCE ($7,186 \pm 742$ years ago), in line with
168 archaeological evidence of domestication occurring at this time (Fig. 1D, S5). Additionally,
169 when modelled from a possible African source, SMC++ trajectories indicated more recent and
170 nearly coincidental expansions into Asia around 2,600 BCE ($4,573 \pm 577$ years ago) and Europe
171 around 2,800 BCE ($4,806 \pm 671$ years ago) (Fig. 1D). This is in line with the unique origin model
172 and the earliest archaeological evidence of donkeys in Asia (Iranian Plateau and the Indus
173 Valley), and Europe (Portugal, Greece and Cyprus) in the mid-to-late 3rd millennia BCE (29-34).
174 Furthermore, Yemen and Oman subpopulations do not branch basal to Clade B according to
175 fineSTRUCTURE (35), in contrast to the expectations of the dual origins model, but within
176 Asian subpopulations (Fig. 2A, 2B). Lastly, pairwise genetic distances between Ethiopia and
177 non-African subpopulations were greater than those from Yemen (Fig. S5). They both increased
178 linearly with geographic distances and supported identical dispersal rates (Fig. S5; p -
179 value=0.775), in line with a single wave of expansion at a constant pace. Therefore, our analyses
180 support an early domestication in Africa, spreading at an even rate into the Arabian Peninsula
181 and Eurasia, and flow back into Nubia and Maghreb. Modern subpopulations from the Horn of
182 Africa and Kenya so far best represent the descendants of earliest donkeys.

183 **Ancient donkey genomes reveal early and rapid dispersal into Asia and secondary contacts**
184 **between Europe and western Africa**

185 Patterns of genetic variation within modern subpopulations may reflect recent breeding history
186 rather than early domestication (36). Additionally, they could under-represent the contribution of
187 lineages that were once important but have since declined (37). Dating population splits also
188 assumes constant, yet unknown generation intervals. To address these caveats and validate the
189 domestication history reconstructed above, we generated a genomic time series spanning the last
190 ~4,000 years, that included 31 ancient donkeys from 11 different sites, ranging from the Atlantic
191 shores (Portugal) to Central Asia (eastern Iran/Turkmenistan) (Fig. 3A, Table S2).

192 Ancient genomes sequenced to 0.77-5.05 fold coverage (Table S6) were analyzed using two
193 complementary methods: pseudo-haploidization following (21) resulting in 4,833,570 nucleotide
194 transversions, and genotype imputation following (38), at 7,161,029 polymorphic sites present at
195 more than 5% frequency in modern donkeys (38, 39). Imputation accuracy was confirmed by
196 high consistency rates between imputed and observed genotypes following down-sampling of
197 high-coverage modern genomes, and downstream analyses largely consistent with those based on
198 pseudo-haploidized data (Fig. S6, S7, S9, S10, S11, S12, S14, Table S6).

199 The three oldest samples from our dataset consist of donkeys from Anatolia (Acemhöyük,
200 Turkey), radiocarbon dated to 2,564-2,039 BCE. Their age and phylogenetic placement within
201 Clade B confirm an early expansion out of Africa by ~2,500 BCE, in agreement with SMC++
202 time estimates (Fig. 2A, S10). These samples, and a donkey from eastern Iran/Turkmenistan
203 affiliated to the Bactria–Margiana Archaeological Complex (BMAC, ~2,050 BCE; Chalow3),
204 branch prior to the formation of modern subpopulations from central Asia (Kazakhstan,
205 Kyrgyzstan, Turkmenistan) and eastern Asia (China, Mongolia, Tibet) (Fig. 2C). These
206 subpopulations thus diverged after ~2,050 BCE, but potentially before the radiocarbon age of the

207 donkey from Doshan Tepe (1,049-928 BCE), which appears closer to modern subpopulations
208 from central Asia in one Treemix analysis (Fig. 2D, S10).

209 Ancient samples from Iran (Shahr-i-Qumis, 800 BCE-800 CE), including one Sassanid (AM805)
210 are not more closely related to central than to eastern Asian modern subpopulations, although
211 their exact phylogenetic placement remains unclear (Fig. 2A, B, S10). Their fineSTRUCTURE
212 affinities to modern Iran, Anatolia (Turkey), the Levant (Syria), and Maghreb (Tunisia) support
213 different genetic ancestry profiles from those inferred at the nearby site of Doshan Tepe. This
214 indicates a population turnover in Iran after ~1,000 BCE but before ~500 CE, corresponding to
215 the radiocarbon time interval of Doshan Tepe and a single specimen from Shahr-i-Qumis.

216 Strikingly, all our ancient specimens from Europe cluster within modern European domesticates,
217 supporting differentiation within this continent prior to the oldest European samples analyzed
218 (Tarquinia, 803–412 BCE, ~2,500 years ago; Fig. 3C). However, a donkey from a Roman
219 context in Marseille, a major seaport trading center in southern France (Centre Bourse Marseille,
220 0–500 CE), displayed strong genetic affinities with modern individuals from western Africa (Fig.
221 3B, 3D). Additionally, SNP and haplotype sharedness with modern western Africa were also
222 found in European donkeys from Islamic era in Portugal (Albufeira, 1,228–1,280 CE) and
223 Roman times in Northern France (Boinville-en-Woëvre, 200-500 CE) (Fig 3B, 3E). This reveals
224 multiple contacts between Europe and western Africa from the Antiquity to Middle Ages.
225 Despite ancient European donkeys showing western African ancestry, these contacts have
226 impacted western Africa more than Europe, in line with Treemix inferring gene flow
227 predominantly in this direction than the reverse (Fig. 1C). Interestingly, all modern Irish donkeys
228 and the two Etruscan samples from Tarquinia are devoid of western African ancestry. This

229 suggests the preservation of old European genetic lineages, at least in some modern
230 subpopulations of this continent.

231 **Donkey management involved inbreeding and introgression from divergent lineages**

232 Inbreeding is a common reproductive strategy for breeding animals with desirable traits (40). To
233 assess whether ancient donkey breeders made use of inbreeding, we measured the proportion of
234 autosomal runs of homozygosity (ROH) using three independent techniques, all of which
235 provided consistent results (Fig. S13, S14). We detected inbreeding, but no significant changes
236 in levels between modern and ancient donkeys (Wilcoxon rank sum test, p -value = 0.3951) (Fig.
237 4A, 4B, 4C). Conversely, modern horses show higher inbreeding levels than their ancient
238 counterparts (Wilcoxon rank sum test, p -value < 0.001), mirroring previous reports of reduced
239 heterozygosity and increased deleterious mutation load in recent times (21, 41) (Fig. 4D, E, F).
240 Longer ROH tracts are more common in modern horses and donkeys than in the past, consistent
241 with inbreeding from closer generations in their genealogies (Fig. 4C, 4F). Overall, our analyses
242 support recent major changes in reproductive management inflating inbreeding in horses, but not
243 in donkeys.

244 Admixture modelling suggests ongoing introgression from African wild asses into modern
245 donkeys from Africa and the southern Arabian Peninsula (with between 0.24–6.99% of
246 admixture, Fig. 1A, S3, Table S5). This is in line with free-ranging local management practices
247 allowing for continued interbreeding with wild and feral subpopulations (4, 42). The limited but
248 significant amount of wild genetic material from kiangs in one modern donkey from China also
249 supports admixture between taxa generally regarded as separate species. This confirms previous
250 reports of mitochondrial introgression (43) and genomic admixture despite different karyotypes

251 (24). Interestingly, all but one ancient donkey (Tur168) carried remnants of outgroup material
252 (0.21-4.15%; Fig. 3B), potentially resulting from recent range contractions of wild
253 subpopulations and ancient management practices providing more opportunities for wild
254 introgression.

255 The genome of MV242, a donkey from Israel dating to the Hellenistic period (350-58 BCE),
256 displayed the largest fraction of divergent genetic material (Fig. 3B, $4.15\% \pm 0.019$). In Treemix,
257 this sample showed a deeper placement than all donkeys present in our panel, except the Somali
258 wild ass (*E.a.som*) (Fig. 2E). Significantly positive $f_4(E.a.som, MV242; Horn+Ken, x)$ statistics
259 revealed MV242-related genetic ancestry in some modern subpopulations (x), especially towards
260 central and eastern Asia (Fig. 5E). This ancestry was already present in the BMAC sample from
261 Iran (Chalow3, Fig. 5F), indicating contact ~ 2050 BCE at the latest. It was, however, absent in
262 Acemhöyük at that time, suggesting that the MV242 divergent lineage ranged into eastern
263 Iran/Turkmenistan, but not Turkey. This lineage also left genetic material in modern Anatolia,
264 the Levant, Nubia, and Maghreb, but not in western Africa, consistent with donkeys carrying
265 MV242-related ancestry flowing back into some African regions. Finally, this ancestry was also
266 present in southwestern European subpopulations (CYK, ESP, PTG), but neither in the modern
267 Balkans and Ireland, nor in any ancient European sample analyzed here (Fig. 5E-F). Combined,
268 our results suggest a range for the MV242-related lineage from the Levant into Asia, rather than
269 Europe and Africa.

270 Despite its divergent genetic makeup, MV242 carries a mitochondrial haplotype characteristic of
271 Clade II (Fig. 5A). Our tip-calibrated coalescent analyses revealed that the time to the most
272 common recent ancestor of that Clade was 32,226 BCE and not 332,580-142,980 BCE (Fig. 5B),
273 as previously reported (12, 44). Since the same holds true for Clade I, both clades could have

274 coexisted in sympatry 25,000 years later as donkeys were first domesticated (Fig. 5B).
275 Additionally, no phylogeographic structure is apparent in patterns of mitochondrial variation,
276 both in modern and ancient subpopulations, as ancient specimens from Asia and Europe,
277 sometimes from the same archaeological sites, were placed across both clades (Fig 5A). Y-
278 chromosomal variation was also associated with little, if any, population structure (Fig. 5C, D).
279 Combined, our results dismiss mitochondrial DNA and the Y-chromosome as reliable markers of
280 domestication history in donkeys.

281 **Romans bred improved donkeys for producing mules essential for their military power and**
282 **economy**

283 Beyond documenting domestication history at the global scale, our genomic dataset also
284 included 3 jennies (females) and 6 jacks (males) from the same archaeological site (Boinville-en-
285 Woëvre) (Fig. 3A). These were found in a dedicated farming area of a Roman villa, providing
286 insights into local management practices in Roman Northern France (200-500 CE). One jack
287 (GVA349) appeared particularly inbred with long ROH indicative of recent consanguinity (Fig.
288 4A) and was genetically related to four jacks and one jenny (family group GVA1, including
289 GVA125, GVA347, GVA348, GVA349, GVA353, and GVA354; Table S10). Additionally, two
290 jennies showed genetic relatedness coefficients equivalent to full siblings (family group GVA2
291 GVA355 and GVA358; Table S10). This indicates breeding management within close kin,
292 potentially aimed at selecting for desirable traits. Genotype imputation at *TBX3* (13) revealed the
293 presence of dun and derived colored coats, but no evidence for the dominant alleles associated
294 with white spots or long hair was found in the sequence alignments at *KIT* (45) and *FGF5* (46)
295 (Table S7-9). The latter two phenotypes are, however, relatively common in modern breeds from
296 France, suggesting post-Roman selection for these traits.

297 The abundance of donkeys at Boinville-en-Woëvre stands as an exception in Roman France, as
298 mules dominated all other assemblages from this time (47). Contemporaneous Roman sites
299 report mules of a large and uniform size, indicating selective breeding in the parental species for
300 expensive animals of exceptional stature (Varo (2, 6)) (48). Interestingly, morphometric
301 measurements previously revealed five donkeys from family group GVA1 as giant (148-156cm
302 at the withers) (47). We found that GVA359 had a similarly large size (144cm) and genetic
303 affinities to western Africa. This may indicate restocking to enhance body size from distant
304 bloodlines carrying divergent ancestry, or from wild populations.

305 Interestingly, outgroup admixture was significantly higher at Boinville-en-Woëvre than in other
306 ancient donkeys except the divergent MV242 specimen (p -value = 0.045). Significantly negative
307 $f_4(\text{kiang, MV242; Fiumarella1, Boinville-en-Woëvre})$ statistics support restocking into family
308 group GVA1 only, from a lineage more divergent than MV242 (Fig. 5G). Additionally, $f_4(\text{kiang,}$
309 $E.a.som; Fiumarella1, GVA1)$ statistics reject unbalanced allele sharedness between $E.a.som$ and
310 GVA1, ruling out restocking from $E.a.som$ or more divergent populations (Fig. 5H). Combined,
311 these findings uncover a lineage, phylogenetically intermediate between MV242 and $E.a.som$,
312 contributing to the genetic makeup of some Roman donkeys at Boinville-en-Woëvre. Together
313 with the evidence of genetic relatedness and inbreeding, this suggests Boinville-en-Woëvre as a
314 likely mule production center that maintained bloodlines of giant donkeys selected through
315 familial breeding and restocking. This center may illustrate how Romans sustained the enormous
316 demand for mules, which is documented in the nearby Rhine frontier (49), and has fueled
317 transportation networks throughout the Empire (47).

318 Discussion

319 Our study solves long-standing debates about donkey domestication. We support domestication
320 starting from a unique African source ~5,000 BCE. Donkeys subsequently spread into Eurasia
321 from ~2,500 BCE, and central and eastern Asian subpopulations differentiated ~2,000-1,000
322 BCE. Genetic affinities characteristic of modern western Europe were already formed by 500
323 BCE. Following early domestication, African donkeys further differentiated in the West and the
324 Horn of Africa plus Kenya, but also received streams of genetic ancestry from western Europe as
325 well as a region encompassing the Levant, Anatolia and Mesopotamia. Donkey domestication
326 involved limited, but significant wild introgression. It did not entail inflated inbreeding in recent
327 times, in contrast to horses. In fact, the processes of donkey and horse domestication
328 dramatically differed, as horses were domesticated twice (50) and rapidly spread across Eurasia
329 from the lower Don-Volga region ~2,000 BCE (21). Their regional differentiation remained
330 relatively limited due to strong connectivity at continental distances early on and until oriental
331 bloodlines were propagated throughout the world during the last 1,000 years (41, 51). The extent
332 to which the different domestication trajectories of donkeys and horses were only driven by their
333 respective roles in human societies or also reflected management practices adapted to their
334 respective mating and social behavior (52), remains to be explored.

335 This work clarifies global patterns of donkey domestication and movements, but also highlights
336 many directions for future research. For example, it remains unknown whether domestic donkeys
337 only dispersed out of Africa by land through the Sinai Peninsula, or across the Red Sea from
338 Ethiopia to Yemen. Additionally, modern subpopulations from the Horn of Africa plus Kenya
339 were found to be the first expanding. This may suggest early domestication there, or donkeys
340 domesticated elsewhere in Africa entering the region more recently. Further research is needed to
341 clarify the timing of pastoral spread into the Red Sea Sudanese region and the Horn of Africa.

342 Current dates range from ~2500 BCE in Ethiopia and Eritrea (53) to ~3000 BCE in northern
343 Kenya (54). Donkeys are not present in the archaeological record of western Africa before the
344 beginning of the common era either (55), which postdates by 3,000 years the time when donkey
345 populations from Horn of Africa plus Kenya and western African are inferred to have split
346 genetically. This may indicate an early, yet undocumented arrival in the region, or a slow
347 migration westward, only reaching the modern range later. Improving the current African
348 archaeological record thus appears paramount to refining the exact context underlying early
349 donkey domestication and subsequent population movements.

350 Further genomic studies in other regions would also largely benefit the understanding of donkey
351 diversity and history. Resolving the genetic structure of equine remains from the 3rd millennia
352 BCE of southwest Asia will be challenging due to postmortem DNA decay, but essential to map
353 the geographic range of the divergent lineage identified here (MV242), as well as to understand
354 dispersal mechanisms in greater detail. The same holds true for Chalcolithic and Bronze Age
355 Europe, which remain genetically undocumented in our dataset, and onwards. Developing
356 genetic knowledge of ancient European donkeys will further clarify patterns of exchange across
357 the Mediterranean region, including during and after Roman times, as revealed in this study. It
358 will also provide insights into the dispersal mechanisms underpinning the genetically supported
359 presence of donkey remains in Portugal ~2,200 BCE (33). Genetic characterization of local
360 archaeological sites at the population scale may uncover additional mule breeding centers, other
361 than the one reported here. This will shed light on the diversity of breeding management
362 strategies developed by Romans to supply their continental-wide economy and military with
363 adequate animal resources (49). For now, both the absence of mules and rarity of horse mares at
364 Boinville-en-Woëvre (47) suggest that mares were brought in for mating before returning

365 pregnant to their owners. Alternatively, donkey breeders may have visited other farms with their
366 jacks to cover mares.

367 Efforts should continue to characterize the modern donkey diversity around the world, especially
368 in Saudi Arabia, which is currently characterized by a single individual, as well as in Africa, for
369 which no populations located south of the Equator have been sampled. Such efforts may not only
370 refine the historical legacy of past populations into the modern world, but also uncover the
371 genetic basis of desert adaptations, which could prove invaluable for future donkey breeding in
372 the face of global warming.

373

374 **References and notes**

- 375 1. P. Mitchell, *The donkey in human history: an archaeological perspective* (Oxford
376 University Press, Oxford, UK, 2018).
- 377 2. S. L. Norris, H. A. Little, J. Ryding, Z. Raw, Global donkey and mule populations:
378 figures and trends. *PLOS ONE* **16**, e0247830 (2021).
- 379 3. B. Kimura, F. Marshall, A. Beja-Pereira, C. Mulligan, Donkey domestication. *Afr*
380 *Archaeol Rev* **30**, 83-95 (2013).
- 381 4. F. Marshall, *Rethinking agriculture: archeological and ethnoarcheological perspectives*
382 (Left Coast Press, Walnut Creek, CA, USA, 2007).
- 383 5. S. Bokonyi, "The animal remains of Maadi, Egypt: A preliminary report" in *Studi di*
384 *paletnologia in onore di Salvatore M. Puglisi* M. Liverani, A. Palmieri, R. Peroni, Eds.
385 (Università di Roma "La Sapienza", Rome, 1985), pp. 495-499.
- 386 6. J. Boesneck, A. Von den Driesch, "Tierreste aus der vorgeschichtlichen siedlung von El-
387 Omari bei" in *El Omari : a neolithic settlement and other sites in the vicinity of Wadi*
388 *Hof, Helwan*, F. Debono, B. Mortensen, Eds. (1990), pp. 99-107.
- 389 7. J. Boesneck, A. von den Driesch, R. Ziegler, "Die Tierreste von Maadi und dem Friedhof
390 am Wadi Digla" in *Maadi III*, I. Rizkana, J. Seeber, Eds. (1989), pp. 87-128.
- 391 8. K. M. Cialowicz, *Les palettes Egyptiennes aux motifs zoomorphes et sans decoration.*
392 *Etudes de l'art predynastique* (Jagiellonian University, Krakow, Poland, 1991).
- 393 9. D. J. Brewer, D. B. Redford, S. Redford, *Domestic plants and animals: the Egyptian*
394 *origins* (Warmister: Aries and Phillips, 1994).

- 395 10. S. Rossel, F. Marshall, J. Peters, T. Pilgram, M. D. Adams, D. Connor, Domestication of
 396 the donkey: timing, processes, and indicators. *Proc. Natl. Acad. Sci. U.S.A.* **105**, 3715
 397 (2008).
- 398 11. A. Beja-Pereira, P. R. England, N. Ferrand, S. Jordan, A. O. Bakhiet, M. A. Abdalla *et*
 399 *al.*, African origins of the domestic donkey. *Science* **304**, 1781 (2004).
- 400 12. B. Kimura, F. B. Marshall, S. Chen, S. Rosenbom, P. D. Moehlman, N. Tuross *et al.*,
 401 Ancient DNA from Nubian and Somali wild ass provides insights into donkey ancestry
 402 and domestication. *Proc. R. Soc. B* **278**, 50-57 (2011).
- 403 13. C. Wang, H. Li, Y. Guo, J. Huang, Y. Sun, J. Min *et al.*, Donkey genomes provide new
 404 insights into domestication and selection for coat color. *Nat. Commun.* **11**, 6014 (2020).
- 405 14. M. Cattani, S. Bokonyi, "Ash-Shumah. An early Holocene settlement of desert hunters
 406 and mangrove foragers in the Yemeni Tihama" in *Essays on the Late Prehistory of the*
 407 *Arabian Peninsula. Serie Orientale Romana XCIII*, S. Cleuziou, T. Maurizio, Z. Juris,
 408 Eds. (Istituto Italiano per l'Africa e l'Oriente, Roma, 2002).
- 409 15. R. H. Meadow, H. P. Uerpmann, *Equids in the ancient world, vol. 2* (Wiesbaden, 1991).
- 410 16. J. Clutton-Brock, The process of domestication. *Mamm Rev.* **22**, 79-85 (1992).
- 411 17. J. Zarins, R. Hauser, The domestication of equidae in third-millennium BCE
 412 Mesopotamia. *Cornell University Studies in Assyriology and Sumerology* **24**, XI + 432
 413 (2014).
- 414 18. E. Vila, "Data on equids from late fourth and third millennium sites in Northern Syria" in
 415 *Equids in Time and Space: Papers in Honour of Véra Eisenmann.*, M. Mashkour, Ed.
 416 (Oxford, Oxbow, 2006), pp. 101-123.

- 417 19. J. Boessneck, A. von den Driesch, U. Steger, Tierknochenfunde der Ausgrabungen des
418 Deutschen Archäologischen Instituts Bagdad in Uruk-Warka, Iraq. *Baghdader*
419 *Mitteilungen* **15**, 149-189 (1984).
- 420 20. A. E. Bennett, J. Weber, W. Bendhafer, S. Champlot, J. Joris Peters, G. M. Schwartz *et*
421 *al.*, The genetic identity of the earliest human-made hybrid animals, the kungas of Syro-
422 Mesopotamia. *Sci. Adv.* **8**, eabm0218 (2022).
- 423 21. P. Librado, N. Khan, A. Fages, M. A. Kusliy, T. Suchan, L. Tonasso-Calvière *et al.*, The
424 origins and spread of domestic horses from the Western Eurasian steppes. *Nature* **598**,
425 634–640 (2021).
- 426 22. S. Rosenbom, V. Costa, S. Chen, L. Khalatbari, G. H. Yusefi, A. Abdulkadir *et al.*,
427 Reassessing the evolutionary history of ass-like equids: Insights from patterns of genetic
428 variation in contemporary extant populations. *Mol. Phylogenet. Evol.* **85**, 88-96 (2015).
- 429 23. G. Renaud, B. Petersen, A. Seguin-Orlando, M. F. Bertelsen, A. Waller, R. Newton *et al.*,
430 Improved de novo genomic assembly for the domestic donkey. *Sci. Adv.* **4**, eaaq0392
431 (2018).
- 432 24. H. Jónsson, M. Schubert, A. Seguin-Orlando, A. Ginolhac, L. Petersen, M. Fumagalli *et*
433 *al.*, Speciation with gene flow in equids despite extensive chromosomal plasticity. *Proc.*
434 *Natl. Acad. Sci. U.S.A.* **111**, 18655 (2014).
- 435 25. L. Zeng, H. Q. Liu, X. L. Tu, C. M. Ji, X. Gou, A. Esmailzadeh *et al.*, Genomes reveal
436 selective sweeps in kiang and donkey for high-altitude adaptation. *Zool. Res.* **42**, 450-460
437 (2021).

- 438 26. A. L. Price, N. J. Patterson, R. M. Plenge, M. E. Weinblatt, N. A. Shadick, D. Reich,
 439 Principal components analysis corrects for stratification in genome-wide association
 440 studies. *Nat. Genet.* **38**, 904-909 (2006).
- 441 27. J. K. Pickrell, J. K. Pritchard, Inference of population splits and mixtures from genome-
 442 wide allele frequency data. *PLoS Genet.* **8**, e1002967 (2012).
- 443 28. J. Terhorst, J. A. Kamm, Y. S. Song, Robust and scalable inference of population history
 444 from hundreds of unphased whole genomes. *Nat. Genet.* **49**, 303-309 (2017).
- 445 29. D. Reese, Faunal remains from early Helladic II Lerna (Argolid-Greece). *Mediterr.*
 446 *Archaeol. Archaeom.* **13**, 289-320 (2013).
- 447 30. B. A. Knapp, Bronze Age Mediterranean Island Cultures and the Ancient Near East. *The*
 448 *Biblical Archaeologist* **55**, 52-72 (1992).
- 449 31. S. Ratnagar, *Trading Encounters: from the Euphrates to the Indus in the Bronze Age*
 450 (Oxford: Oxford University Press, 2004).
- 451 32. M. A. Zeder, "The equid remains from Tal-e Malyan, southern Iran" in *Equids in the*
 452 *Ancient World*, R. H. Meadow, H. P. Uerpmann, Eds. (Wiesbaden: Reichert, 1986), pp.
 453 164-193.
- 454 33. J. L. Cardoso, J. T. Vilstrup, V. Eisenmann, L. Orlando, First evidence of *Equus asinus* L.
 455 in the Chalcolithic disputes the Phoenicians as the first to introduce donkeys into the
 456 Iberian Peninsula. *J. Archaeol. Sci.* **40**, 4483-4490 (2013).
- 457 34. S. Amiri, M. Mashkour, F. Mohaseb, Naseri R, "The Subsistence Economy of a Highland
 458 Settlement in the Zagros during the Bronze and Iron Ages. The Case of Gūnespān
 459 (Hamadan, Iran)" in *Archaeozoology of Southwest Asia and Adjacent Areas XIII:*
 460 *Proceedings of the Thirteenth International Symposium, University of Cyprus, Nicosia,*

- 461 *Cyprus, June 7-10, 2017.* , J. Daujat, A. Hadjikoumis, R. Berthon, J. Chahoud, V.
 462 Kassianidou, J. D. Vigne, Eds. (2021), pp. 199-219.
- 463 35. D. J. Lawson, G. Hellenthal, S. Myers, D. Falush, Inference of population structure using
 464 dense haplotype data. *PLoS Genet.* **8**, e1002453 (2012).
- 465 36. L. Girdland Flink, R. Allen, R. Barnett, H. Malmström, J. Peters, J. Eriksson *et al.*,
 466 Establishing the validity of domestication genes using DNA from ancient chickens. *Proc.*
 467 *Natl. Acad. Sci. U.S.A.* **111**, 6184-6189 (2014).
- 468 37. L. A. F. Frantz, D. G. Bradley, G. Larson, L. Orlando, Animal domestication in the era of
 469 ancient genomics. *Nat. Rev. Genet.* **21**, 449-460 (2020).
- 470 38. R. Hui, E. D'Atanasio, L. M. Cassidy, C. L. Scheib, T. Kivisild, Evaluating genotype
 471 imputation pipeline for ultra-low coverage ancient genomes. *Sci. Rep.* **10**, 18542 (2020).
- 472 39. B. I. Browning, S. R. Browning, Genotype imputation with millions of reference samples.
 473 *Am. J. Hum. Genet.* **98**, 116-126 (2016).
- 474 40. T. N. Kristensen, A. C. Sørensen, Inbreeding – lessons from animal breeding,
 475 evolutionary biology and conservation genetics. *Animal Science* **80**, 121-133 (2007).
- 476 41. A. Fages, K. Hanghøj, N. Khan, C. Gaunitz, A. Seguin-Orlando, M. Leonardi *et al.*,
 477 Tracking five millenia of horse management with extensive ancient genome time series.
 478 *Cell* **177**, 1419-1435.e1431 (2019).
- 479 42. F. Marshall, L. Weissbrod, "The consequences of women's use of donkeys for pastoral
 480 flexibility: Maasai ethnoarchaeology" in *Tracking Down the Past. Ethnohistory Meets*
 481 *Archaeozoology*, G. Grupe, J. Peters, G. McGlynn, Eds. (Rahden/Westf. : M. Leidor,
 482 2009), pp. 59-79.

- 483 43. E. A. Bennett, S. Champlot, J. Peters, B. S. Arbuckle, S. Guimaraes, M. Pruvost *et al.*,
484 Taming the late Quaternary phylogeography of the Eurasian wild ass through ancient
485 and modern DNA. *PLOS ONE* **12**, e0174216 (2017).
- 486 44. L. Wang, G. Sheng, M. Preick, S. Hu, T. Deng, U. H. Taron *et al.*, Ancient mitogenomes
487 provide new insights into the origin and early introduction of Chinese domestic donkeys.
488 *Front. Genet.* **12**, (2021).
- 489 45. B. Haase, S. Rieder, T. Leeb, Two variants in the KIT gene as candidate causative
490 mutations for a dominant white and a white spotting phenotype in the donkey. *Anim.*
491 *Genet.* **46**, 321-324 (2015).
- 492 46. R. Legrand, L. Turet, M. Abitbol, Two recessive mutations in FGF5 are associated with
493 the long-hair phenotype in donkeys. *Genet. Sel. Evol* **46**, 65 (2014).
- 494 47. S. Lepetz, B. Clavel, D. Alioğlu, L. Chauvey, S. Schiavinato, L. Tonasso-Calvière *et al.*,
495 Historical management of equine resources in France from the Iron Age to the Modern
496 Period. *J. Archaeol. Sci. Rep.* **40**, 103250 (2021).
- 497 48. G. K. Kunst, Archaeozoological evidence for equid use, sex structure and mortality in a
498 Roman auxiliary fort (Carnuntum-Petronell, lower Austria). *Anthropozoologica* **31**, 109-
499 118 (2000).
- 500 49. C. Johnstone, "Commodities or logistics? : The role of equids in Roman supply
501 networks" in *Feeding the Roman Army: The Archaeology of Production and Supply in*
502 *NW Europe*, S. Stalibrass, R. Thomas, Eds. (Oxbow Books, Oxford, 2008).
- 503 50. C. Gaunitz, A. Fages, K. Hanghøj, A. Albrechtsen, N. Khan, M. Schubert *et al.*, Ancient
504 genomes revisit the ancestry of domestic and Przewalski's horses. *Science* **360**, 111-114
505 (2018).

- 506 51. S. Felkel, C. Vogl, D. Rigler, V. Dobretsberger, B. P. Chowdhary, O. Distl *et al.*, The
507 horse Y chromosome as an informative marker for tracing sire lines. *Sci. Rep.* **9**, 6095
508 (2019).
- 509 52. F. B. Marshall, K. Dobney, T. Denham, J. M. Capriles, Evaluating the roles of directed
510 breeding and gene flow in animal domestication. *Proc. Natl. Acad. Sci. U.S.A.* **111**, 6153-
511 6158 (2014).
- 512 53. J. Lesur, E. A. Hildebrand, G. Abawa, X. Gutherz, The advent of herding in the Horn of
513 Africa: new data from Ethiopia, Djibouti and Somaliland. *Quat* **343**, 148-158 (2014).
- 514 54. E. A. Hildebrand, K. M. Grillo, E. A. Sawchuk, S. K. Pfeiffer, L. B. Conyers, S. T.
515 Goldstein *et al.*, A monumental cemetery built by eastern Africa's first herders near Lake
516 Turkana, Kenya. *Proc. Natl. Acad. Sci. U.S.A.* **115**, 8942-8947 (2018).
- 517 55. K. MacDonald, R. Hutton MacDonald, "The origins and development of domesticated
518 animals in arid West Africa" in *The origins and development of African livestock:
519 archaeology, genetics, linguistics and ethnography.*, R. M. Blench, K. MacDonald, Eds.
520 (University College London Press, London, UK, 2000).
- 521 56. D. H. Alexander, K. Lange, Enhancements to the ADMIXTURE algorithm for individual
522 ancestry estimation. *BMC Bioinform.* **12**, 246 (2011).
- 523 57. N. Patterson, A. L. Price, D. Reich, Population structure and eigenanalysis. *PLoS Genet.*
524 **2**, e190 (2006).
- 525 58. N. Patterson, P. Moorjani, Y. Luo, S. Mallick, N. Rohland, Y. Zhan *et al.*, Ancient
526 admixture in human history. *Genetics* **192**, 1065 (2012).
- 527 59. F. G. Vieira, A. Albrechtsen, R. Nielsen, Estimating IBD tracts from low coverage NGS
528 data. *Bioinformatics* **32**, 2096-2102 (2016).

- 529 60. B. Q. Minh, H. A. Schmidt, O. Chernomor, D. Schrempf, M. D. Woodhams, A. von
530 Haeseler *et al.*, IQ-TREE 2: new models and efficient methods for phylogenetic inference
531 in the genomic era. *Mol. Biol. Evol.* **37**, 1530-1534 (2020).

532

533 **Fig. 1: Modern donkey dataset and population evolutionary history.** A) Number and
 534 geographical distribution of modern donkey samples ($n=207$). Pie charts show the
 535 ADMIXTURE proportion of domestic ancestry (grey), African wild ass ancestry (white) and
 536 kiang ancestry (black) averaged across all individuals from each country (56). For visualization,
 537 the total surface of each pie chart is scaled to 2%. B) Smartpca (57) of modern donkeys, with the
 538 imputed ancient samples in black. C) Treemix phylogeny of modern domesticates (excluding
 539 individuals with high wild introgression, $n=201$) (27). Node supports are estimated from 100
 540 bootstrap pseudo-replicates (confidence < 90% in red). Percentage values indicate admixture
 541 proportions inferred from Treemix (27). D) SMC++ demographic trajectories (colored) and split
 542 time estimates (black) for pairs of main geographic regions (28), repeating the analysis on two
 543 datasets of three individuals per population (the second dataset is shown in semi-transparency).
 544 Modern donkeys are colored and shaped according to geographical location and continents in all
 545 panels.

546 **Fig. 2: Haplotype sharedness and phylogenetic placement of ancient European donkeys.** A)
 547 Haplotype sharedness clustering of modern ($n=168$) and ancient donkeys ($n=31$) reconstructed
 548 using fineSTRUCTURE (35). Modern domesticates are colored following Fig. 1 and ancient
 549 individuals are numbered according to Fig. 3A. Cluster supports are shown in percentage on each
 550 node if >0.8. MV242 placement is incongruent with Treemix (Fig. 2E), due to the limited
 551 representation of divergent ancestries in the modern reference panel used for imputation. B) Co-
 552 ancestry matrix based on haplotype sharedness. Co-ancestry values averaged for co-clustered
 553 individuals. C-E) Treemix phylogenies of three ancient specimens shown in black (C: Chalow3,
 554 D: Doshan Tepe, E: MV242) placed within the subpopulations defined in Fig. 1C (27). Branches
 555 that are not scaled are shown as dashed lines.

556 **Fig. 3: Ancient donkey dataset, genetic affinities to outgroups and modern donkeys.** A)
 557 Geographical distribution, estimated age and sample names of ancient donkeys ($n=31$). Pie charts
 558 represent the proportion of individuals with dun coat color (white), heterozygotes (grey), and
 559 derived coat color (red) at each site. Genotype probabilities ≥ 0.99 denoted with ** and ≥ 0.9
 560 with *. B) Heatmap displaying outgroup f_3 -statistics in the form of (modern, ancient; kiang)
 561 (58). Bar charts represent the proportion of wild ancestry (kiang, onager, zebra, *E.a.som*) in each
 562 ancient individual with standard errors estimated from ADMIXTURE with 100 bootstrap
 563 pseudo-replicates (56). C-E) Treemix phylogenies of ancient specimens from three
 564 archaeological sites shown in black (C: Tarquinia (Tarquinia214, Tarquinia501), D: Bourse
 565 (BourseB, BourseC), E: Albufeira) placed within the subpopulations defined in Fig. 1C (27).
 566 Branches that are not scaled are shown as dashed lines.

567

568 **Fig 4: Inbreeding in domestic donkeys and horses.** A) Distribution of total runs of
 569 homozygosity (ROH) length in modern versus ancient donkeys. B) The total length of ROH in
 570 donkey genomes through time. C-D) Same as A-B, but for 79 modern and 75 ancient horses.
 571 ROH tracts were identified using ngsF-HMM (59).

572

573 **Fig. 5: Uniparental marker phylogenies and introgression of divergent lineages.** A)
 574 Mitochondrial phylogeny constructed using IQ-TREE (60) with 100 bootstrap pseudo-replicates
 575 marked with a black triangle if $>90\%$. B) Posterior distributions of the time to the most recent
 576 common ancestors of all mitochondrial haplotypes, Clade I and Clade II labelled with their
 577 modes. C-D) Same as A-B for the Y-chromosome. E-H) f_4 -statistics (58) exploring the genetic

578 contribution of divergent lineages into modern and ancient donkeys. Z scores were corrected for
579 multiple testing, and red bars with asterisks show p -value <0.05 .

580 **Acknowledgments:**

581 **Funding:** LKH would like to thank the director of the Tel es-Safi/Gath excavation, Prof.
582 Aren Maeir, for facilitating sampling. The DonkeyBank collection of modern donkey DNA
583 samples is supported by the European Union's Horizon 2020 Research and Innovation
584 Programme (Grant Agreement Number 857251). Lucia Perez-Pardal is funded by national
585 funds from FCT – Fundação para a Ciência e a Tecnologia, I.P. Genoscope and GeT-PlaGe
586 sequencing platforms are partly funded by France Génomique National infrastructure, funded
587 as part of Investissement d 'avenir' program managed by Agence Nationale pour la Recherche
588 (contract ANR-10-INBS-09). This project has received funding from the CNRS, University
589 Paul Sabatier (AnimalFarm IRP), and the European Research Council (ERC) under the
590 European Union's Horizon 2020 research and innovation programme (Grant Agreements
591 885729-AncestralWeave, 295729-CodeX, 853272-PALAEOFARM, and; 681605-
592 PEGASUS).

593 **Author contributions:**

594 Conceptualization: LO

595 Materials and Reagents: JMA, AP, PW, ABP, DDW, LO

596 Archaeological samples and contextual information: MV, EV, MM, OP, UT, GBG, AT,
597 VT, FA, JLC, MJV, MTA, NB, AG, LKH, AÖ, BA, OV, BC, SL, AAV, HD, AM, MM.

598 Investigation: SBB, DLA, MPW, WCB.

599 Sampled modern donkeys: ABP, DDW, LPR, SAB.

600 Radiocarbon dating: JS.

601 DNA sequencing: MTC, LC, SS, ASO, AP, OB, CD, PW.

602 Data analysis: ETT, PL, LO.

603 Writing – Supplemental Information: ETT, with input from LO

604 Writing – Main Article: ETT, PL, LO, with input from all co-authors.

605 **Competing interests:** Authors declare that they have no competing interests.

606 **Data and materials availability:** The sequence data generated in this study is available for
607 download at the European Nucleotide Archive (Accession number = PRJEB52849). The
608 accession numbers for each individual sample and all other data used in this study are
609 included in Table S1, S2 and S11 of the Supplementary Information.

610 **Supplementary Materials:**

611 Materials and Methods

612 Figs. S1 to S15

613 Tables S1 to S11

614 References 61-137

Supplementary Materials for

The genomic history and global expansion of domestic donkeys

Evelyn T. Todd, Laure Tonasso-Calvière, Lorelei Chauvey, Stéphanie Schiavinato, Antoine Fages, Andaine Seguin-Orlando, Pierre Clavel, Naveed Khan, Lucía Perez Pardal, Laura Patterson Rosa, Pablo Librado, Harald Ringbauer, Marta Verdugo, John Southon, Jean-Marc Aury, Aude Perdereau, Emmanuelle Vila, Matilde Marzullo, Ornella Prato, Umberto Tecchiati, Giovanna Bagnasco Gianni, Antonio Tagliacozzo, Vincenzo Tinè, Francesca Alhaique, João Luís Cardoso, Maria João Valente, Miguel Telles Antunes, Laurent Frantz, Beth Shapiro, Daniel G. Bradley, Nicolas Boulbes, Armelle Gardeisen, Liora Kolska Horwitz, Aliye Öztan, Benjamin S. Arbuckle, Vedat Onar, Benoît Clavel, Sébastien Lepetz, Ali Akbar Vahdati, Hossein Davoudi, Azadeh Mohaseb, Marjan Mashkour, Olivier Bouchez, Cécile Donnadieu, Patrick Wincker, Samantha A. Brooks, Albano Beja-Pereira, Dong-Dong Wu, Ludovic Orlando.

Correspondence to: ludovic.orlando@univ-tlse3.fr

This PDF file includes:

Materials and Methods

Figs. S1 to S15

Tables S1 to S11

References 61-137

1 **Summary**

2 This document describes the methods that have been involved in this study. The first part of
3 these analyses focusses on a panel of 207 modern donkey and 15 wild equid genomes, 49 of
4 which are newly described in this study. These genomes were used to: 1) call variants
5 (GraphTyper (version 2.5.1) (61)); 2) create a recombination map (LDHat (version 2.2) (62));
6 3) call phased haplotypes (BEAGLE (version 5.1) (39)) ; and 4) infer the population history
7 and structure (PLINK (version 1.9) (63), ADMIXTURE (version 1.3.0) (56), qpAdm (version
8 810) (64), Treemix (version 1.13) (27), SMC++ (version 1.15.4) (28) and ADMIXTOOLS2
9 (58, 65)).

10 Additionally, the second part of the analysis leverages the modern genome panel, supplemented
11 with 31 ancient donkey genomes spread across central Asia to western Europe and spanning
12 the last 4,500 years. We created two datasets to fully exploit the genetic information of these
13 samples, both pseudo-haploidising genomes at transversion sites (n= 4,833,570), and imputing
14 genomes for the set of variants identified in the modern panel (n=7,161,029) (BEAGLE
15 versions 4.0 and 5.1). Those datasets were used to infer the past population dynamics and assess
16 breeding management through ADMIXTURE, PLINK, Treemix, fineSTRUCTURE (version
17 4.1.1) (35), KING (version 2.2.7) (66), NgsRelate (version 2) (67), NgsF-HMM (version 1)
18 (59) and qpDstat (version: 751) (58, 65).

19 Finally, modern and ancient sequences aligned against the mitochondrial genome and Y-
20 chromosome were used to infer phylogenetic relationships within both maternal and paternal
21 lineages and reconstruct their past demographic trajectory (IQ-TREE (version 1.6.12) (60) and
22 BEAST (version 2.6.5)) (68-70).

23 **Materials and Methods**

24 Sample collection, DNA extraction and genome sequencing of modern samples

25 We extracted and sequenced DNA from 48 tissue samples of domestic donkeys kindly provided
26 from the existing collection of Dr. Albano Beja-Pereira, which were collected between 2000
27 and 2002 (DonkeyBank, CIBIO-InBIO, University of Porto). The sampling was revised and
28 approved by CIBIO bioethic board. Samples from this collection have been used across the
29 years in several published studies (11, 12, 71). The curation of this sample bank is oriented by
30 the principles of the 3Rs, avoiding unnecessary sampling of animals whenever the collection
31 has samples representing a region or the desired donkey phenotype. Only from 2015 onward,
32 did export and ethical and animal welfare permits start to be required from the samples stored
33 in this collection. Up to this date, it was not a general practice to require such permits from
34 domestic animals, and unfortunately, even less in the case of the donkey. When these samples
35 were collected, the owners first approached the animal to calm them down. The marginal region
36 of the ear was cleaned with 70% ethanol and a single-use sterile punch biopsy was used to take
37 a tiny piece of skin about 0.2 cm³ from each individual. Particular attention was devoted to
38 collecting the tissue along the margin and not across the ear, as this area is poorly irrigated and
39 not sensitive. The punch biopsy device automatically cauterizes the possible small capillary
40 vessels from the place where a sample was taken. Usually, this takes a split second and does
41 not require holding the animals for blood sampling and animals do not generally react. After
42 sampling, blue spray disinfectant was applied to the region. Nervous or frightened animals
43 were avoided and the animal was observed for some minutes after having been sampled.

44 Around 20 plucked hairs (with roots) were instead collected from animals for which the owner
45 expressed a preference for plucking hairs instead of tissue. Normally, dorsum or neck hairs
46 were individually plucked from the animal without the need of restraining the animal. The
47 collected hairs or tissues were stored in the plastic tube and completely submerged in
48 preservative (96% alcohol) with at least three parts of ethanol for each part of the tissue. DNA
49 from DonkeyBank tissues were extracted from the tissues using the JetQuick™ Tissue DNA
50 Spin Kit (Genomed, GmbH) and the concentration of DNA extracts was measured using a
51 Qubit Fluorimeter (Thermo Fisher Scientific).

52 A single specimen from a Pega donkey was provided by the Brooks Equine Genetics Lab
53 (University of Florida, Gainesville, FL, USA). The sampling was revised and approved by the
54 UF - IACUC Protocol #201408411. The hair sample, including hair roots, was pulled from the
55 tail of the individual, and stored in a clean paper envelope. DNA from this sample was extracted
56 using a modified lysis protocol described by Cook and colleagues (72).

57 Publicly available fastq files for 158 domestic donkeys, 2 Asiatic wild asses, 1 *E. africanus*
58 *somaliensis* (*E.a.som*), 1 *E. zebra hartmannae*, 1 *E. zebra grevyi*, 1 *E. zebra burchelli*, 2 *E.*
59 *hemionous* and 7 *E. kiang* were downloaded from the National Library of Medicine and
60 Genome Sequence Archive database (13, 24, 73).

61 Details and accession numbers for all samples sequenced and downloaded from public
62 databases can be found in Table S1.

63 Archaeological samples and context (Provenance)

64 The following section describes the archaeological contexts associated with all ancient donkeys
65 sequenced in this study. The full name of each site is composed of the modern country where
66 the excavation site lays followed by the age in Before Common Era (BCE) or Common Era
67 (CE) as estimated from radiocarbon dating or inferred from archaeological context. The
68 accession number and associated metadata for each ancient donkey genome included in this
69 paper can be found in Table S2.

- 70 • **TUK_2564-2039BCE:** Acemhöyük, Turkey (samples: AC14380, AC14415, MV051).

71 Acemhöyük is a large mound site located in the Aksaray province of central Turkey
72 representing an important urban center in the Early and Middle Bronze Age (EBA and MBA,
73 ~2,800-1,700 BCE). The site is located at an elevation of approximately 950 m above sea level
74 on the alluvial fan of the Melendiz river near the central Anatolian Great Salt Lake (Tüz Gölü).
75 Acemhöyük consists of twelve major occupational levels with deposits representing EBA,
76 MBA, Early Iron Age, Hellenistic, and modern occupations. The site is best known for its well-
77 preserved Sarıkaya and Hatıplar ‘palace’ structures, which were built in the early 18th century
78 BCE and destroyed by a violent fire in the mid-18th century BCE (74). These remains were
79 excavated and studied by Dr. Nimet Özgüç, who documented extensive connections between
80 the Sarıkaya palace at Acemhöyük and Kültepe-Kanesh, the kingdom of Karkemis on the
81 Syrian-Turkish border, as well as the Assyrian kingdom of Šamši Adad (75). More recent
82 excavations by Dr. Aliye Öztan have explored administrative buildings within the city center
83 associated with the MBA occupation (including the ‘Hizmet binası’), which were also
84 destroyed by the fire that likely ended the settlement’s role as a political center towards the end
85 of the MBA (74). Moreover, Öztan’s excavations have uncovered extensive exposures of the
86 EBA occupation including 75 meters length of the EBA city wall on the south-eastern margin

87 of the mound as well as associated buildings dating to mid to late 3rd millennium BCE (EBIII)
88 (76-78). Deposits associated with EBA levels XI and X include evidence for the destruction of
89 city wall including as many as 1500 biconical clay balls interpreted as sling stones, human
90 remains subject to violent death, as well as extensive pits filled with burnt and ashy deposits
91 (79, 80). Based on a direct radiocarbon date on human bone from area AB/52 associated with
92 these deposits (Sk4: BETA464596, 3920±30 bp, 95% 2480 - 2299 cal BC), this destruction is
93 dated to the second half of the 3rd millennium BCE (80).

94 All three donkey specimens from Acemhöyük utilized in this study are petrosal portions of the
95 temporal bone derived from grid square EB/50 and assigned to stratigraphic level XI or X
96 dating to the EBA (EBIII). Specimen AC14380 (derived from mekan C) was recovered on the
97 23rd of July, 2012. The specimen AC14415 was recovered on the 24th of July 2015; while
98 specimen MV051 (recorded as specimen AC13084 in the Acemhöyük zooarchaeological
99 database) was recovered on August 17th, 2012. All of these specimens derive from deposits
100 representing multiple complete or partial donkey burials located in close proximity to the level
101 XI city wall (MNI of 8 donkeys recovered from this area). They were recovered from shallow
102 deposits directly under the remains of structures associated with the modern village, which
103 currently surrounds the mound and were initially thought to be modern pits related to the
104 disposal of donkey remains. However, it became clear that these donkey burials, as well as
105 others in adjacent areas DB/50 (MNI=3) and DB/48 (MNI=3) are associated with the EBA
106 occupation of the city. Specimen MV051 has been directly dated by radiocarbon assay placing
107 it in the last quarter of the 3rd millennium BCE, which corresponds with the phasing of the
108 stratigraphic context to levels XI and X (UBA-30288, 3784±41 BP; 2285-2141 cal. BCE).
109 Samples AC14380 and AC14415 were also radiocarbon dated and returned the same
110 measurement (UCIAMS-199621 and UCIAMS-199619, 3945±20 BP; 2564-2346 cal. BCE)
111 (Table S2).

112 • **IRA_2400BCE-2039BCE:** Chalow, Iran (sample: Chalow3)

113 Chalow cemetery is located in the North Khorasan Province in the North East of Iran. It was
114 first located by Dr. Ali Akbar Vahdati in 2006 and the discovery of material culture placed this
115 site in the Middle-Late Bronze / Bactria-Margiana Archaeological Complex (BMAC) (2200 to
116 1900 BCE) (81). In Trench 41E, Grave 6 East, excavated by Dr. Vahdati and Dr. Raffaele
117 Biscione in 2015, an equid was discovered buried beside a human skeleton. This equid was
118 later identified as a donkey and included in the current study (Table S2).

119 • **IRA_1049BCE-928BCE:** Doshan Tepe, Iran (sample: DoshanTepe).

120 Doshan Tepe is one of the five archaeological sites of the Ozbaki archaeological zone located
121 in the Savojbolagh plain, 75 kilometers towards the north-west of Tehran, with excavations
122 starting in 1998. The site of Doshan Tepe is located 250 meters to the west of the Main Tepe
123 (Ozbaki Median Fortress). The plain was occupied from the 6th millennium BCE with
124 excavations leading to the identification of 3 periods of the Iron Age. The latest is
125 contemporaneous to the Median period and the two earliest periods are dated from the second
126 half of the second millennium to the advent of the Median dynasty. The presence of grey
127 pottery suggests non-local traditions. Doshan Tepe had also an important role in the region
128 since cuneiform tablets were found in the Ozbaki archaeological zone. Studies of the faunal
129 remains identified numerous equids at this sites, including 29 donkeys, 11 hemiones, 8 horses
130 and 4 probable hybrids and 93 unidentified equids (82). The donkey sample in this study

131 belongs to the Iron Age II chronology in Iran. It was directly radiocarbon dated to 1049-928
132 cal. BCE (UCIAMS-223195, 2840±15 BP) (Table S2).

133 • **ITA_803-412BCE:** Tarquinia, Italy (samples :Tarquinia214, Tarquinia501).

134 The ‘monumental complex’ of Tarquinia offers the extraordinary opportunity to monitor the
135 cultural development of an Etruscan area sacred to the major female goddess of the Etruscans.
136 Archaeological evidence sheds light on the continuity and memory of the sacred area over the
137 centuries up to the encounter with Rome. From the end of the 10th century BCE, offerings
138 located by a natural cavity show the cult of a divinity of Nature, who catalyzed the very first
139 community. Ritual sealing of a number of votive pits of different size contain a considerable
140 number of animal bones (83). Samples Tarquinia214 and Tarquinia501 were found in the
141 texture of pavements of structures belonging to the Archaic phase of the site. Both samples
142 were directly radiocarbon dated. The date obtained for specimen Tarquinia214, 750-412 BCE
143 (UCIAMS-224884, 2445±20 BP), overlaps the archaeological context (~550BCE). Two dates
144 were obtained for specimen Tarquinia501, which returned a range slightly older than those
145 estimated based on the archaeological context (803-547 BCE vs 520-500BCE) (UCIAMS-
146 224885 and UCIAMS-224886, 2515±20 BP and 2656±20 BP) (Table S2).

147 • **ISR_350_58BCE:** Nizzana, Israel (sample: MV242).

148 Nizzana (sometimes also written as Nessana) is located 52km to the South-West of the city
149 Beersheba. The site was first occupied in the Hellenistic period, and settlement continued
150 throughout the Roman and Byzantine periods until its abandonment in the Early Islamic
151 period. Architectural remains include residential buildings, a Late Roman military fort, three
152 Byzantine churches and a monastery and notably was a 6–7th century CE papyrus archive (84-
153 86). The sample MV242 dates back to the Hellenistic period and was radiocarbon dated to 350-
154 58 cal. BCE (UCIAMS-199283, 2150±20 BP) (Table S2).

155 • **IRA_800BCE-800CE:** Shahr-i-Qumis, Iran (samples: AM39, AM44, AM66, AM71,
156 AM805, AM89).

157 Shahr-i-Qumis is a site in Northeast Iran, consisting of several isolated mounds spread across
158 an area of 28 kilometers. This site dates back to the Parthian and Sassanian periods, although
159 some recent radiocarbon dating of faunal remains show a longer period of occupation, from
160 the 8th century BCE to the 8th century CE (87, 88). The site has been identified as Hekatompylos
161 (41, 88), the capital of the Parthian Empire and major hub of the Silk Road and Great Khorasan
162 Road. Excavations at Shahr-i-Qumis revealed a very large quantity of equine skeletons. Sample
163 AM805 was radiocarbon dated to 415-542 CE (UCIAMS-223584 and UCIAMS0223188,
164 1615±20 and 1585±15; Table S2). This places it either during the kingdom of Yazdegerd II
165 (438–457 CE) or his brother Peroz I (457–484 CE). In the beginning of the 5th century CE,
166 nomadic groups (in particular the Hephthalites or White Huns) attacked Persia several times,
167 invading parts of eastern Persia for several years. These events may have also impacted the
168 equine population. A large set of animal bones including an important assemblage of equine
169 bones has been studied by Dr. Marjan Mashkour and Dr. Azadeh Mohaseb from 2002 and later
170 other collaborators (Hossein Davoudi, Homa Fathi, Sansaz Beizae Doost and Roya Khazaeli)
171 at the British Institute of Persian studies in Tehran (89). The assemblage was then transferred
172 to the National Museum of Iran where Azadeh Mohaseb is currently performing a
173 morphometric geometric study of the equid bones.

174 • **FRA_200-500CE:** Boinville-en-Woëvre, France (samples : GVA125, GVA347,
175 GVA348, GVA349, GVA353, GVA354, GVA355, GVA358, GVA359).

176 The Gallo-Roman villa of Boinville-en-Woëvre, Déviation Est d'Etain, is located in the
177 department of Meuse, in Northern France. The excavation was carried out in 2005 under the
178 direction of S. Viller (Inrap). Within the Pars Rustica, approximately fifteen pits were
179 discovered, containing 22 complete or sub-complete skeletons of horses and donkeys (9 of
180 which were included in this study, Table S2). Individuals are dated from the Late Antiquity
181 (200-500 CE) (47).

182 • **FRA_0-500CE:** Centre Bourse Marseille, France (samples: BourseB, BourseC)

183 The equid bones come from ancient excavations carried out in 1968-1969 at the horn of the
184 ancient port of Marseille. They are dated to late Roman times and were studied by Lucien
185 Jourdan who delivered one of the first archaeozoological theses for the Roman period in 1976.
186 Although the chronological resolution is limited, the assemblages can be associated to a
187 complex of carcass deposits accumulated by marine movements between 0-500 CE (90). A
188 horse and two donkeys were identified from this site (47).

189 • **TUK_552-987CE:** Yenikapi, Turkey (samples: Tur168, Tur177, Tur179, Tur277)

190 Yenikapi excavations area is located at the Yenikapi section of Istanbul which lies at the west
191 of Namik Kemal Avenue leading from Aksaray down to the Marmara Sea. The site occupies
192 approximately 58,000 m² and covers 1.5 km inland from the Marmara Sea. During the
193 construction work of the Marmaray and Metro railway project at Yenikapi a large number of
194 antique shipwrecks and animal skeletons were discovered. In the light of these important
195 findings, organized excavations began as early as 2004. The results of the analyses indicate
196 various dates ranging from the early through to the late Byzantine period. About 57 animal
197 species have been identified from the faunal assemblage of the site, and the majority of them
198 are comprised from horse, donkey and mule remains (91-93).

199 • **PTG_1228-1280CE:** Albufeira, Portugal (sample: Albufeira1x1)

200 This site is in the historic center of Albufeira, on an old peninsula which is surrounded by an
201 inlet to the east and the north. Two silos were found located to the east of the small church of
202 Misericórdia. One silo, that was uncovered during construction work was filled with
203 archaeological material. The finding of coins indicated that this material is no older than the
204 13th century, during the last phase of Islamic Rule (Almohad Period). The Almohad dominion
205 of Albufeira lasts until 1249 and was the last Alcazaba (city) to be conquered by the Christians.
206 The ceramic materials found at this site are typical from the Almohad period and one of the
207 coins is from the reign of King Afonso III (1248-1279).

208 Abundant remains of mammological and malacological fauna were identified, including
209 deciduous teeth of a horse and donkey on the top layer of the silo (94). The radiocarbon date
210 for the donkey sample (1228-1280 cal. CE; UCIAMS-208877, 765±15 BP, Table S2) suggests
211 its death in the last decades of the Almohad period or shortly after the conquest. However,
212 Islamic people remained in Algarve under the rule of the Christians, so the sample has been
213 considered as Late Islamic.

214 • **ITA_1683-1936CE:** Fiumarella, Italy (sample: Fiumarella1)

215 The site of Riparo della Fiumarella di Tortora is located in the valley of the Fiumarella di
216 Tortora stream, close to the modern town of Tortora (Cosenza, Calabria, Southern Italy) and

217 not far from the Tyrrhenian coast. This strategic position, along one of the routes between the
218 coast and more inland territories, may hint to the importance of the site in the region.

219
220 The site was excavated in 2000 by the Soprintendenza Speciale al Museo Preistorico
221 Etnografico “Luigi Pigorini”, now part of the Museo delle Civiltà (Rome). The stratigraphic
222 sequence and the archaeological materials evidenced that the site was in use from at least the
223 late Chalcolithic to the MBA (95). The chronological and cultural attributions are based on
224 ceramic typology and few bronze artifacts.

225
226 The site is now a rock-shelter, but in the past, possibly until the beginning of the MBA, it was
227 a larger cave that collapsed just before the last phases of prehistoric occupation. The relatively
228 small faunal assemblage (n=299) from all the archaeological layers includes mainly domestic
229 mammals, although some remains of red deer and wild boar as well as tortoise were also
230 recovered. Most of the remains represent food refuses although animals probably used for other
231 purposes (e.g., dog, equids) are also present.

232
233 Caprine herding represents the main economic activity especially in the MBA when there is a
234 corresponding decrease in the number of pig remains, while cattle rearing was not relevant
235 throughout the archeological sequence. Dogs were extremely rare. Hunting was moderately
236 important during the EBA occupation (20% of the identified specimens). Of particular interest
237 to this study is the presence of two remains of small equids: a femur head from the EBA 2
238 levels (ca. 1950-1650 BCE), and a third lower molar belonging to a young individual from the
239 MBA 3 - Apennine Culture levels (ca. 1450-1350 BCE). Based on genetic analyses, both
240 specimens were identified as donkey and the latter one was included in the present study due
241 to its high content in endogenous DNA.

242 The presence of donkeys at such an early date was unexpected because according to current
243 archaeozoological data the earliest occurrence of domestic donkey in Italy is documented only
244 at sites referable to more recent phases of the Bronze age (e.g., Spina, Monte Titano, Coppa
245 Nevigata, Madonna del Petto; (96-99)). Therefore, to assess the actual antiquity of the tooth,
246 the specimen was directly dated (UCIAMS-229410, 165±25 BP; Table S2). Unfortunately, the
247 results indicated that the specimen represents modern intrusive material within the Bronze Age
248 levels, however its genetic data have been integrated in this research.

249 DNA extraction and genome sequencing of ancient samples

250 The procedures of DNA extraction, library construction and shallow sequencing followed the
251 procedures outlined by Seguin-Orlando and colleagues (100) and Librado and colleagues (21).
252 The drilling and DNA extractions from osseous material of ancient equids were carried out in
253 the ancient DNA facilities of the Centre for Anthropobiology and Genomics of Toulouse
254 (CAGT), France. Briefly, the methods involved: 1) powdering a total of 100-590mg of osseous
255 material using the Mixel Mill MM200 (Retsch) Micro-dismembrator; 2) extracting the DNA
256 following the procedure outlined by (101), which was tailored to facilitate the recovery of even
257 the shortest DNA fragments; 3) treating DNA extracts with the USER™ (NEB) enzymatic
258 cocktail to eliminate a fraction of post mortem DNA damage (102); 4) constructing from
259 double-stranded DNA templates DNA libraries in which two internal indexes are added during
260 adapter ligation and one external index is added during PCR amplification; and 5)
261 amplification, purification and quantification of DNA libraries before pooling 20–50 DNA

262 libraries for low-depth sequencing. After screening for library content using a Miniseq
263 instrument (high-output 80PE mode) at the CAGT (France), sequencing was performed on
264 various Illumina platforms, including HiSeq2500 instruments, at the Centre for GeoGenetics
265 (University of Copenhagen, Denmark) and HiSeq4000 instruments at the Genoscope (Evry,
266 France). Sequence trimming, mapping, filtering and base calibration at damaged sites were
267 carried out following the methodology from Librado and colleagues (21).

268 Radiocarbon dating

269 Radiocarbon dates were estimated for 14 of the 31 (45%) ancient donkey samples in this
270 study. Dating was carried out at the Keck Carbon Cycle AMS Laboratory, UC Irvine
271 following collagen extraction and ultra-filtration from approximately 1 g of osseous material.
272 IntCal20 calibration (103) was performed using OxCalOnline (104). Calibrated dates are
273 provided in Table S2. The ages of ancient samples that were not radiocarbon dated were
274 inferred from their established archaeological contexts.

275 Read alignment, rescaling and trimming

276 For each raw fastQ file, sequencing reads were demultiplexed, collapsed and trimmed using
277 AdapterRemoval2 (version 2.3.0) (105) following the methodology from Gaunitz and
278 colleagues (50) for single indexed DNA libraries, and the methodology from Librado and
279 colleagues (21) for triple indexed libraries. AdapterRemoval2 also ensured that paired-end
280 reads showing sufficient sequence overlap were collapsed and trimmed (truncated) if ends
281 showed insufficient qualities. Collapsed, truncated and those paired end reads not collapsed
282 (paired) were then parsed through PALEOMIX version 1.2.13.2 (106) for Bowtie2 mapping
283 against the donkey mitochondrial (CM027722.1), and nuclear reference sequence
284 (GCA_016077375.1, https://ftp.ncbi.nlm.nih.gov/genomes/genbank/vertebrate_mammalian/Equus_asinus/all_assembly_versions/GCA_016077325.1_EquAsi1.0). Finally, the optimized
285 parameters recommended by Poulet and Orlando (107) were considered for mapping, and
286 alignments were locally realigned around indels using the IndelRealigner procedure from
287 GATK (13). Sequence alignments shorter than 25 nucleotides, and/or representing PCR
288 duplicates were removed, as well as reads with mapping quality scores inferior to 25.

290 Subject to trimming, the software mapDamage2 (24) was used to check for the presence of
291 nucleotide mis-incorporation profiles characteristic of ancient DNA data at the library level,
292 randomly selecting 100,000 reads. We observed the expected increase of C to T (G to A) mis-
293 incorporation rates at read starts (read ends) for both USER™-treated and non-USER™-treated
294 data, although of lower magnitude for the former, as expected. Furthermore, genomic positions
295 preceding read starts were higher in purines in non-USER™ read alignments, consistently with
296 post-mortem DNA fragmentation being depurination-driven. In USER™-treated read
297 alignments, these positions were enriched in cytosine residues, in line with the excision of
298 deaminated cytosines by the sequential activities of Uracil DNA
299 glycosylase and Endonuclease VIII enzymes present in the USER™ mix. In order to limit the
300 impact of remnant mis-incorporations in downstream analyses, we applied the computational
301 procedure combining end trimming and base quality rescaling based on the post-mortem DNA
302 damage profiles, as described in Seguin-Orlando and colleagues (100) and Librado and
303 colleagues (21). Briefly, this procedure relies on PMDtools (108) to sort read alignments into
304 those likely affected by and those devoid of post-mortem DNA damage. The former alignments
305 were then subjected to base rescaling at those positions likely incorporating nucleotide mis-

306 incorporations reflecting post-mortem cytosine deamination using mapDamage2 (109), before
307 trimming their ends for 10 nucleotides, while the latter were directly subjected to end trimming
308 for 5 nucleotides.

309 Variant calling pipeline

310 • **Alignment to the reference genome and rescaling of modern individuals**

311 We determined the sex of each individual by comparing the relative depth of reads between
312 the autosomes and X chromosomes in the bam files using the “depth” function in SAMtools
313 (version 1.7-12-g17a2483)(110). Individuals with a relative depth of 1 between the autosomes
314 and X chromosome were considered to be female and an autosomal depth twice that of the X
315 chromosome were considered to be male (Table S1, S2).

316 • **Variant calling and quality control filtering of modern individuals**

317 We called variants (single nucleotide polymorphisms (SNPs) and insertions or deletions of
318 bases (INDELs)) from the mapped and rescaled bam files of modern equids using GraphTyper,
319 running each chromosome in parallel (version 2.5.1) (61) ($n=45,031,411$ variants, Table S3).
320 We then applied the recommended variant filters using the “vcffilter” function from Vcflib
321 (version 1.0) (111): $ABHet < 0.0$, $ABHet > 0.33$, $BHom < 0.0$, $ABHom > 0.97$, $MaxAASR >$
322 0.4 , $MQ > 30$. We used GATK (version 4.0.8.1) (112) and BCFtools (version 1.8) (110) to
323 apply the following genotype filters: Phred score > 20 , minor allele frequency (MAF) ≥ 0.01 ,
324 Hardy-Weinberg equilibrium p-value ≥ 0.001 and genotype missingness ≤ 0.2 , and
325 conditioning on biallelic variants only. After filtering, we removed the 18 scaffolds with no
326 variants remaining and the sex chromosomes, leaving the variants on the 30 autosomes for
327 further analysis ($n=13,013,551$ variants, Table S4).

328 • **Generation of the recombination map and phasing of modern individuals**

329 We selected 25 donkeys to generate a recombination map for all autosomal variants that passed
330 QC filters ($n=13,013,551$). In order to select individuals that provided a representative subset
331 of all subpopulations, we constructed a Principal Component Analysis (PCA) using PLINK
332 (version 1.9) (63) with all domestic donkey samples ($n=206$). We finally selected 25 domestic
333 donkeys representing the different geographical locations sampled, so no two individuals were
334 chosen from the same country. In order to prevent selecting individuals with high levels of
335 inbreeding, we estimated levels of inbreeding as runs of homozygosity (ROH) across all
336 autosomes using PLINK (version 1.9) (63). Considering that the data used to generate the
337 recombination map were unimputed, we also selected individuals with the lowest proportion
338 of missing SNPs (Table S1).

339 To calculate the effective population size of the 25 donkeys, we used the formula $N_e = \theta / 4\mu$,
340 where μ is the per generation mutation rate, N_e is the effective population size, and θ is the
341 nucleotide diversity. We used a per generation per site μ value of $7.242e-09$ as estimated for
342 horses (113), assuming a generation interval of 8 years. We calculated theta (θ) for the 25
343 selected individuals by calling variants using ANGSD (version 0.930) (114), conditioning only
344 on variants that passed the previous quality control filters with the parameters: “-GL 1 -C 50 -
345 minQ 25 -minmapq 30 -doMaf 1 -baq 1”. We estimated θ as 0.000875 for autosomal variants,
346 and N_e for domestic donkeys as 30,222.

347 To generate the recombination map, we first calculated the population scaled recombination
348 rate (ρ) between each variant using of LDHat (version 2.2) (62). To achieve this, we split each
349 chromosome into overlapping windows of 2,000 variants with an overlap of 200 variants
350 between each window. We generated a log likelihood lookup table for 50 chromosomes for the
351 25 diploid individuals using the θ estimated using ANGSD with the “complete” function of
352 LDHat. We then estimated ρ for each region using the “intervals” function of LDHat with the
353 parameters: “-its 10000000 -samp 2000 -bpen 5”. We discarded the first 20 million burnins and
354 averaged the remaining iterations using the “stat” function of LDHat with the parameter: “-
355 burn 50”, before combining the ρ values for each window back into complete chromosomes
356 and converting the ρ values to centimorgans (cM) using the estimated N_e value (Table S4, Fig.
357 S1). We found that the average rate of recombination 0.599 cM/Mb per chromosome, which is
358 lower than a previous estimate for horses (1.16 cM/Mb)(115), and in the lower range for
359 mammalian species. Next, we used the recombination map to phase missing variants for each
360 individual using BEAGLE (version 5.1) (39).

361 Population genetic analysis of modern donkeys

362 We used the phased variants to construct PCA analyses using PLINK for three subsets of the
363 population: all individuals (n=222 individuals, Fig. S2), domestic donkeys and *E.a.som* (n=208
364 individuals, Fig. S3), domestic donkeys only (n=206 individuals, Fig. 1B).

365 A PCA of all samples (n=222, Fig. S2) showed that domestic donkeys clustered closely
366 together compared to the wild equids, which is consistent with all individuals originating from
367 a single domestication process. The closest wild equid to the cluster of domestic donkeys was
368 *E.a.som*, in agreement with previous findings that donkeys were most likely domesticated from
369 wild African ass species (11-13). Early evidence of hunted *Equus a. africanus* at Gebel Gharbi
370 (modern day Libya, radiocarbon dated to 16,750 years ago) suggests a long history of human
371 contact with wild asses in Africa (116). However, the absence of the other two African wild
372 ass subspecies in the dataset (*E. a. africanus* or *E. a. atlanticus*) makes it impossible to
373 determine which of these subspecies is genetically closest to the donkey. Interestingly, the 7
374 kiangs in the dataset separated into two clusters which diverged on the PC2 axis only, which
375 may represent two different subspecies of kiang that have previously been found to be
376 genetically distinct (22). Of the two publicly available samples labelled as “Asiatic Wild Ass”
377 (Accession numbers: AW_1 (SRS3167373) and AW_2 (SRS3167374)), one clustered with a
378 group of kiangs and the other was most genetically similar to *E.hemionus*.

379 The PCA including only domestic donkeys and their closest relative showed *E.a.som* as
380 divergent from the domestic donkeys but closest to East African donkeys (Fig. S3). One donkey
381 from Ethiopia clustered between *E.a.som* and the other domesticates, which is indicative of
382 wild genetic material being present in the genome of this individual (Fig. S3). Additionally,
383 another donkey from Ethiopia and one from Algeria also shifted closer to *E.a.som* compared
384 to PCA plots with domesticates only, also indicating the presence of wild genetic material in
385 these individuals.

386 Within the domestic donkey population only, we observed strong sub-structuring of donkeys
387 from different geographical locations (Fig. 1B). African donkeys were diverged from the rest
388 of the donkeys on all PCA plots. European donkeys were genetically differentiated on the PC1
389 axis, with Irish donkeys highly drifted from individuals sampled from mainland Europe. There

390 was a further spread of donkeys along the bottom half of the PC2 axis moving through Asia
391 with all Chinese, Mongolian and Tibetan donkeys clustering together at the bottom of the PC2
392 axis.

393 We also found genetic differentiation between donkeys sampled from the same country.
394 Ethiopian donkeys cluster closely together with other African individuals, except for one
395 donkey clustering close to individuals from the Balkans (Macedonia and Croatia). One
396 individual from Turkey clustered distinctly as well, between Egyptian and European donkeys,
397 so was most likely the product of interbreeding between donkeys from different regions.
398 Additionally, Somalian donkeys form two distinct clusters. Two donkeys cluster with
399 individuals from the neighbouring countries of Ethiopia and Algeria. However, three donkeys
400 are more genetically similar to individuals sampled from Tunisia, Turkey, Syria and Iran,
401 seemingly the result of secondary translocations of donkeys from the Middle East back into
402 this region of the world.

403 We conducted an admixture analysis for all modern equids using ADMIXTURE (version 1.3.0)
404 (56) (Fig. S4). We thinned the variants using the "--indep-pairwise 50 10 0.2 --maf 0.05"
405 parameters in PLINK, leaving 531,322 unlinked variants. We used these variants for
406 ADMIXTURE analysis, with K values between 2-5. The ADMIXTURE analysis showed a
407 distinctive (red) ancestral component that differentiates wild equids from domestic donkeys for
408 all K values. The optimal K value of 4 showed a green ancestral component, which almost
409 completely makes up the genetic material of Irish donkeys with the navy component
410 predominating the genetic makeup of Asian donkeys, with the Kenyan samples showing a
411 yellow ancestral component. The additional (blue) ancestral component at K=5 was
412 predominate in donkeys from the Canary Islands, Spain and Portugal. These findings agree
413 with the substructures seen on the PCA and indicate that genetic drift has occurred in some
414 subpopulations of donkeys, mostly those from more geographically isolated locations such as
415 Ireland, Iberia and the Horn of Africa plus Kenya.

416 We found that the genomes of all kiangs, onagers and zebras consisted entirely of the red
417 ancestral component (named "wild ancestry"). However, only half the genome of the single
418 *E.a.som* individual only consisted of wild ancestry, which may be due to high levels of
419 inbreeding and genetic drift due to low population size in this species or because it is the closest
420 genetic ancestor to domesticates (23, 24). We found that the red ancestral component was also
421 present in the genomes of some domesticated individuals (named "wild ancestry"). To
422 determine the proportion of wild ancestry in the genome of each domestic donkey, we reran
423 the ADMIXTURE analysis with 100 bootstrap pseudo-replicates. We estimated the average
424 proportion of wild ancestry and the standard deviation for each domestic donkey across the
425 bootstraps Individuals with a standard deviation larger than the average wild ancestry
426 proportion (with ancestry proportion estimates intercepting zero) were assigned a wild ancestry
427 proportion of 0 (Fig. 1A). Donkeys with a proportion of wild ancestry larger than their standard
428 deviation were considered to carry significant admixture proportions and were named
429 "admixed donkeys" ($n=20$ individuals).

430 Within the domestic samples, one individual sampled from Ethiopia had a high proportion of
431 wild ancestry (6.99%), and was also identified on the PCA as showing a closer genetic
432 relationship with *E.a.som* compared to the other domesticates. We found measurable levels of

433 wild introgression in 18 other individuals from Africa and the southern Arabian Peninsula
434 (Yemen and Oman), and one individual from China (Fig. 1A).

435 To determine which wild equid population contributed wild ancestry to the hybrid donkeys, we
436 constructed qpAdm models (version 810) (64). The right (reference) populations consisted of
437 two outgroup domestic donkey populations (determined as donkey populations on different
438 clades to the individual of interest with no admixture from Treemix models and with
439 differential genetic components from the ADMIXTURE analysis) and two wild populations
440 (Table S5). To investigate possible sources of admixture, we selected domestic donkeys that
441 showed a similar genetic makeup to the target individuals based on the ADMIXTURE analysis
442 and a wild equid population as another potential ancestral group.

443 Population modelling with qpAdm identified the source of wild admixture in all individuals
444 from the Horn of Africa + Kenya and the southern Arabian Peninsula was from a closely related
445 source to *E.a.som*. However, without whole genome sequence data for the other African wild
446 ass species, it was not possible to determine whether this wild admixture occurred from *E.a.som*
447 directly or another sister subspecies. One individual from China showed admixture from kiangs
448 which are a native wild equid species found in the area and may have been the result of human
449 experimentation.

450 Interestingly, donkeys from Yemen and Oman also showed introgression from African wild
451 asses despite being outside the species historical and current habitat range. This is possibly due
452 to sustained trade of donkeys across the Red Sea with Africa. Additionally, introgression of
453 wild African asses was also found in donkeys sampled from western Africa despite this region
454 also being outside the species historical and current habitat range, which may be due to the
455 wider distribution of African wild asses in the past (12). Wild introgression into domestic
456 donkeys is consistent with the extensive reporting of interbreeding between donkeys and wild
457 asses throughout history (52, 117, 118), as well as observations in other domesticated species
458 including sheep (119) and cattle (120, 121). Such practices may have aimed to a further fitness
459 advantage by providing a new phenotype or increasing heterozygosity levels. Further sampling
460 of domestic donkeys in the future would confirm if wild introgression is continuing to occur or
461 if management practices have changed in recent times.

462 We constructed phylogenetic models using Treemix (version 1.13) (27) with 0-5 migration
463 edges for domestic donkeys + *E.a.som* (n=200). We excluded donkeys with the highest levels
464 of wild genetic material (n=6 with over 0.5% wild genetic material, as determined by the
465 ADMIXTURE analysis, and n=2 that were hybrids between multiple subpopulations), as they
466 introduced unnecessary complexity to the graph. Inclusion of these individuals resulted in
467 strong migration edges to the outgroup and each other, making it impossible to see admixture
468 between other groups of donkeys. We grouped the remaining donkeys into subpopulations
469 based on their geographical location, and then thinned the variants using the "--indep-pairwise
470 50 10 0.2 --maf 0.05" parameters in PLINK (632,429 variants remaining after pruning). We
471 estimated the optimal number of migration edges using a mixed linear model implemented in
472 the optM R package (<https://cran.r-project.org/web/packages/OptM/index.html>). Using the tree
473 with the optimal number of migration edges (m=3), we estimated bootstrap confidence
474 intervals for each node using modified scripts from the BITE package with 100 pseudo-
475 replicates (122) (Fig. 1C).

476 The Treemix analyses showed distinctive population sub-structuring within domestic donkeys
477 from different geographical locations, with two main branches forming between African (Clade
478 A) and African and non-African donkeys (Clade B), with further differentiation of Asian and
479 European donkeys into separate clusters. The Pega donkey from Brazil was highly divergent
480 but most genetically similar to individuals from the Canary Islands and Iberia. Therefore, the
481 genetic makeup of this rare breed of donkey suggests that is most likely the result of importation
482 of stocks from Iberia during Portuguese colonisation.

483 With the optimal number of migration edges ($m=3$) and exclusion of hybrid individuals, there
484 was evidence of shared genetic material between donkeys from the Clade A (Horn of Africa +
485 Kenya and western Africa) with individuals from Sudan (34.5%), which cluster on Clade B.
486 Bootstrapping the tree revealed low confidence at this node (Fig. 1C), which is likely due to
487 the high level of admixture with donkeys from Clade A. Most likely donkeys in this region are
488 bred from stocks sourced from Egypt in the north and other donkey populations in Africa. A
489 migration edge with a lower weight (21.7%) is also observed between the cluster of donkeys
490 from Spain, Portugal, the Canary Islands, Saudi Arabia and Brazil with individuals from
491 western Africa, which likely reflects trade over the Mediterranean, resulting in the importation
492 of donkeys between these regions. Finally, a migration edge between the single donkeys
493 sampled from Saudi Arabia and Brazil (39.8%) was also observed. The genetic similarity
494 between the donkey sampled from Saudi Arabia with the European donkeys compared to others
495 from the Arabian Peninsula (Yemen and Oman) is likely due to translocations of stocks back
496 into this region.

497 To further elucidate whether modern individuals are derived from one or two domestication
498 processes, we plotted the correlation between the genetic versus the geographic distance of
499 each subpopulation compared to donkeys from Ethiopia (Clade A) and Yemen (Clade B) (Fig.
500 S5). First, we determined regions of the genome contributed by wild ancestors by modelling
501 the admixed individuals in PCAdmix (123) with the ancestral populations as determined by
502 ADMIXTURE and qpAdm using the default parameters. We then created a masked VCF file
503 of all domestic donkeys by removing all variants from regions attributed to wild ancestry
504 ($n=11,576,248$ variants remaining after filtering). We then estimated the genetic distance (f_2)
505 between populations using ADMIXTOOLS2 (124, 125) and the geographic distance between
506 populations as the haversine distance using the geosphere package in R ([https://cran.r-](https://cran.r-project.org/web/packages/geosphere/index.html)
507 [project.org/web/packages/geosphere/index.html](https://cran.r-project.org/web/packages/geosphere/index.html)).

508 To avoid closely related subpopulations confounding regression trends, we excluded those
509 from the same geographic regions which clustered on Treemix with Ethiopia (Kenya and
510 Somalia) and Oman (Yemen). We calculated a separate regression line for individuals from
511 western Africa (Ghana, Mauritania, Nigeria and Senegal), as our demographic trajectories
512 indicated that they split from the subpopulations in the Horn of Africa+ Kenya early on before
513 the expansion out of Africa (Fig. 1D). We also excluded individuals that were translocations
514 back into geographic regions (ALG, BRA, SAU).

515 We found a strong linear trend of increasing genetic distance verses geographic distance from
516 Ethiopia ($r=0.767$, $r^2=0.460$) and Oman ($r=0.662$, $r^2=0.438$). The strong linear correlations fits
517 with modern donkeys being derived from a single source population similar to Ethiopia, as a
518 break in the trend would indicate that individuals out-of-Africa contained genetic material from
519 another source. The Z-statistic between the coefficients of the two models found no significant

520 difference (p-value=0.775). The same rate of regression from Oman and Ethiopia further
521 suggests that donkeys expanded out from a single source in Africa into the Arabian Peninsula
522 and then into Eurasia.

523 To determine the demographic history and split timing of donkey subpopulations, we selected
524 4 main subpopulations based on Treemix modelling, ADMIXTURE and PCA analysis
525 comprising of individuals from the Horn of Africa + Kenya (Horn+Ken), western Africa
526 (WAfrica), Asia and Europe. We selected three individuals from each subpopulation and
527 converted the variants in the VCF file to SMC++ format, masking regions with wild
528 introgression and tandem repeats using the “vcf2smc” function in the SMC++ package (version
529 1.15.4) (28). We then constructed pseudo-bootstrap replicates of each file by randomly
530 resampling 90% of each chromosome in chunks with 10 replicates based on a modified script
531 from MSMC2 package (126, 127), which was developed and implemented by Zheng and
532 colleagues (127). We then modelled the population split timing between subpopulations using
533 the split function in SMC++. Next, we obtained the split times from each model using the
534 standard plot function from SMC++ with a generational interval of 8 years (Fig. 1D, S6). We
535 estimated the mean and standard deviation for the split times of each model across the 10
536 bootstrap pseudo-replicates (Table S14). Additionally, we repeated the same analysis using a
537 different subset of three individuals from each subpopulation to confirm the robustness of the
538 model outputs.

539 Our demographic modelling using SMC++ showed a decrease followed by a rapid expansion
540 in effective population size for all donkey subgroups around 5,000 BCE, in line with theories
541 that donkeys are derived from a domestication process in Africa around the time of the
542 aridification of the Sahara desert (1) (Fig. S6). Further, the models estimated that the first
543 population split occurred between donkeys now found in the Horn of Africa plus Kenya and
544 western Africa, indicative of early genetic isolation occurring within the African continent (Fig.
545 1D).

546 Concurrent population split times of European and Asian subpopulation with donkeys from the
547 Horn of Africa plus Kenya indicates a rapid population expansion out of Africa, which suggests
548 that donkeys spread almost simultaneously and extremely rapidly throughout the Old World
549 by the third millennium BCE. This, and the strong phylogeographic structure detected amongst
550 modern populations, indicate that early herders maintained high local reproductive stocks
551 within the areas where donkeys were imported to sustain their further geographic spread. In
552 contrast, effective population size of the donkeys now found in western African only achieved
553 stabilisation around 1,000 years ago.

554 Imputation of ancient genomes

555 We imputed the ancient genomes based on the pipeline developed and tested by Hui and
556 colleagues (38). In line with this method, we created a reference panel consisting of all modern
557 domestic donkeys ($n=206$) and variants with a MAF ≥ 0.05 . We selected only ancient donkeys
558 with a genome coverage of over 0.75X as candidates for imputation ($n=31$ individuals, Fig.
559 3A, Table S2). Before imputation we pseudo-haploidized the ancient individuals using the
560 “dohaplo” flag in ANGSD, conditioning only on positions found in the modern reference panel.
561 We then projected the ancient individuals onto the PCA of modern domesticates using the
562 “lsqproject” function in the smartpca program from the EIGENSOFT package (version 6.1.4)
563 (26, 57) (Fig. S7). We found that all ancient individuals clustered closely with the modern

564 domesticates, indicating that they have a similar genetic makeup and that the reference panel
565 of modern variants can be used for the imputation of the ancient samples.

566 After confirming that the ancient samples clustered with the modern individuals, we genotyped
567 all variants found in the modern reference panel using ANGSD with the following parameters:
568 “-doMajorMinor 3 -GL 1 -doMaf 1 -snp_pval 1e-6 -doGeno 4 -doPost 1 -postCutoff 0.99 -
569 remove_bads 1 -C 50 -minMapQ 25 -minQ 30 -uniqueOnly 1 -baq 1”. After variant calling the
570 genotypes in the ancient samples from the reference panel of variants, we compared the
571 proportion of missing variants to the level of coverage in each sample (Table S7). We found
572 that the level of coverage was approximately inversely proportional to missingness in our
573 ancient samples. The lowest rate of missing variants was 0.558 (55.8%) in a sample with 4.92X
574 coverage and the highest proportion of missing variants was 0.973 for the samples with the
575 lowest level of coverage (0.77X and 0.93X).

576 We applied a pre-imputation filter of “GP >=0.99” using BEAGLE (version 4.0) to our ancient
577 variant panel We then imputed the genotypes of our ancient individuals with BEAGLE (version
578 5.1), using only the filtered variants, the reference panel of modern donkeys and the
579 recombination map previously generated. We reapplied the filter “GP >=0.99” post-imputation
580 ($n=7,161,029$ variants (TI/TV=2.17), and $n=2,245,992$ variants (TI/TV=2.21) that were present
581 in all ancient individuals after post-imputation filtering). We then merged the variants from
582 ancient and modern individuals into a single file using the “merge” function in BCFtools.

583 To examine the accuracy of this method on the imputation of donkey genomes, we randomly
584 knocked out an increasing proportion of variants (0.2, 0.5, 0.5, 0.9, 0.92, 0.94, 0.96 and 0.99)
585 from ten modern individuals with the lowest rates of missing SNPs (pre-phasing and excluding
586 the donkey that was used for the reference genome). We then re-imputed the variants for these
587 individuals using the same imputation pipeline as outlined above. and after filtering, compared
588 them with the original variants for the same sample to measure the accuracy of imputing
589 samples with different rates of missingness (Fig. S8). Based on this imputation accuracy test,
590 we predicated that all samples have an overall imputation accuracy between 98.1% and 98.6%
591 (Fig. S8, Table S6).

592 After imputation, we projected the ancient, imputed samples onto the PCA with the non-
593 imputed, pseudo-haploidized data for the same ancient donkeys and the modern donkeys used
594 in the reference dataset (Fig. S7). We found that after imputation each ancient individual
595 clustered very similarly to the non-imputed data, albeit moving away from the 0,0-axis due to
596 more data being available (including heterozygous variants). This further provided an
597 indication that the imputation did not change the genetic makeup of the ancient samples relative
598 to the modern individuals, but helped gain resolution.

599 To test for the effects of post-mortem damage on the accuracy of imputation in ancient samples,
600 we genotyped alleles for the ancient donkey with the highest coverage (GVA348, 5.05X), using
601 ANGSD and conditioning on sites with a coverage of at least 8X (“setMinDepth 8”). We then
602 compared these genotyped alleles to the imputed variants and found that we recovered the same
603 alleles for 99.99% of sites (541,969 out of 541,981 sites), further providing evidence that our
604 method is highly accurate for imputing variants in samples with post-mortem damage.

605 Population genetic analysis using imputed variants

606 We performed an ADMIXTURE analysis conditioning on all modern equids and ancient
607 donkeys using imputed variants (Fig. S4). We first thinned all imputed autosomal variants in
608 PLINK using the parameters: “--indep-pairwise 50 10 0.2 --maf 0.05”, then calculated
609 admixture proportions for models with K values between 2 and 5 using ADMIXTURE ($n=253$

610 individuals and $n=494,050$ variants after filtering). An optimal K value of 4 was estimated by
611 comparing the cross-validation values of the different models.

612 PCA analysis showed that ancient donkeys clustered most closely with modern donkeys, and
613 also showed a similar genetic makeup on the ADMIXTURE analysis. However, an ancient
614 donkey from Israel (MV242; Nizzana, 350-58BCE) showed high amounts of ancestry from a
615 divergent wild outgroup. Bootstrapped ADMIXTURE (100 bootstrap pseudo-replicates) found
616 that MV242 contained 4.15 ± 0.19 % wild genetic material (Fig. 2C).

617 We conducted a haplotype-based clustering analysis of all modern and ancient domestic
618 donkeys using fineSTRUCTURE (version 4.1.1) (35). We converted the variants in the VCF
619 file and the recombination map present in all individuals ($n=2,245,992$) to the required input
620 file formats using custom R scripts and the provided perl scripts from the fineSTRUCTURE
621 package. We excluded 58 Chinese and Tibetan donkeys so as to avoid overrepresenting this
622 region. Additionally, we removed modern individuals that were identified in the previous
623 ADMIXTURE analysis as having a high proportion of wild admixture ($n=6$) and admixture
624 between different populations ($n=2$), which were found to confound the output, resulting in a
625 final dataset of 172 individuals. FineSTRUCTURE was run with default parameters to paint
626 the chromosomes and model haplotype sharing between individuals. The maximum likelihood
627 tree and co-ancestry matrix was plotted from the output files using modified versions of the R
628 scripts provided with the fineSTRUCTURE package (Fig. 2A, 2B, S9).

629 To estimate the genetic sharedness between each ancient individual with the modern
630 subpopulations, we calculated outgroup f3-statistics in the form of (modern, ancient; kiang)
631 using ADMIXTOOLS2 (58, 65), using only variants present in all individuals
632 ($n=2,245,992$). We used the mean and standard error from the outgroup f3-statistics to plot a
633 heatmap comparing relatedness between the ancient individuals to the modern populations
634 (Fig. 3B).

635 To further confirm the genetic makeup of our ancient individuals, as inferred by
636 fineSTRUCTURE analysis and outgroup f3-statistics, we constructed Treemix models using
637 the imputed matrix with variants present in all individuals, first pruning the matrix in PLINK
638 using the parameter "--indep-pairwise 50 10 0.2" ($n=175,093$ variants after filtering). In
639 accordance with earlier Treemix models (Fig. 1B), we removed modern donkeys with high
640 proportions of wild admixture or that were hybrids between different regions, and included
641 *E.a.som*, with the kiangs as an outgroup ($n=207$ modern individuals). We then grouped modern
642 donkeys according to the branches on Fig. 1B into HORN+KEN (ETH,KEN,SOM), WAFR
643 (GHA, MAU,NIG, SEN), SAPEN (OMA,YEM), CASIA (TKM,KYR,KAZ), EASIA
644 (CHI,TIB,MON), IRA (IRA), TTS (TUK, TUN, SYR), NUBIA (EGY,SUD), EEUR
645 (YUM,YUC), IRE (IRE,Eas), and WEUR (ESP,PTG,CYK,BRA). Ancient donkeys were
646 added to the Treemix model separately, grouped according to their archaeological site (Table
647 S2, Fig. S10). However, in two sites, fineSTRUCTURE analysis showed potentially different
648 genetic makeup in individuals from Yenikapi and Shahr-i-Qumis, so were modelled separately.
649 Each Treemix model was run for 0-10 migration events with 5 replicates and a k value of 1000.
650 The optimal migration edges were inferred using optM, and the 100 bootstraps were performed
651 using the BITE package as above (Fig. 2C, 2D, 2E 3C, 3D, 3E, S10).

652 A deletion in *TBX3* has been found to be responsible to the phenotypic change from a grey dun
653 coat to a coloured coat in donkeys (13). A single nucleotide deletion in the *TBX3* gene (CT>C-

654) results in derived coat colours in homozygous individuals, which has previously been
655 annotated to JADWZW010000009.1:42742556 on this version of the assembly (13). We
656 genotyped all ancient and modern individuals in our dataset. As a confirmation of the validity
657 of this genotyping, we found that all wild individuals were genotyped for the dun coat colour,
658 but the reference individual (a black donkey) was genotyped for a derived coat colour.

659 With a post-imputation filter of $GP \geq 0.99$, 19 out of 31 ancient donkeys were genotyped for
660 the *TBX3* locus. However, with a $GP \geq 0.9$, the *TBX3* genotype of 25 ancient individuals could
661 be inferred. Coat color phenotypes in ancient donkeys showed that derived coat colors were
662 present across multiple locations, ranging from western Asia (Iran, Shahr-i-Qumis) to Iberia
663 (Portugal, Albufeira) (Fig. 3A). Colored coats appeared almost simultaneously in our dataset
664 in samples from Shahr-i-Qumis and Boinville-en-Woëvre. However, one of our oldest samples
665 (Chalow3) was heterozygous, indicating that this variant was segregating in donkeys by at least
666 this time (~2050BCE). The presence of black donkeys have been recorded in Iraq (Assur) in
667 the 2nd millennium BCE, which further suggests that the mutation in the *TBX3* gene was present
668 in early donkey populations (128). Derived coat colors appeared at high frequencies in modern
669 domesticates out of Africa, indicating that selection in more modern times may have favored
670 derived coat colors in donkeys in some regions of the world (Fig. S11).

671 However, we found that variants underlying long hair and white spots were not present in our
672 phased variant panel for modern donkeys. Two recessive mutations in the *FGF5* gene have
673 been associated with long hair in donkeys (46). The missense mutation (G>A) was mapped to
674 JADWZW010000004.1:161390091 and a frameshift deletion (delAT) to
675 JADWZW010000004.1:161397694 on the reference genome used in this study. Additionally,
676 a dominant mutation associated with white spotting has been identified in splice donor site in
677 the *KIT* gene (T>A, JADWZW010000004.1:139925278) (45). Analysis of sequence
678 alignments of the 31 ancient donkeys did not find any individuals homozygous for either *FGF5*
679 mutation, although one individual was heterozygous for the missense mutation (AM89) (Table
680 S7), and another for the deletion (Tur179) (Table S8). This indicates that these mutations were
681 segregating in ancient donkeys, but likely reached higher frequency in some modern breeds at
682 later dates. None of the ancient donkeys carried the mutation associated with white spotting,
683 suggesting that this phenotype was not commonly found in the past (Table S9).

684 To gain insights into the breeding management of ancient donkeys, we estimated the level of
685 relatedness between ancient donkeys from the same site using KING (version 2.2.7) (66) on
686 the panel of imputed variants, conditioning on transversions that were common across all
687 individuals ($n=31$ individuals, $n=619,981$ transversions, Table S10). We found evidence of
688 close familial relatedness between 6 donkeys from Boinville-en-Woëvre. Two other donkeys
689 from this site had a high level of genetic relatedness, indicative of full siblings. Additionally,
690 the two donkeys from Tarquinia showed a 4th degree of genetic relatedness. No close genetic
691 relatedness was inferred between donkeys at any other site. However, ancient donkeys from
692 the same site may be from different generations, which could explain the lack of genetic
693 relatedness between them.

694 Errors in imputation may lead to over- or underestimates of relatedness between ancient
695 individuals. Therefore, we also estimated the relatedness between modern and ancient donkeys
696 using NgsRelate (version 2) (67). Variants were first called using ANGSD for all modern and
697 ancient donkeys ($n=238$) separately for each chromosome with the following parameters: “-

698 `baq 1 -doCounts 1 -C 50 -skipTriallelic 1 -doMajorMinor 1 -SNP_pval 1e-6 -doMaf 1 -`
699 `rmTriallelic 1e-4 - -minQ 30 -minMapQ 25 -uniqueOnly 1 -remove_bads 1 -doPost 1 -`
700 `beagleProb 1 -doGlf 2 -GL 2 -P 2 -MAF 0.05`", with sites covered in at least 75% of individuals.
701 Transitions were removed and the separate chromosome files were merged together, before
702 running NgsRelate ($n=473,263$ variants). High correlations between the KING coefficient
703 estimated using NgsRelate and the IBD coefficient estimated for the phased and imputed data
704 using the KING software ($r=0.871$, $r^2=0.759$) showed that accurate relationship inferences
705 could be inferred using imputed data (Fig. S12).

706 We estimated inbreeding as runs of homozygosity (ROH) for all modern and ancient donkeys
707 using three methods. First, using PLINK using the "--homozyg" function for all imputed
708 transversions ($n=238$ individuals, $n=1,949,850$ transversions), with a cut off length of at least
709 1 MB. Estimating runs of homozygosity requires dense haplotypes, however imputation errors
710 in the low-coverage ancient samples may lead to inaccurate calculations of inbreeding levels.
711 To account for imputation errors which may break up ROHs, we allowed for up to 4
712 heterozygous variants in each 50 SNP sliding window (Fig. S13A).

713 We examined the effects of imputation errors on ROH estimations using imputed variants in
714 PLINK by down-sampling and re-imputing 10 high coverage modern donkey genomes: 5 with
715 the highest ROH and 5 with the lowest total length of ROH (as estimated by PLINK). We found
716 little change in the total length of ROH when up to 96% of variants were knocked out and re-
717 imputed, which was the highest rate of missingness in our ancient samples (Fig. S14A). This
718 agrees with the estimations of high imputation accuracy in these samples and provides evidence
719 that ROHs can still be inferred using PLINK with a low rate of errors.

720 To further test the robustness of the imputed data in accurately estimating ROHs in our ancient
721 samples, we also estimated ROHs using the method implemented NgsF-HMM (version 1) (59)
722 on the unimputed data from all modern and ancient donkeys ($n=238$ individuals). We estimated
723 ROHs using NgsF-HMM, using the same files as generated for NgsRelate ($n=473,263$
724 variants), and using a minimum epsilon of $1e-8$. We then filtered the ROHs to only select those
725 with a total length over 1MB, containing more than 100 SNPs and with at least one SNP per
726 50KB on average, in line with the parameters defining an ROH in PLINK (Fig. 4A, Fig. 4B).

727 We also estimated ROHs from the bam files of the modern and ancient donkeys by searching
728 for regions with a low density of heterozygous variants. First, we down sampled the bam file
729 for each modern and ancient donkey to the lowest coverage sample in our dataset (0.77X) using
730 SAMtools. Next, we generated counts files using ANGSD with the parameters: "--doCounts 1
731 -dumpCounts 4", conditioning only on sites with a MAF ≥ 0.05 in modern donkeys. We then
732 filtered the sites for each individual for a depth greater than 2, then grouped the remaining sites
733 into bins of 200 SNPs. Bins with less than 6 heterozygous variants (a frequency of 0.03) were
734 considered to be a ROH. These parameters were optimised by comparing the size and
735 distribution of ROHs in high coverage modern individuals to those estimated in PLINK. We
736 then summed the length of all ROH bins together to obtain the total proportion of the genome
737 in ROH for each individual (Fig. S13B). We then compared the total ROH in the genome of
738 each individual to that estimated by PLINK and ngsF-HMM. The three methods showed high
739 correlation, indicating that the estimates were robust to imputation or phasing errors (Fig. S14).

740 We plotted the total length of ROH in the genome of each donkey as a function of time for
741 each of the three methods (Fig. 5B, Fig. S13), separating the modern donkeys by continent and

742 grouping the ancient donkeys by site and inferring their age through radiocarbon dates where
743 available or the archaeological context of the sample. Visually, little change was seen in the
744 overall proportion of ROH in the genomes of modern versus ancient donkeys. A Wilcoxon
745 rank sum test using the NgsF-HMM output confirmed that there was no significant difference
746 in the total length of ROH between the two groups ($W=2904$ p -value=0.395, $n=238$) (Fig. 5A).
747 In line with their close familial relationships, a Wilcoxon rank sum test determined that the five
748 donkeys from Boinville-en-Woëvre had significantly higher proportions of their genomes in
749 ROH compared to the other ancient individuals (Wilcoxon rank sum test, $W = 139$, p -value =
750 0.045, $n=31$).

751 Next, we estimated ROH from publicly available whole genome sequences of 75 ancient and
752 79 modern horses, using NgsF-HMM with the same method as for donkeys (Table S11, Fig.
753 4C, 4D, $n=963,418$ transversions). A Wilcoxon rank sum test confirmed that modern horses
754 were more significantly inbred than ancients ($W= 4541$, p -value>0.001, $n=154$), in contrast to
755 donkeys (Fig. 5C). The total ROH for each horse was plotted as a function of time, as for
756 donkeys (Fig. 5D).

757 Pseudo-haploidized matrix

758 Variation in ancient individuals that is not represented in modern populations may affect the
759 accuracy of population models conditioning on modern variation only. To confirm the accuracy
760 of our analyses using imputed ancient genomes that were conditioned on modern variation, we
761 constructed a pseudo-haploidized matrix for the ancient and modern individuals included in
762 the Treemix analysis, following the procedure from Gaunitz and colleagues (2018) and Librado
763 and colleagues (2021) (21, 50). Variants were called in ANGSD with the parameters: “-minQ
764 20 -minMapQ 25 -remove_bads 1 =uniqueOnly 1 -baq 1 -C 50 -doHaploCall 1”, conditioning
765 only on transversions ($n=4,833,570$ transversions). We used this matrix for Treemix analyses
766 using the same method as above, LD pruning the variants ($n=496,697$ after pruning). We added
767 ancient donkeys from each site to the Treemix models separately, then estimating the optimal
768 number of migration edges and performed 100 bootstrap pseudo-replicates for each model. We
769 found that placement on ancient donkeys on the Treemix models constructed using imputed
770 and pseudo-haploidized data was highly similar, confirming the accuracy of our imputation
771 panel (Fig. S10). Next, we constructed a neighbour joining tree to further confirm the
772 population structure of the modern and ancient donkeys. We first calculated pairwise genetic
773 distances between all samples using PLINK, then retrieved the tree topology by implementing
774 the bioNJ algorithm in FastME (version 2.1.4)(129), with 100 bootstrap pseudo-replicates to
775 assess node supports (Fig. S15).

776 The genome of MV242 was found to contain divergent genetic material, as confirmed by
777 ADMIXTURE analysis and Treemix phylogenies using imputed data (Fig. 2E, 3A, S4, S10,
778 S15). However, because there may be errors in the imputed haplotypes of this individual due
779 to the divergent genetic makeup, we used pseudo-haploidized data for further analysis. We
780 modelled $f_4(E.a.som, MV242; HORN+KEN, x)$ statistics to determine whether genetic
781 material from this lineage was present in modern donkey subpopulations (x) using qpDstat
782 (version 751) from the Admixtools package (58, 65). We grouped modern donkeys into the
783 same subpopulations used on the Treemix models (Fig. S10). P -values were obtained through
784 multiple test correction of Z -scores with a significance threshold of 0.05. Positive and

785 significant f4-statistics provided evidence of MV242 ancestry in modern donkeys from eastern
786 Asia, Nubia, central Asia, Turkey, Syria, Tunisia, Iran and western Europe (Fig. 5E).

787 Next, we tested for the presence of genetic material in the ancient donkeys with $f_4(E.a.som,$
788 $MV242; Fiumarella1, x)$ statistics, where x are the ancient donkeys grouped by site according
789 to the Treemix models (Fig. S10). An excess of sharedness with the MV242 lineage was found
790 in the individual Chalow3 as the f_4 -statistics were positive and significant (Fig. 5F). However,
791 significantly negative f_4 -statistics showed a deficit in sharedness in a family group of 6
792 donkeys from Boinville-en-Woëvre (GVA125, GVA347, GVA348, GVA349, GVA353,
793 GVA354) (Fig. 5G), which showed evidence of wild genetic material in ADMIXTURE
794 analysis (Fig. 3A). To determine whether this wild genetic material is derived from a source
795 more divergent than MV242 we tested $f_4(kiang, MV242; Fiumarella1, x)$ statistics, where x
796 are the three family groups from Boinville-en-Woëvre. This statistic was negative and
797 significant for family group GVA1 only, which supports restocking in this population from a
798 lineage more divergent than MV242. The $f_4(kiang, E.a.som; Fiumarella1, x)$ statistics, for the
799 family groups at Boinville-en-Woëvre were balanced, which suggests that this wild genetic
800 material is not from a population more divergent than *E.a.som* (Fig. 5H).

801 Uniparental markers

802 To construct the mitochondrial phylogeny, we called variants with “-doHaploCall 1 -minMapQ
803 25 -minQ 30 -doDepth 5” using ANGSD. Additionally, we included the mitochondrial
804 genomes of three *Equus hemionus hemippus* (accession numbers: ERS7669491, ERS7669492,
805 ERS7669493) (20) ($n=2,805$ variants, $n=256$ individuals). We generated a tree with IQ-TREE
806 (version 1.6.12) (60), using 100 bootstrap pseudo-replicates for assessing node support (Fig.
807 5A). The tree was rooted between the zebras and hemiones+ kiangs, as per Jónsson and
808 colleagues (24).

809 To construct the Y-chromosome phylogeny, we called variants using ANGSD with the
810 parameters: “-isHap 1 -baq 1 -remove_bads 1 -uniqueOnly 1 -minMapQ 25 -minQ 30 -
811 -rmTriallelic 1e-4-SNP_pval 1e-6 -C 50” for all male equids in our dataset ($n=125$),
812 conditioning on transversions only and including only variants present in more than 90% of
813 individuals, leaving a total of 3,171 variants in the final dataset. We generated a tree with IQ-
814 TREE (version 1.6.12) (60), using the same parameters as those used to generate the
815 mitochondrial tree (Fig. 5B).

816 To estimate the time to the most recent common ancestor (TMRCA), we constructed Bayesian
817 skyline plots using mitochondrial and Y-chromosome variation of domestic donkeys only
818 ($n=238$ and 121 individuals, respectively) using BEAST (version 2.6.5) (68-70). We estimated
819 the optimal substitution model for both datasets using the BIC scores estimated from IQ-TREE.
820 we converted the multi-alignment fasta files to BEAST input files using BEAUTi (version
821 2.5.26) (68-70) specifying the following parameters: 1) the optimal model for all three datasets
822 was GTR, with an empirical distribution and a gamma category count of 4. 2) Tips of the
823 ancient individuals were dating in years before present using radiocarbon dates, where
824 available, or the mean of the time period estimated from archaeological context. For ancient
825 donkeys from Shahr-i-Qumis, their age was inferred from the single individual radiocarbon
826 dated at this site (AM805). 3) Selecting the Bayesian skyline demographic model and
827 uncorrelated log-Normal relaxed molecular clocks with mean values= [1e-07] per site per year
828 [sampling from a uniform prior between 1e-08 and 1e-05]. BEAST (version 2.5.1) (68-70) was

829 run for a total of 500,000,000 iterations for Y-chromosomal and 350,000,000 for mitochondrial
830 reconstructions. The posterior distributions of the tree heights were generated using Tracer
831 (version 1.7.1) (130) with 20% as burn-in (Fig. 4B, D).

832

833 **Table S1:** Sample information for all modern donkeys and wild equids ($n=222$). The country
834 of origin, short country code, genome depth-of-coverage, the proportion of missing variants
835 after variant calling and accession number are reported. Accessions numbers starting with
836 “SRS” were downloaded from the National Library of Medicine, “ERS” from the European
837 Nucleotide Archive, and those starting with “SAMC” from the Genome Sequence Archive
838 database.

| ID | Species | coverage | Proportion missing variants | sex | Country | short country code | Accession |
|-------------------------|---------------------|----------|-----------------------------|-----|---------------|--------------------|-------------|
| ALG_01 | <i>Equus asinus</i> | 25.378 | 0.008 | M | Algeria | ALG | ERS12239254 |
| IRE_EnglishWpureIrish_1 | <i>Equus asinus</i> | 10.369 | 0.271 | F | Ireland | IRE | SRS3167383 |
| IRE_EnglishWpureIrish_2 | <i>Equus asinus</i> | 9.086 | 0.35 | F | Ireland | IRE | SRS3167384 |
| IRE_pureIrish_3 | <i>Equus asinus</i> | 8.589 | 0.377 | F | Ireland | IRE | SRS3167387 |
| IRE_pureIrish_4 | <i>Equus asinus</i> | 8.33 | 0.402 | F | Ireland | IRE | SRS3167408 |
| IRE_pureIrish_5 | <i>Equus asinus</i> | 9.339 | 0.344 | F | Ireland | IRE | SRS3167409 |
| IRE_pureIrish_6 | <i>Equus asinus</i> | 10.265 | 0.28 | F | Ireland | IRE | SRS3167406 |
| IRE_pureIrish_7 | <i>Equus asinus</i> | 9.055 | 0.367 | F | Ireland | IRE | SRS3167407 |
| IRE_pureIrish_8 | <i>Equus asinus</i> | 9.021 | 0.369 | M | Ireland | IRE | SRS3167410 |
| Aw_1 | Asiatic wild ass | 11.057 | 0.178 | M | NA | AW | SRS3167373 |
| Aw_2 | Asiatic wild ass | 11.464 | 0.163 | F | NA | AW | SRS3167374 |
| CHI_dz | <i>Equus asinus</i> | 150.067 | 0.003 | F | China (plain) | CHI | SRS7835299 |
| CHI_Guangling_3 | <i>Equus asinus</i> | 9.817 | 0.28 | M | China (plain) | CHI | SRS3167352 |
| CHI_Guangling_4 | <i>Equus asinus</i> | 10.497 | 0.23 | F | China (plain) | CHI | SRS3167350 |
| CHI_HetianGray_1 | <i>Equus asinus</i> | 10.168 | 0.253 | M | China (plain) | CHI | SRS3167356 |
| CHI_HetianGray_2 | <i>Equus asinus</i> | 9.831 | 0.274 | F | China (plain) | CHI | SRS3167354 |
| CHI_HetianGray_3 | <i>Equus asinus</i> | 9.527 | 0.292 | F | China (plain) | CHI | SRS3167361 |
| CHI_HetianGray_4 | <i>Equus asinus</i> | 9.993 | 0.253 | F | China (plain) | CHI | SRS3167381 |
| CHI_BY02A | <i>Equus asinus</i> | 13.477 | 0.105 | F | China (plain) | CHI | SRS3167450 |
| CHI_BY03A | <i>Equus asinus</i> | 11.341 | 0.176 | F | China (plain) | CHI | SRS3167463 |
| CHI_BY06A | <i>Equus asinus</i> | 12.584 | 0.11 | M | China (plain) | CHI | SRS3167461 |
| CHI_BY07A | <i>Equus asinus</i> | 10.626 | 0.211 | M | China (plain) | CHI | SRS3167462 |
| CHI_GL03A | <i>Equus asinus</i> | 11.589 | 0.152 | F | China (plain) | CHI | SRS3167460 |
| CHI_GL04A | <i>Equus asinus</i> | 12.789 | 0.119 | F | China (plain) | CHI | SRS3167357 |
| CHI_HL06 | <i>Equus asinus</i> | 5.968 | 0.641 | F | China (plain) | CHI | SAMC048978 |
| CHI_HL28 | <i>Equus asinus</i> | 6.461 | 0.571 | M | China (plain) | CHI | SAMC048979 |
| CHI_HL29 | <i>Equus asinus</i> | 6.229 | 0.597 | M | China (plain) | CHI | SAMC048980 |
| CHI_JM01A | <i>Equus asinus</i> | 11.482 | 0.152 | F | China (plain) | CHI | SRS3167380 |
| CHI_JM05A | <i>Equus asinus</i> | 10.701 | 0.183 | M | China (plain) | CHI | SRS3167379 |
| CHI_JM06A | <i>Equus asinus</i> | 11.65 | 0.149 | F | China (plain) | CHI | SRS3167378 |
| CHI_JM07A | <i>Equus asinus</i> | 11.037 | 0.174 | M | China (plain) | CHI | SRS3167377 |
| CHI_JM11A | <i>Equus asinus</i> | 10.004 | 0.24 | M | China (plain) | CHI | SRS3167392 |
| CHI_KL02A | <i>Equus asinus</i> | 10.818 | 0.192 | F | China (plain) | CHI | SRS3167391 |
| CHI_KL03A | <i>Equus asinus</i> | 13.283 | 0.105 | F | China (plain) | CHI | SRS3167389 |

| | | | | | | | |
|----------------|------------------------|--------|-------|---|---------------|------|-------------|
| CHI_KL04A | <i>Equus asinus</i> | 11.804 | 0.147 | F | China (plain) | CHI | SRS3167390 |
| CHI_KL05A | <i>Equus asinus</i> | 9.689 | 0.266 | F | China (plain) | CHI | SRS3167388 |
| CHI_XJ1 | <i>Equus asinus</i> | 5.939 | 0.635 | F | China (plain) | CHI | SAMC049000 |
| CHI_XJ2 | <i>Equus asinus</i> | 5.798 | 0.65 | F | China (plain) | CHI | SAMC049001 |
| CHI_XJ3 | <i>Equus asinus</i> | 5.891 | 0.641 | F | China (plain) | CHI | SAMC049002 |
| CHI_XJ5 | <i>Equus asinus</i> | 7.545 | 0.476 | F | China (plain) | CHI | SAMC049003 |
| CHI_XJ6 | <i>Equus asinus</i> | 6.481 | 0.576 | F | China (plain) | CHI | SAMC049004 |
| CHI_YM01 | <i>Equus asinus</i> | 6.365 | 0.591 | M | China (plain) | CHI | SAMC049023 |
| CHI_YM04 | <i>Equus asinus</i> | 6.346 | 0.588 | M | China (plain) | CHI | SAMC049024 |
| CHI_YM05 | <i>Equus asinus</i> | 5.749 | 0.655 | F | China (plain) | CHI | SAMC049025 |
| CHI_YM12 | <i>Equus asinus</i> | 5.585 | 0.676 | F | China (plain) | CHI | SAMC049026 |
| CHI_Qingyang_1 | <i>Equus asinus</i> | 10.453 | 0.228 | M | China (plain) | CHI | SRS3167413 |
| CHI_Qingyang_2 | <i>Equus asinus</i> | 10.786 | 0.224 | F | China (plain) | CHI | SRS3167414 |
| CHI_Qingyang_3 | <i>Equus asinus</i> | 10.631 | 0.239 | M | China (plain) | CHI | SRS3167415 |
| CHI_Qingyang_4 | <i>Equus asinus</i> | 10.647 | 0.251 | M | China (plain) | CHI | SRS3167411 |
| CHI_Turfan_1 | <i>Equus asinus</i> | 10.508 | 0.246 | F | China (plain) | CHI | SRS3167412 |
| CHI_Turfan_2 | <i>Equus asinus</i> | 8.709 | 0.386 | F | China (plain) | CHI | SRS3167424 |
| CHI_Turfan_3 | <i>Equus asinus</i> | 7.963 | 0.421 | M | China (plain) | CHI | SRS3167423 |
| CHI_Turfan_4 | <i>Equus asinus</i> | 8.699 | 0.367 | F | China (plain) | CHI | SRS3167422 |
| CHI_Turfan_5 | <i>Equus asinus</i> | 7.969 | 0.441 | F | China (plain) | CHI | SRS3167421 |
| CHI_Xinjiang_1 | <i>Equus asinus</i> | 11.005 | 0.215 | F | China (plain) | CHI | SRS3167454 |
| CHI_Xinjiang_2 | <i>Equus asinus</i> | 9.063 | 0.336 | M | China (plain) | CHI | SRS3167473 |
| CHI_Xinjiang_3 | <i>Equus asinus</i> | 9.652 | 0.285 | M | China (plain) | CHI | SRS3167474 |
| CHI_Xinjiang_4 | <i>Equus asinus</i> | 8.417 | 0.393 | M | China (plain) | CHI | SRS3167475 |
| CHI_Xinjiang_5 | <i>Equus asinus</i> | 9.763 | 0.3 | F | China (plain) | CHI | SRS3167470 |
| CHI_Yunnan_1 | <i>Equus asinus</i> | 10.606 | 0.247 | M | China (plain) | CHI | SRS3167371 |
| CHI_Yunnan_2 | <i>Equus asinus</i> | 10.24 | 0.271 | F | China (plain) | CHI | SRS3167369 |
| CHI_Yunnan_3 | <i>Equus asinus</i> | 10.891 | 0.212 | M | China (plain) | CHI | SRS3167370 |
| Easi_Willy2 | <i>Equus asinus</i> | 28.839 | 0.025 | M | Denmark | Eas | SRS431817 |
| Eboe_0227A | <i>Equus burchelli</i> | 22.537 | 0.142 | F | NA | Eboe | ERS559290 |
| EGY_1 | <i>Equus asinus</i> | 11.642 | 0.166 | F | Egypt | EGY | SRS3167452 |
| EGY_2 | <i>Equus asinus</i> | 10.872 | 0.225 | F | Egypt | EGY | SRS3167456 |
| EGY_3 | <i>Equus asinus</i> | 10.963 | 0.221 | M | Egypt | EGY | SRS3167455 |
| EGY_4 | <i>Equus asinus</i> | 7.997 | 0.436 | M | Egypt | EGY | SRS3167382 |
| EGY_5 | <i>Equus asinus</i> | 7.275 | 0.506 | F | Egypt | EGY | SRS3167358 |
| Egre_0228A | <i>Equus grevyi</i> | 18.65 | 0.126 | F | NA | Egre | SRS1208552 |
| EGY_155 | <i>Equus asinus</i> | 14.498 | 0.136 | M | Egypt | EGY | SRS3167349 |
| EGY_161 | <i>Equus asinus</i> | 8.868 | 0.39 | M | Egypt | EGY | SRS3167353 |
| EGY_169 | <i>Equus asinus</i> | 8.949 | 0.368 | M | Egypt | EGY | SRS3167359 |
| EGY_02 | <i>Equus asinus</i> | 27.085 | 0.007 | M | Egypt | EGY | ERS12239300 |
| EGY_14 | <i>Equus asinus</i> | 35.048 | 0.004 | F | Egypt | EGY | ERS12239301 |
| EGY_17 | <i>Equus asinus</i> | 29.792 | 0.005 | M | Egypt | EGY | ERS12239302 |

| | | | | | | | |
|-------------|------------------------------------|--------|-------|---|------------|------|-------------|
| Ehar_0229A | <i>Equus hartmannae</i> | 19.301 | 0.144 | F | NA | Ehar | SRS861660 |
| Eki_0231A | <i>Equus kiang</i> | 14.887 | 0.125 | F | NA | Eki | SRS861663 |
| Ekiang_XZYL | <i>Equus kiang</i> | 7.79 | 0.587 | F | NA | Eki | SAMC049022 |
| Ekiang_YP21 | <i>Equus kiang</i> | 6.723 | 0.679 | F | NA | Eki | SAMC049027 |
| Ekiang_ZYL | <i>Equus kiang</i> | 6.649 | 0.667 | F | NA | Eki | SAMC049051 |
| Ekiang_kun1 | <i>Equus kiang</i> | 5.825 | 0.636 | M | NA | Eki | SAMC048991 |
| Ekiang_kun2 | <i>Equus kiang</i> | 6.132 | 0.592 | F | NA | Eki | SAMC048992 |
| Eona_0230A | <i>Equus hemionus</i> | 21.498 | 0.102 | M | NA | Eon | SRS474403 |
| Eona_0261A | <i>Equus hemionus</i> | 9.497 | 0.29 | F | NA | Eon | SRS693024 |
| Esom_0226A | <i>Equus africanus somaliensis</i> | 25.869 | 0.087 | F | NA | Esom | SRS861674 |
| ETH_1 | <i>Equus asinus</i> | 9.15 | 0.291 | M | Ethiopia | ETH | SRS3167398 |
| ETH_10 | <i>Equus asinus</i> | 8.783 | 0.352 | M | Ethiopia | ETH | SRS3167432 |
| ETH_2 | <i>Equus asinus</i> | 8.508 | 0.388 | M | Ethiopia | ETH | SRS3167445 |
| ETH_3 | <i>Equus asinus</i> | 8.565 | 0.379 | M | Ethiopia | ETH | SRS3167444 |
| ETH_4 | <i>Equus asinus</i> | 9.482 | 0.289 | M | Ethiopia | ETH | SRS3167442 |
| ETH_5 | <i>Equus asinus</i> | 8.008 | 0.478 | M | Ethiopia | ETH | SRS3167443 |
| ETH_6 | <i>Equus asinus</i> | 8.088 | 0.41 | M | Ethiopia | ETH | SRS3167430 |
| ETH_7 | <i>Equus asinus</i> | 8.006 | 0.426 | F | Ethiopia | ETH | SRS3167433 |
| ETH_8 | <i>Equus asinus</i> | 9.409 | 0.29 | F | Ethiopia | ETH | SRS3167428 |
| ETH_9 | <i>Equus asinus</i> | 8.617 | 0.362 | M | Ethiopia | ETH | SRS3167431 |
| ETH_14B | <i>Equus asinus</i> | 32.065 | 0.005 | M | Ethiopia | ETH | ERS12239255 |
| ETH_5B | <i>Equus asinus</i> | 35.773 | 0.051 | M | Ethiopia | ETH | ERS12239256 |
| ETH_6B | <i>Equus asinus</i> | 28.247 | 0.037 | M | Ethiopia | ETH | ERS12239257 |
| GHA_01 | <i>Equus asinus</i> | 20.988 | 0.014 | M | Ghana | GHA | ERS12239258 |
| GHA_07 | <i>Equus asinus</i> | 29.092 | 0.005 | F | Ghana | GHA | ERS12239259 |
| IRA_D2 | <i>Equus asinus</i> | 10.35 | 0.423 | F | Iran | IRA | SAMC048970 |
| IRA_D7 | <i>Equus asinus</i> | 6.842 | 0.572 | M | Iran | IRA | SAMC048971 |
| IRA_D9 | <i>Equus asinus</i> | 7.274 | 0.546 | M | Iran | IRA | SAMC048972 |
| IRA_D10 | <i>Equus asinus</i> | 10.796 | 0.338 | M | Iran | IRA | SAMC048965 |
| IRA_D11 | <i>Equus asinus</i> | 6.628 | 0.613 | M | Iran | IRA | SAMC048966 |
| IRA_D13 | <i>Equus asinus</i> | 9.359 | 0.46 | F | Iran | IRA | SAMC048967 |
| IRA_D14 | <i>Equus asinus</i> | 12.299 | 0.267 | M | Iran | IRA | SAMC048968 |
| IRA_D16 | <i>Equus asinus</i> | 10.518 | 0.332 | F | Iran | IRA | SAMC048969 |
| KAZ_04 | <i>Equus asinus</i> | 27.202 | 0.006 | F | Kazakhstan | KAZ | ERS12239260 |
| KAZ_07 | <i>Equus asinus</i> | 29.988 | 0.005 | F | Kazakhstan | KAZ | ERS12239261 |
| KEN_YPO86 | <i>Equus asinus</i> | 12.269 | 0.262 | M | Kenya | KEN | SAMC049038 |
| KEN_YPO97 | <i>Equus asinus</i> | 10.148 | 0.452 | F | Kenya | KEN | SAMC049048 |
| KEN_YPO98 | <i>Equus asinus</i> | 8.334 | 0.491 | M | Kenya | KEN | SAMC049049 |
| KEN_YPO101 | <i>Equus asinus</i> | 7.208 | 0.6 | M | Kenya | KEN | SAMC049028 |
| KEN_YPO102 | <i>Equus asinus</i> | 8.117 | 0.544 | M | Kenya | KEN | SAMC049029 |

| | | | | | | | |
|-------------|---------------------|--------|-------|---|--------------|------|-------------|
| KEN_YPO104 | <i>Equus asinus</i> | 8.768 | 0.391 | F | Kenya | KEN | SAMC049030 |
| KEN_YPO106 | <i>Equus asinus</i> | 11.438 | 0.261 | M | Kenya | KEN | SAMC049031 |
| KEN_YPO89 | <i>Equus asinus</i> | 12.803 | 0.231 | M | Kenya | KEN | SAMC049041 |
| KEN_YPO99 | <i>Equus asinus</i> | 8.575 | 0.494 | M | Kenya | KEN | SAMC049050 |
| KEN_YPO87 | <i>Equus asinus</i> | 9.529 | 0.353 | M | Kenya | KEN | SAMC049039 |
| KEN_YPO88 | <i>Equus asinus</i> | 10.558 | 0.353 | M | Kenya | KEN | SAMC049040 |
| KEN_YPO90 | <i>Equus asinus</i> | 12.444 | 0.275 | F | Kenya | KEN | SAMC049042 |
| KEN_YPO91 | <i>Equus asinus</i> | 11.092 | 0.335 | M | Kenya | KEN | SAMC049043 |
| KEN_YPO92 | <i>Equus asinus</i> | 11.048 | 0.36 | M | Kenya | KEN | SAMC049044 |
| KEN_YPO93 | <i>Equus asinus</i> | 12.105 | 0.191 | M | Kenya | KEN | SAMC049045 |
| KEN_YPO95 | <i>Equus asinus</i> | 10.662 | 0.34 | M | Kenya | KEN | SAMC049046 |
| KEN_YPO96 | <i>Equus asinus</i> | 12.505 | 0.27 | M | Kenya | KEN | SAMC049047 |
| Kia_1 | <i>Equus asinus</i> | 27.447 | 0.067 | F | NA | Eki | SRS3167376 |
| KYR_Sdonk3 | <i>Equus asinus</i> | 8.328 | 0.478 | F | Kyrgyzstan | KYR | SAMC048996 |
| KYR_Sdonk6 | <i>Equus asinus</i> | 29.255 | 0.487 | F | Kyrgyzstan | KYR | SAMC048997 |
| KYR_Sdonk7 | <i>Equus asinus</i> | 8.071 | 0.585 | M | Kyrgyzstan | KYR | SAMC048998 |
| KYR_Sdonk9 | <i>Equus asinus</i> | 6.826 | 0.28 | F | Kyrgyzstan | KYR | SAMC048999 |
| KYR_Sdonk12 | <i>Equus asinus</i> | 5.903 | 0.006 | M | Kyrgyzstan | KYR | SAMC048993 |
| KYR_16 | <i>Equus asinus</i> | 9.971 | 0.406 | F | Kyrgyzstan | KYR | ERS12239262 |
| KYR_31 | <i>Equus asinus</i> | 9.053 | 0.346 | F | Kyrgyzstan | KYR | ERS12239263 |
| KYR_Sdonk1 | <i>Equus asinus</i> | 29.519 | 0.524 | M | Kyrgyzstan | KYR | SAMC048994 |
| KYR_Sdonk2 | <i>Equus asinus</i> | 9.799 | 0.007 | M | Kyrgyzstan | KYR | SAMC048995 |
| MAU_2990 | <i>Equus asinus</i> | 23.125 | 0.009 | F | Mauritania | MAU | ERS12239299 |
| MAU_3094 | <i>Equus asinus</i> | 24.434 | 0.007 | F | Mauritania | MAU | ERS12239298 |
| MAU_3261 | <i>Equus asinus</i> | 27.093 | 0.006 | F | Mauritania | MAU | ERS12239297 |
| MON_08 | <i>Equus asinus</i> | 28.569 | 0.005 | F | Mongolia | MON | ERS12239264 |
| MON_10 | <i>Equus asinus</i> | 27.899 | 0.006 | F | Mongolia | MON | ERS12239265 |
| NIG_YPO62 | <i>Equus asinus</i> | 10.673 | 0.389 | M | Nigeria | NIG | SAMC049032 |
| NIG_YPO63 | <i>Equus asinus</i> | 11.36 | 0.327 | F | Nigeria | NIG | SAMC049033 |
| NIG_YPO64 | <i>Equus asinus</i> | 8.866 | 0.458 | M | Nigeria | NIG | SAMC049034 |
| NIG_YPO65 | <i>Equus asinus</i> | 10.422 | 0.318 | M | Nigeria | NIG | SAMC049035 |
| NIG_YPO66 | <i>Equus asinus</i> | 10.574 | 0.349 | F | Nigeria | NIG | SAMC049036 |
| NIG_YPO67 | <i>Equus asinus</i> | 14.534 | 0.224 | M | Nigeria | NIG | SAMC049037 |
| OMA_38 | <i>Equus asinus</i> | 28.817 | 0.005 | F | Oman | OMA | ERS12239266 |
| OMA_39 | <i>Equus asinus</i> | 25.459 | 0.022 | M | Oman | OMA | ERS12239267 |
| OMA_46 | <i>Equus asinus</i> | 28.281 | 0.005 | F | Oman | OMA | ERS12239268 |
| PTGm_02 | <i>Equus asinus</i> | 32.589 | 0.004 | F | Portugal | PTGM | ERS12239269 |
| PTGm_10 | <i>Equus asinus</i> | 23.579 | 0.008 | F | Portugal | PTGM | ERS12239270 |
| SAU_11 | <i>Equus asinus</i> | 28.634 | 0.007 | M | Saudi Arabia | SAU | ERS12239271 |
| SEN_10 | <i>Equus asinus</i> | 28.175 | 0.005 | F | Senegal | SEN | ERS12239272 |
| SOM_01 | <i>Equus asinus</i> | 29.409 | 0.045 | F | Somalia | SOM | ERS12239273 |
| SOM_05 | <i>Equus asinus</i> | 31.333 | 0.028 | F | Somalia | SOM | ERS12239274 |

| | | | | | | | |
|-----------------------|---------------------|--------|-------|---|----------------|-----|-------------|
| SOM_19 | <i>Equus asinus</i> | 31.999 | 0.005 | F | Somalia | SOM | ERS12239275 |
| SOM_20 | <i>Equus asinus</i> | 34.065 | 0.004 | F | Somalia | SOM | ERS12239276 |
| SOM_21 | <i>Equus asinus</i> | 36.165 | 0.004 | F | Somalia | SOM | ERS12239277 |
| ESP_Andalusian_1 | <i>Equus asinus</i> | 9.683 | 0.36 | M | Spain | ESP | SRS3167402 |
| ESP_Basque_10 | <i>Equus asinus</i> | 11.632 | 0.186 | F | Spain | ESP | SRS3167401 |
| ESP_Basque_11 | <i>Equus asinus</i> | 9.909 | 0.267 | F | Spain | ESP | SRS3167400 |
| ESP_Basque_12 | <i>Equus asinus</i> | 10.066 | 0.268 | M | Spain | ESP | SRS3167399 |
| ESP_Basque_13 | <i>Equus asinus</i> | 9.553 | 0.304 | F | Spain | ESP | SRS3167404 |
| ESP_ZamoranoLeones_14 | <i>Equus asinus</i> | 10.128 | 0.282 | F | Spain | ESP | SRS3167403 |
| ESP_ZamoranoLeones_15 | <i>Equus asinus</i> | 12.438 | 0.192 | F | Spain | ESP | SRS3167405 |
| ESP_ZamoranoLeones_16 | <i>Equus asinus</i> | 11.581 | 0.232 | F | Spain | ESP | SRS3167385 |
| ESP_ZamoranoLeones_17 | <i>Equus asinus</i> | 11.841 | 0.187 | F | Spain | ESP | SRS3167386 |
| ESP_Baleares_18 | <i>Equus asinus</i> | 9.217 | 0.457 | F | Spain | ESP | SRS3167372 |
| ESP_Andalusian_2 | <i>Equus asinus</i> | 11.462 | 0.215 | F | Spain | ESP | SRS3167368 |
| ESP_Andalusian_3 | <i>Equus asinus</i> | 9.061 | 0.455 | F | Spain | ESP | SRS3167367 |
| CYK_IslasCanarias_4 | <i>Equus asinus</i> | 10.154 | 0.248 | M | Canary Islands | CYK | SRS3167465 |
| CYK_IslasCanarias_5 | <i>Equus asinus</i> | 12.988 | 0.15 | M | Canary Islands | CYK | SRS3167464 |
| CYK_IslasCanarias_6 | <i>Equus asinus</i> | 9.165 | 0.353 | F | Canary Islands | CYK | SRS3167472 |
| CYK_IslasCanarias_7 | <i>Equus asinus</i> | 11.042 | 0.203 | M | Canary Islands | CYK | SRS3167441 |
| CYK_IslasCanarias_8 | <i>Equus asinus</i> | 9.904 | 0.273 | M | Canary Islands | CYK | SRS3167469 |
| CYK_IslasCanarias_9 | <i>Equus asinus</i> | 9.155 | 0.332 | M | Canary Islands | CYK | SRS3167471 |
| SUD_20 | <i>Equus asinus</i> | 25.12 | 0.007 | F | Sudan | SUD | ERS12239278 |
| SUD_49 | <i>Equus asinus</i> | 30.011 | 0.005 | M | Sudan | SUD | ERS12239279 |
| SUD_55 | <i>Equus asinus</i> | 31.734 | 0.004 | M | Sudan | SUD | ERS12239280 |
| SYR_06 | <i>Equus asinus</i> | 32.131 | 0.005 | F | Syria | SYR | ERS12239281 |
| SYR_19 | <i>Equus asinus</i> | 32.954 | 0.004 | F | Syria | SYR | ERS12239282 |
| TIB_DQFS2 | <i>Equus asinus</i> | 9.408 | 0.4 | F | Tibet | TIB | SAMC048957 |
| TIB_XZCD05 | <i>Equus asinus</i> | 8.972 | 0.382 | F | Tibet | TIB | SAMC048958 |
| TIB_XZCM09 | <i>Equus asinus</i> | 8.816 | 0.399 | M | Tibet | TIB | SAMC048959 |
| TIB_XZCM18 | <i>Equus asinus</i> | 10.206 | 0.285 | M | Tibet | TIB | SAMC048960 |
| TIB_DQFS1 | <i>Equus asinus</i> | 6.518 | 0.578 | F | Tibet | TIB | SAMC048973 |
| TIB_DQFS4 | <i>Equus asinus</i> | 6.837 | 0.537 | F | Tibet | TIB | SAMC048974 |
| TIB_DQFS6 | <i>Equus asinus</i> | 6.658 | 0.555 | F | Tibet | TIB | SAMC048975 |
| TIB_XZCD01 | <i>Equus asinus</i> | 7.04 | 0.526 | F | Tibet | TIB | SAMC049005 |
| TIB_XZCD02 | <i>Equus asinus</i> | 5.867 | 0.64 | M | Tibet | TIB | SAMC049006 |
| TIB_XZCD06 | <i>Equus asinus</i> | 5.985 | 0.63 | F | Tibet | TIB | SAMC049007 |
| TIB_XZCM01 | <i>Equus asinus</i> | 6.331 | 0.588 | F | Tibet | TIB | SAMC049008 |
| TIB_XZCM02 | <i>Equus asinus</i> | 5.934 | 0.627 | M | Tibet | TIB | SAMC049009 |
| TIB_XZCM05 | <i>Equus asinus</i> | 5.968 | 0.623 | M | Tibet | TIB | SAMC049010 |
| TIB_XZCM06 | <i>Equus asinus</i> | 6.112 | 0.62 | M | Tibet | TIB | SAMC049011 |
| TIB_XZCM10 | <i>Equus asinus</i> | 6.77 | 0.534 | M | Tibet | TIB | SAMC049012 |
| TIB_XZCM12 | <i>Equus asinus</i> | 5.808 | 0.652 | F | Tibet | TIB | SAMC049013 |

| | | | | | | | |
|----------------|---------------------|--------|-------|---|--------------|-----|-------------|
| TIB_XZCM17 | <i>Equus asinus</i> | 6.1 | 0.599 | M | Tibet | TIB | SAMC049014 |
| TIB_XZSNQS02 | <i>Equus asinus</i> | 6.194 | 0.607 | F | Tibet | TIB | SAMC049015 |
| TIB_XZSNQS03 | <i>Equus asinus</i> | 5.695 | 0.66 | M | Tibet | TIB | SAMC049016 |
| TIB_XZSNQS04 | <i>Equus asinus</i> | 5.636 | 0.667 | M | Tibet | TIB | SAMC049017 |
| TIB_XZSNQS05 | <i>Equus asinus</i> | 5.97 | 0.632 | M | Tibet | TIB | SAMC049018 |
| TIB_XZSNQS06 | <i>Equus asinus</i> | 5.97 | 0.647 | F | Tibet | TIB | SAMC049019 |
| TIB_XZSNQS07 | <i>Equus asinus</i> | 6.327 | 0.585 | M | Tibet | TIB | SAMC049020 |
| TIB_XZSNQS23 | <i>Equus asinus</i> | 7.006 | 0.516 | M | Tibet | TIB | SAMC049021 |
| TKM_107 | <i>Equus asinus</i> | 31.802 | 0.005 | M | Turkmenistan | TKM | ERS12239283 |
| TUK_07 | <i>Equus asinus</i> | 32.266 | 0.004 | M | Turkey | TUK | ERS12239284 |
| TUK_08 | <i>Equus asinus</i> | 31.102 | 0.005 | F | Turkey | TUK | ERS12239285 |
| TUK_26 | <i>Equus asinus</i> | 28.86 | 0.005 | F | Turkey | TUK | ERS12239286 |
| TUN_06 | <i>Equus asinus</i> | 30.823 | 0.005 | M | Tunisia | TUN | ERS12239287 |
| TUN_11 | <i>Equus asinus</i> | 35.539 | 0.004 | F | Tunisia | TUN | ERS12239288 |
| TUN_19 | <i>Equus asinus</i> | 40.152 | 0.004 | F | Tunisia | TUN | ERS12239289 |
| BRA_PegaDonkey | <i>Equus asinus</i> | 13.706 | 0.065 | F | Brazil | BRA | ERS12239290 |
| YEM_08 | <i>Equus asinus</i> | 29.615 | 0.005 | F | Yemen | YEM | ERS12239291 |
| YEM_11 | <i>Equus asinus</i> | 40.052 | 0.003 | M | Yemen | YEM | ERS12239292 |
| YEM_17 | <i>Equus asinus</i> | 31.904 | 0.004 | F | Yemen | YEM | ERS12239293 |
| YUC_08 | <i>Equus asinus</i> | 27.058 | 0.007 | M | Croatia | YUC | ERS12239294 |
| YUM_08 | <i>Equus asinus</i> | 28.304 | 0.006 | M | Macedonia | YUM | ERS12239295 |
| YUM_13 | <i>Equus asinus</i> | 24.307 | 0.009 | M | Macedonia | YUM | ERS12239296 |

840 **Table S2:** Sample information and naming for each ancient individual. Radiocarbon dates
841 were calibrated using Oxcal online and the IntCal20 calibration curve (103, 104). Ages
842 marked with a star are inferred from radiocarbon dates and archaeological context is shown
843 outside the bracket.

| ID | Site | Country | Latitude | Longitude | Radiocarbon dated age | Age | Estimated Time period (years) | Period | Sex | Accession number |
|--------------|---------------------|---------|----------|-----------|--|----------------------|-------------------------------|-----------------------------|-----|------------------|
| AC14380 | Acemhöyük | Türkiye | 38.41123 | 33.83569 | 3945±20 (UCIAMS 199621) | 2455BCE | 2564BCE-2346BCE | Bronze Age | M | ERS12239303 |
| AC14415 | Acemhöyük | Türkiye | 38.41123 | 33.83569 | 3945±20 (UCIAMS 199619) | 2455BCE | 2564BCE-2346BCE | Bronze Age | M | ERS12239304 |
| MV051 | Acemhöyük | Türkiye | 38.41123 | 33.83569 | 3784±41 (UBA-30288) | 2219BCE | 2400BCE-2039BCE | Bronze Age | M | ERS12239305 |
| Chalow3 | Chalow | Iran | 37.10355 | 56.88528 | N/A | 2050BCE | 2200BCE- | BMAC | F | ERS12239306 |
| DoshanTepe | Doshan Tepe | Iran | 35.6833 | 51.5 | 2840±15 (UCIAMS 223195) | 989BCE | 1049BCE-928BCE | Iron Age | F | ERS12239307 |
| Tarquinoa214 | Tarquinoa | Italy | 42.0542 | 11.7576 | 2445±20 (UCIAMS 224884) | 550BCE (*581BCE) | 750BCE- | Etruscan (Archaic Period) | M | ERS12239308 |
| Tarquinoa501 | Tarquinoa | Italy | 42.0542 | 11.7576 | 2515±20 and 2565±20 (UCIAMS 224885 and 224886) | 520-500BCE (*680BCE) | 803BCE-594BCE and | Etruscan (Archaic Period) | F | ERS12239309 |
| MV242 | Nizzana | Israel | 30.88569 | 34.84694 | 2150±20 (UCIAMS 199283) | 204BCE | 350BCE- | Hellenistic Period | F | ERS12239310 |
| AM39 | Shahr-i-Qumis | Iran | 36.5511 | 54.0175 | N/A | 800BCE-800CE | 800BCE- | Parthian & Sassanian Period | F | ERS12239311 |
| AM44 | Shahr-i-Qumis | Iran | 36.5511 | 54.0175 | N/A | 800BCE-800CE | 800BCE- | Parthian & Sassanian Period | M | ERS12239312 |
| AM66 | Shahr-i-Qumis | Iran | 36.5511 | 54.0175 | N/A | 800BCE-800CE | 800BCE- | Parthian & Sassanian Period | M | ERS12239313 |
| AM71 | Shahr-i-Qumis | Iran | 36.5511 | 54.0175 | N/A | 800BCE-800CE | 800BCE- | Parthian & Sassanian Period | M | ERS12239314 |
| AM805 | Shahr-i-Qumis | Iran | 36.5511 | 54.0175 | 1615±20 and 1585±15 (UCIAMS 223584 and 223188) | 481CE | 415-538CE and 421-542CE | Parthian & Sassanian Period | M | ERS12239315 |
| AM89 | Shahr-i-Qumis | Iran | 36.5511 | 54.0175 | N/A | 800BCE-800CE | 800BCE- | Parthian & Sassanian Period | M | ERS12239316 |
| BourseB | Marseille | France | 43.29774 | 5.374613 | N/A | 0CE-500CE | 0CE- | Late Antiquity | M | ERS12239317 |
| BourseC | Marseille | France | 43.29774 | 5.374613 | N/A | 0CE-500CE | 0CE- | Late Antiquity | M | ERS12239318 |
| GVA125 | Boinville-en-Woëvre | France | 49.1858 | 5.6733 | N/A | 200CE- | 200CE- | Roman Period | M | ERS12239319 |
| GVA347 | Boinville-en-Woëvre | France | 49.1858 | 5.6733 | N/A | 200CE- | 200CE- | Roman Period | M | ERS12239320 |
| GVA348 | Boinville-en-Woëvre | France | 49.1858 | 5.6733 | N/A | 200CE- | 200CE- | Roman Period | M | ERS12239321 |
| GVA349 | Boinville-en-Woëvre | France | 49.1858 | 5.6733 | N/A | 200CE- | 200CE- | Roman Period | M | ERS12239322 |

| | | | | | | | | | | |
|--------------|---------------------|----------|---------|---------|-------------------------------|--------|-------------------|------------------------------|---|-------------|
| GVA353 | Boinville-en-Woëvre | France | 49.1858 | 5.6733 | N/A | 200CE- | 200CE- | Roman Period | M | ERS12239323 |
| GVA354 | Boinville-en-Woëvre | France | 49.1858 | 5.6733 | N/A | 200CE- | 200CE- | Roman Period | F | ERS12239324 |
| GVA355 | Boinville-en-Woëvre | France | 49.1858 | 5.6733 | N/A | 200CE- | 200CE- | Roman Period | F | ERS12239325 |
| GVA358 | Boinville-en-Woëvre | France | 49.1858 | 5.6733 | N/A | 200CE- | 200CE- | Roman Period | F | ERS12239326 |
| GVA359 | Boinville-en-Woëvre | France | 49.1858 | 5.6733 | N/A | 200CE- | 200CE- | Roman Period | M | ERS12239327 |
| Tur168 | Yenikapi | Türkiye | 40.9997 | 28.9498 | 1485±20 (UCIAMS 250285) | 596CE | 552CE- 640CE | Byzantine Period | M | ERS12239328 |
| Tur177 | Yenikapi | Türkiye | 40.9997 | 28.9498 | 1125±15 (UCIAMS 250291) | 937CE | 887CE- 986CE | Byzantine Period | F | ERS12239329 |
| Tur179 | Yenikapi | Türkiye | 40.9997 | 28.9498 | 1140±20 (UCIAMS 250292) | 881CE | 774CE- 987CE | Byzantine Period | M | ERS12239330 |
| Tur277 | Yenikapi | Türkiye | 40.9997 | 28.9498 | 1295±15 (UCIAMS 250363) | 721CE | 666CE- 775CE | Byzantine Period | M | ERS12239331 |
| Albufeira1x1 | Albufeira | Portugal | 37.0891 | -8.2479 | 765±15 (UCIAMS 208877) | 1254CE | 1228CE- 1280CE | Islamic Period | F | ERS12239332 |
| Fiumarella1 | Fiumarella | Italy | 39.589 | 16.8127 | 165±25 (UCIAMS 229410) | 1810CE | 1683CE- 1936CE | Bronze Age (Intrusive) | M | ERS12239333 |

844

845 **Table S3:** The number of variants identified by GraphTyper (version 2.5.1)(61) for modern
846 individuals ($n=222$) before and after filtering for high quality variants.

| | Number of variants | SNPs | INDELs |
|---|---------------------------|-------------|---------------|
| Raw (all scaffolds) | 45,031,411 | 40,234,452 | 4,796,959 |
| After filtering (all scaffolds) | 13,267,291 | 11,655,167 | 1,680,089 |
| After filtering (autosomes only) | 13,013,551 | 11,426,298 | 1,587,253 |

847

848 **Table S4:** The number of variants remaining per autosome for the modern individuals
849 ($n=222$) before and after filtering. The length of each autosome in base pairs and
850 centimorgans, and the rate of recombination in cM/Mb is also reported.

| Chromosome | Raw variants | Filtered variants | cM | Base pairs (bp) | cM/Mb |
|-------------------|--------------|-------------------|----------------|----------------------|--------------|
| JADWZW010000002.1 | 2169745 | 637112 | 53.924 | 119293623 | 0.452 |
| JADWZW010000003.1 | 4493039 | 1328891 | 120.098 | 238843737 | 0.503 |
| JADWZW010000004.1 | 3304316 | 1021216 | 93.066 | 183770576 | 0.506 |
| JADWZW010000005.1 | 1646778 | 474536 | 50.987 | 92920267 | 0.549 |
| JADWZW010000006.1 | 2151743 | 628929 | 61.797 | 112287698 | 0.55 |
| JADWZW010000007.1 | 1726889 | 500863 | 51.792 | 93367529 | 0.555 |
| JADWZW010000008.1 | 2350964 | 689712 | 60.556 | 123522326 | 0.49 |
| JADWZW010000009.1 | 2124123 | 714987 | 63.363 | 104245332 | 0.608 |
| JADWZW010000010.1 | 1191724 | 342829 | 39.723 | 64678186 | 0.614 |
| JADWZW010000011.1 | 1769988 | 531435 | 47.142 | 90664430 | 0.52 |
| JADWZW010000012.1 | 1660121 | 525478 | 44.934 | 85786229 | 0.524 |
| JADWZW010000013.1 | 1965805 | 578347 | 46.365 | 106341547 | 0.436 |
| JADWZW010000014.1 | 1107198 | 307520 | 43.321 | 64917852 | 0.667 |
| JADWZW010000015.1 | 876130 | 249858 | 36.895 | 47664211 | 0.774 |
| JADWZW010000016.1 | 991742 | 284692 | 33.995 | 50230352 | 0.677 |
| JADWZW010000017.1 | 941418 | 276091 | 30.639 | 50732407 | 0.604 |
| JADWZW010000018.1 | 986503 | 315280 | 37.799 | 47651278 | 0.793 |
| JADWZW010000019.1 | 670734 | 202542 | 20.526 | 33165847 | 0.619 |
| JADWZW010000020.1 | 545920 | 165635 | 20.42 | 26995809 | 0.756 |
| JADWZW010000021.1 | 1931507 | 585299 | 54.196 | 100519399 | 0.539 |
| JADWZW010000022.1 | 1817414 | 517089 | 49.405 | 98587405 | 0.501 |
| JADWZW010000023.1 | 705216 | 202045 | 21.852 | 38358317 | 0.57 |
| JADWZW010000024.1 | 875823 | 262496 | 25.965 | 47367245 | 0.548 |
| JADWZW010000025.1 | 865649 | 260065 | 23.107 | 46609582 | 0.496 |
| JADWZW010000026.1 | 817711 | 237991 | 26.279 | 47151018 | 0.557 |
| JADWZW010000027.1 | 581105 | 182904 | 22.156 | 28688911 | 0.772 |
| JADWZW010000028.1 | 672875 | 208766 | 23.347 | 32167345 | 0.726 |
| JADWZW010000029.1 | 1226740 | 356584 | 42.517 | 63892262 | 0.665 |
| JADWZW010000030.1 | 754861 | 227618 | 24.809 | 37452155 | 0.662 |
| JADWZW010000031.1 | 623338 | 196741 | 22.059 | 30281758 | 0.728 |
| Total | | | 1293.04 | 2,308,154,633 | 0.599 |

851

852 **Table S5:** Ancestral populations and ancestry proportions for hybrid individuals, calculated
 853 using qpAdm modelling (version 810) (64). Significant *p*-values are indicated with a *.

| ID | Source 1 | Source 2 | Weight 1 | Weight 2 | <i>p</i> -value |
|--------------|----------|----------------|----------|----------|-----------------|
| ETH_5B | ETH | <i>E.a.som</i> | 0.818 | 0.182 | <0.001* |
| SOM_19 | IRA | <i>E.a.som</i> | 0.951 | 0.049 | <0.001* |
| ETH_6B | ETH | <i>E.a.som</i> | 0.956 | 0.044 | <0.001* |
| SOM_20 | IRA | <i>E.a.som</i> | 0.963 | 0.038 | <0.001* |
| SOM_21 | IRA | <i>E.a.som</i> | 0.968 | 0.032 | <0.001* |
| ALG_01 | ETH | <i>E.a.som</i> | 0.974 | 0.026 | <0.001* |
| YEM_08 | EGY | <i>E.a.som</i> | 0.981 | 0.019 | <0.001* |
| SUD_49 | SUD | <i>E.a.som</i> | 0.981 | 0.019 | <0.001* |
| YEM_11 | EGY | <i>E.a.som</i> | 0.983 | 0.017 | <0.001* |
| OMA_46 | EGY | <i>E.a.som</i> | 0.983 | 0.017 | <0.001* |
| YEM_17 | EGY | <i>E.a.som</i> | 0.984 | 0.016 | <0.001* |
| OMA_38 | EGY | <i>E.a.som</i> | 0.985 | 0.015 | <0.001* |
| MAU_3261 | NIG | <i>E.a.som</i> | 0.987 | 0.013 | 0.021* |
| OMA_39 | EGY | <i>E.a.som</i> | 0.988 | 0.012 | 0.005* |
| MAU_2990 | NIG | <i>E.a.som</i> | 0.991 | 0.009 | 0.568 |
| GHA_07 | NIG | <i>E.a.som</i> | 0.993 | 0.007 | 0.183 |
| SEN_10 | NIG | <i>E.a.som</i> | 0.995 | 0.005 | 0.281 |
| CHI_Turfan_2 | CHI | <i>E.kiang</i> | 0.995 | 0.005 | 0.003* |
| MAU_3094 | NIG | <i>E.a.som</i> | 0.996 | 0.004 | 0.626 |
| NIG_YPO67 | NIG | <i>E.a.som</i> | 0.997 | 0.003 | 0.259 |

854

855 **Table S6:** Genome coverage, proportion of missing variants and predicted accuracy of
856 imputation based on tests conducted on modern variants for all ancient samples ($n=31$
857 individuals, $n=7,161,029$ variants, $TI/TV=2.17$).

| Sample | Missingness | Coverage | Predicted Imputation Accuracy (all variants) |
|--------------|-------------|----------|--|
| AM66 | 0.558 | 4.920 | 0.986 |
| GVA348 | 0.600 | 5.050 | 0.986 |
| Tur168 | 0.604 | 4.640 | 0.986 |
| Tur179 | 0.612 | 4.693 | 0.986 |
| Tur177 | 0.727 | 3.693 | 0.985 |
| GVA349 | 0.731 | 4.090 | 0.985 |
| AC14415 | 0.785 | 3.370 | 0.985 |
| TarquiniA501 | 0.799 | 2.900 | 0.985 |
| AM805 | 0.812 | 2.870 | 0.985 |
| Tur277 | 0.827 | 2.951 | 0.984 |
| BourseC | 0.858 | 2.240 | 0.984 |
| GVA125 | 0.862 | 2.060 | 0.984 |
| TarquiniA214 | 0.864 | 2.250 | 0.984 |
| MV242 | 0.879 | 2.510 | 0.984 |
| GVA347 | 0.883 | 2.100 | 0.984 |
| AC14380 | 0.892 | 2.120 | 0.984 |
| Chalow3 | 0.895 | 2.110 | 0.984 |
| MV051 | 0.901 | 1.270 | 0.984 |
| AM89 | 0.901 | 1.570 | 0.984 |
| AM44 | 0.903 | 1.670 | 0.984 |
| AM71 | 0.910 | 1.540 | 0.984 |
| BourseB | 0.915 | 1.600 | 0.984 |
| Albufeira1x1 | 0.919 | 1.620 | 0.983 |
| Fiumarella1 | 0.930 | 1.440 | 0.983 |
| DoshanTepe | 0.938 | 1.540 | 0.983 |
| GVA359 | 0.944 | 1.230 | 0.983 |
| GVA355 | 0.953 | 1.210 | 0.983 |
| GVA353 | 0.963 | 1.060 | 0.982 |
| GVA358 | 0.963 | 1.105 | 0.982 |
| AM39 | 0.973 | 0.770 | 0.981 |
| GVA354 | 0.973 | 0.953 | 0.981 |

858

859 **Table S7:** The depth of reads and variants 5 base pairs either side of the missense mutation
 860 (G>A) at position JADWZW010000004.1:161390091 in *FGF5* (46) for 31 ancient donkeys.

861

| sample | depth of reads | C | C | A | G | T | G/A | G | A | G | C | C |
|--------------|----------------|---|---|---|---|---|------|---|---|---|-------|---|
| AC14380 | 3 | . | . | . | . | . | . | . | . | . | . | . |
| AC14415 | 4 | . | . | . | . | . | . | . | . | . | . | . |
| Albufeira1x1 | 1 | . | . | . | . | . | . | . | . | . | . | . |
| AM39 | 2 | . | . | . | . | . | . | . | . | . | . | . |
| AM44 | 1 | . | . | . | . | . | . | . | . | . | . | . |
| AM66 | 5 | . | . | . | . | . | . | . | . | . | . | . |
| AM71 | 4 | . | . | . | . | . | . | . | . | . | . | . |
| AM805 | 6 | . | . | . | . | . | . | . | . | . | . | . |
| AM89 | 3 | . | . | . | . | . | A(1) | . | . | . | . | . |
| BourseB | 0 | . | . | . | . | . | . | . | . | . | . | . |
| BourseC | 0 | . | . | . | . | . | . | . | . | . | . | . |
| Chalow3 | 2 | . | . | . | . | . | . | . | . | . | . | . |
| DoshanTepe | 1 | . | . | . | . | . | . | . | . | . | . | . |
| Fiumarella1 | 1 | . | . | . | . | . | . | . | . | . | . | . |
| GVA125 | 0 | . | . | . | . | . | . | . | . | . | . | . |
| GVA347 | 3 | . | . | . | . | . | . | . | . | . | . | . |
| GVA348 | 4 | . | . | . | . | . | . | . | . | . | . | . |
| GVA349 | 3 | . | . | . | . | . | . | . | . | . | . | . |
| GVA353 | 0 | . | . | . | . | . | . | . | . | . | . | . |
| GVA354 | 0 | . | . | . | . | . | . | . | . | . | . | . |
| GVA355 | 0 | . | . | . | . | . | . | . | . | . | . | . |
| GVA358 | 1 | . | . | . | . | . | . | . | . | . | . | . |
| GVA359 | 4 | . | . | . | . | . | . | . | . | . | . | . |
| MV051 | 0 | . | . | . | . | . | . | . | . | . | . | . |
| MV242 | 3 | . | . | . | . | . | . | . | . | . | . | . |
| Tarquinoa214 | 1 | . | . | . | . | . | . | . | . | . | . | . |
| Tarquinoa501 | 4 | . | . | . | . | . | . | . | . | . | . | . |
| Tur168 | 3 | . | . | . | . | . | . | . | . | . | . | . |
| Tur177 | 2 | . | . | . | . | . | . | . | . | . | G (1) | . |
| Tur179 | 3 | . | . | . | . | . | . | . | . | . | . | . |
| Tur277 | 2 | . | . | . | . | . | . | . | . | . | . | . |

862

863 **Table S8:** The depth of reads and variants 5 base pairs either side of the frameshift deletion
 864 (delAT) at position (JADWZW010000004.1:161397694) in *FGF5* (46) for 31 ancient
 865 donkeys.

| Sample | depth of reads | T | A | G | C | G | A/- | T/- | G | T | C | A | A |
|--------------|----------------|---|---|---|------|------|------|------|------|------|------|---|---|
| AC14380 | 2 | . | . | . | . | . | . | . | . | . | . | . | . |
| AC14415 | 6 | . | . | . | . | . | . | . | . | . | . | . | . |
| Albufeira1x1 | 0 | . | . | . | . | . | . | . | . | . | . | . | . |
| AM39 | 1 | . | . | . | . | . | . | . | . | . | . | . | . |
| AM44 | 1 | . | . | . | . | . | . | . | . | . | . | . | . |
| AM66 | 8 | . | . | . | . | A(1) | . | . | . | . | . | . | . |
| AM71 | 0 | . | . | . | . | . | . | . | . | . | . | . | . |
| AM805 | 5 | . | . | . | . | . | . | . | . | . | . | . | . |
| AM89 | 2 | . | . | . | . | . | . | . | . | . | . | . | . |
| BourseB | 2 | . | . | . | T(1) | . | . | . | . | . | . | . | . |
| BourseC | 4 | . | . | . | . | . | . | . | . | . | . | . | . |
| Chalow3 | 3 | . | . | . | . | A(1) | . | . | . | . | . | . | . |
| DoshanTepe | 1 | . | . | . | . | . | . | . | . | . | . | . | . |
| Fiumarella1 | 1 | . | . | . | . | . | . | . | . | . | . | . | . |
| GVA125 | 5 | . | . | . | . | A(1) | . | . | A(1) | G(1) | G(1) | . | . |
| GVA347 | 3 | . | . | . | . | . | . | . | . | . | . | . | . |
| GVA348 | 10 | . | . | . | . | . | . | . | . | . | . | . | . |
| GVA349 | 2 | . | . | . | . | . | . | . | . | . | . | . | . |
| GVA353 | 3 | . | . | . | . | . | . | . | . | . | . | . | . |
| GVA354 | 1 | . | . | . | . | . | . | . | . | . | . | . | . |
| GVA355 | 0 | . | . | . | . | . | . | . | . | . | . | . | . |
| GVA358 | 1 | . | . | . | T(1) | . | . | . | . | . | . | . | . |
| GVA359 | 1 | . | . | . | . | . | . | . | . | . | . | . | . |
| MV051 | 1 | . | . | . | . | . | . | . | . | . | . | . | . |
| MV242 | 4 | . | . | . | . | . | . | . | . | . | . | . | . |
| Tarquinoa214 | 4 | . | . | . | . | A(1) | . | . | . | . | . | . | . |
| Tarquinoa501 | 5 | . | . | . | . | . | . | . | . | . | . | . | . |
| Tur168 | 4 | . | . | . | . | . | . | . | . | . | . | . | . |
| Tur177 | 6 | . | . | . | T(1) | . | . | . | . | . | . | . | . |
| Tur179 | 3 | . | . | . | -(1) | -(1) | -(1) | -(1) | . | . | . | . | . |
| Tur277 | 5 | . | . | . | . | . | . | . | . | . | . | . | . |

866

867

868 **Table S9:** The depth of reads and variants 5 base pairs either side of the T>A splice site
 869 mutation in *KIT* at position JADWZW010000004.1:139925278 for 31 ancient donkeys (45).

| Sample | depth of reads | G | A | G | G | T/A | A | A | A | G | C |
|--------------|----------------|---|------|---|------|-----|---|---|---|------|------|
| AC14380 | 0 | . | . | . | . | . | . | . | . | . | . |
| AC14415 | 5 | . | T(1) | . | . | . | . | . | . | T(1) | T(1) |
| Albufeiralx1 | 2 | . | . | . | . | . | . | . | . | . | . |
| AM39 | 0 | . | . | . | . | . | . | . | . | . | . |
| AM44 | 1 | . | . | . | . | . | . | . | . | . | . |
| AM66 | 3 | . | . | . | . | . | . | . | . | . | . |
| AM71 | 2 | . | . | . | . | . | . | . | . | . | . |
| AM805 | 3 | . | . | . | . | . | . | . | . | . | . |
| AM89 | 5 | . | . | . | . | . | . | . | . | . | . |
| BourseB | 1 | . | . | . | . | . | . | . | . | . | . |
| BourseC | 8 | . | . | . | . | . | . | . | . | . | . |
| Chalow3 | 1 | . | . | . | . | . | . | . | . | . | . |
| DoshanTepe | 1 | . | . | . | . | . | . | . | . | . | . |
| Fiumarella1 | 1 | . | . | . | . | . | . | . | . | . | . |
| GVA125 | 1 | . | . | . | . | . | . | . | . | . | . |
| GVA347 | 1 | . | . | . | . | . | . | . | . | . | . |
| GVA348 | 3 | . | . | . | . | . | . | . | . | . | . |
| GVA349 | 3 | . | . | . | . | . | . | . | . | . | . |
| GVA353 | 0 | . | . | . | . | . | . | . | . | . | . |
| GVA354 | 2 | . | . | . | . | . | . | . | . | . | . |
| GVA355 | 0 | . | . | . | . | . | . | . | . | . | . |
| GVA358 | 2 | . | . | . | . | . | . | . | . | . | . |
| GVA359 | 0 | . | . | . | . | . | . | . | . | . | . |
| MV051 | 2 | . | . | . | . | . | . | . | . | . | . |
| MV242 | 3 | . | . | . | T(1) | . | . | . | . | . | . |
| Tarquinia214 | 4 | . | . | . | . | . | . | . | . | . | . |
| Tarquinia501 | 2 | . | . | . | . | . | . | . | . | . | . |
| Tur168 | 6 | . | . | . | . | . | . | . | . | . | . |
| Tur177 | 6 | . | . | . | . | . | . | . | . | . | . |
| Tur179 | 5 | . | . | . | . | . | . | . | . | . | . |
| Tur277 | 2 | . | . | . | . | . | . | . | . | . | . |

870

871 **Table S10:** Levels of relatedness between ancient individuals estimated using KING (version
872 2.2.7) (66) with the imputed variant panel, conditioning on transversions only ($n=31$
873 individuals, $n=619,981$ transversions). Only relationships between individuals inferred to
874 show genetic relatedness are shown.

| ID1 | ID2 | Proportion of IBD | Degree of relatedness |
|---------------|---------------|--------------------------|------------------------------|
| GVA355 | GVA358 | 0.705 | 1st |
| GVA125 | GVA353 | 0.250 | 2nd |
| GVA347 | GVA353 | 0.238 | 2nd |
| GVA125 | GVA348 | 0.201 | 2nd |
| GVA348 | GVA353 | 0.189 | 2nd |
| GVA348 | GVA354 | 0.188 | 2nd |
| GVA125 | GVA354 | 0.178 | 2nd |
| GVA347 | GVA354 | 0.166 | 3rd |
| GVA125 | GVA347 | 0.162 | 3rd |
| GVA347 | GVA348 | 0.159 | 3rd |
| GVA353 | GVA354 | 0.154 | 3rd |
| GVA348 | GVA349 | 0.138 | 3rd |
| GVA347 | GVA349 | 0.125 | 3rd |
| GVA349 | GVA353 | 0.124 | 3rd |
| GVA125 | GVA349 | 0.108 | 3rd |
| GVA349 | GVA354 | 0.101 | 3rd |
| Tarquinius214 | Tarquinius501 | 0.081 | 4th |
| GVA348 | GVA355 | 0.052 | 4th |
| GVA348 | GVA358 | 0.051 | 4th |

875

876

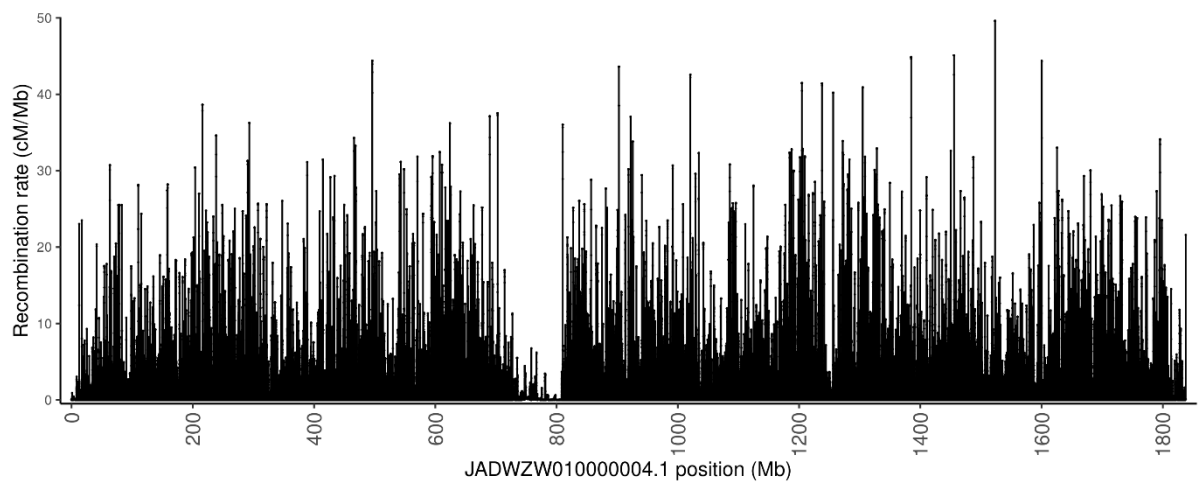
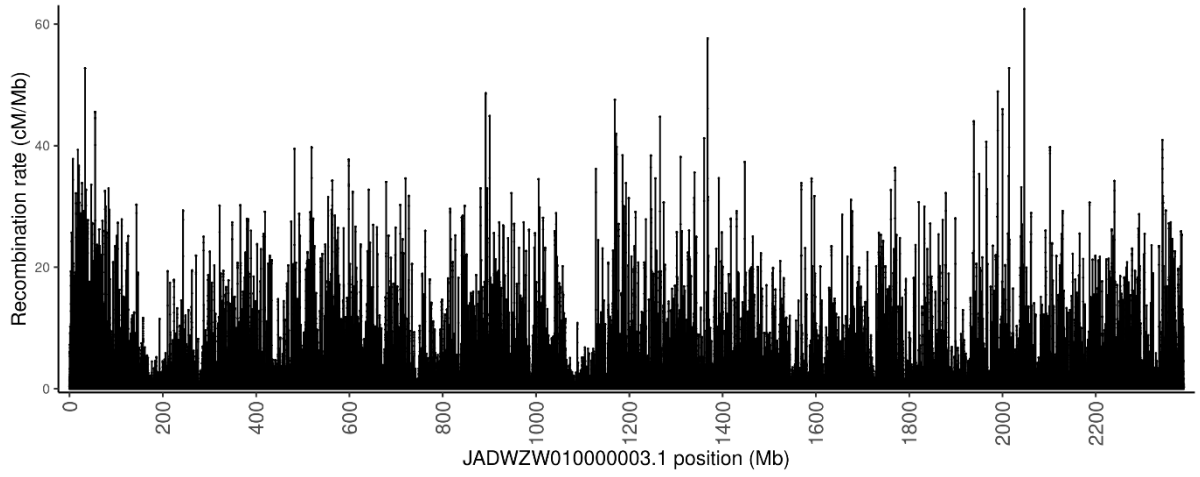
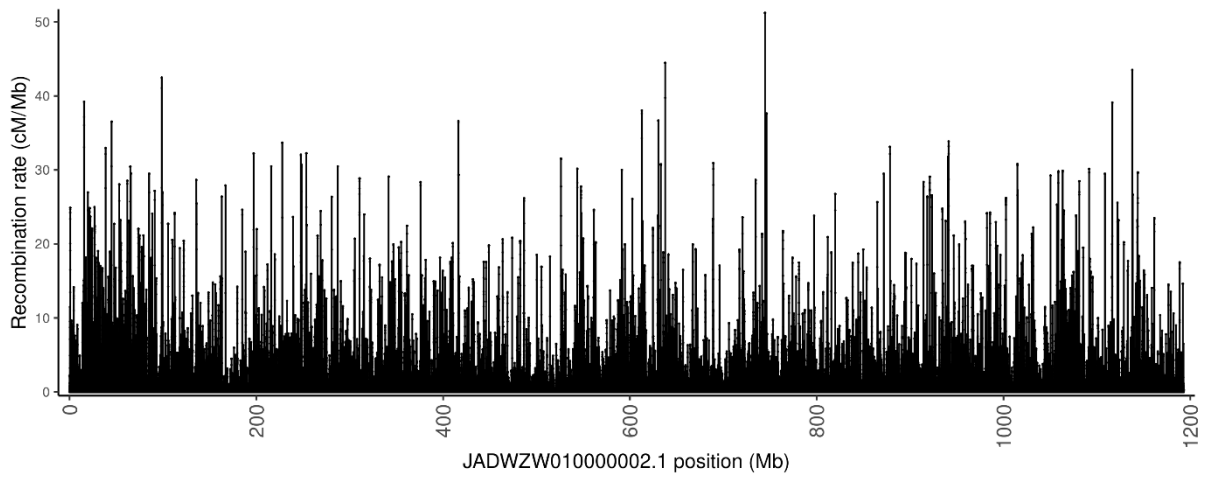
877 **Table S11:** Sample information and accession numbers for each modern ($n=79$) and ancient
878 horse ($n=75$) used for estimating inbreeding levels (Fig. 4D, E, F). Whole-genome sequence
879 data and metadata on the site, country and age (inferred from the radiocarbon dates) for the
880 ancient horses were obtained from (21, 41, 50, 131). Whole-genome sequence data for
881 modern horses were obtained from (132-137)

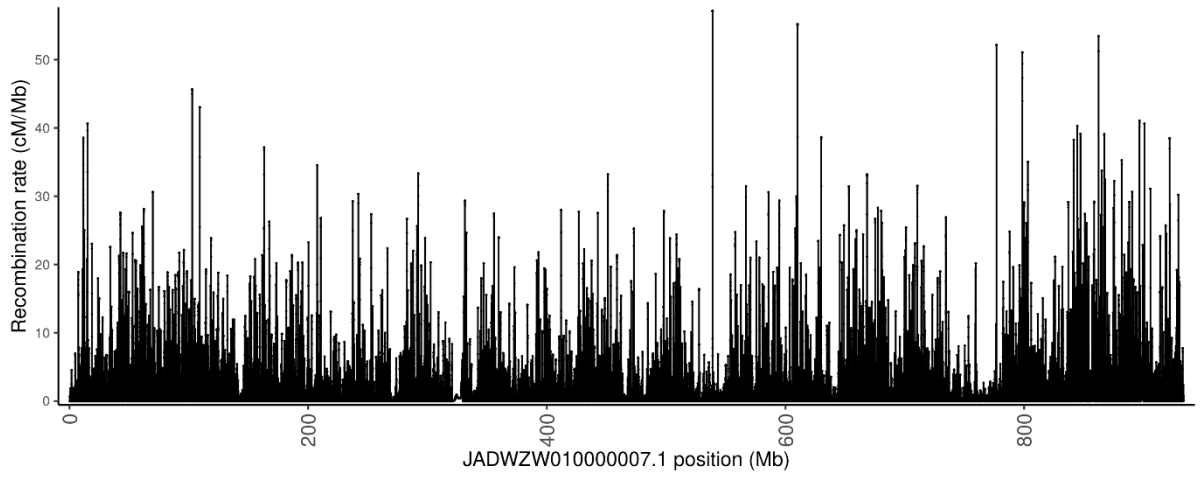
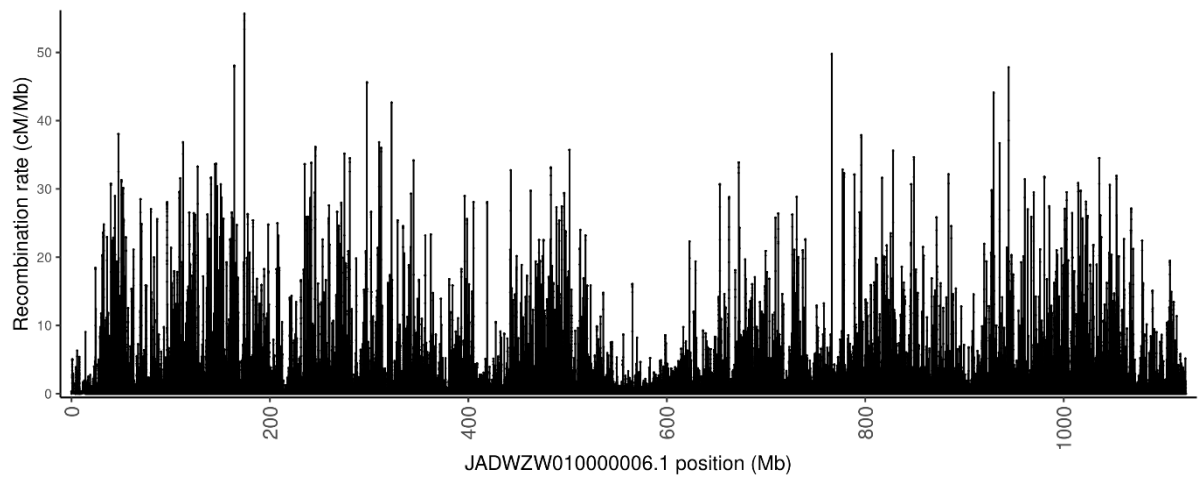
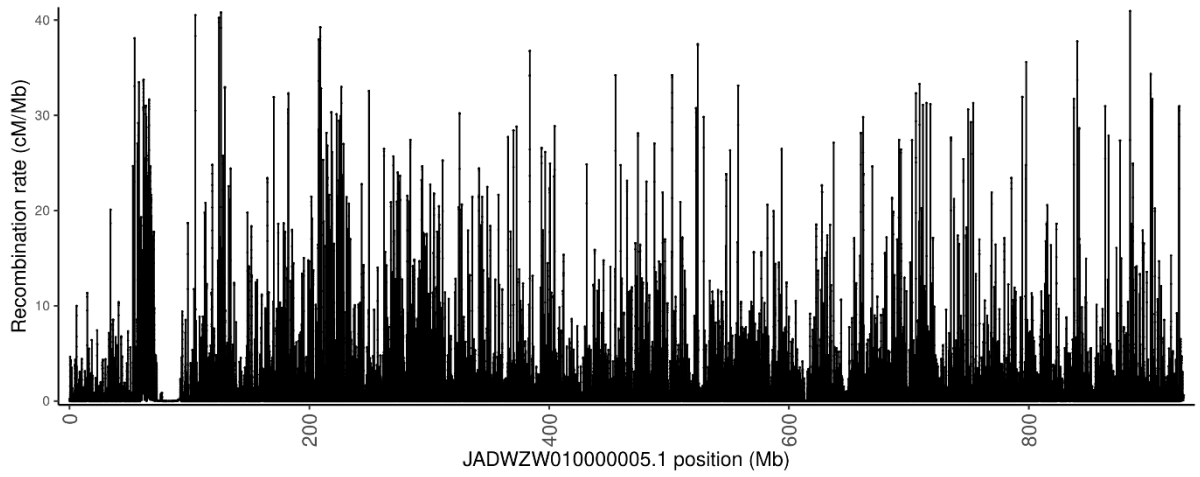
| ID | Site | Country | Age | age2 | label | Accession number |
|--------------------------------|------|---------|--------|------|-------|------------------|
| Akha_0248A_AKT001 | NA | NA | 2000CE | 2000 | M1 | ERS1246351 |
| Akha_0302A_AKT003 | NA | NA | 2000CE | 2000 | M2 | ERS1246352 |
| Arabian_UFL_948_ERR3465834 | NA | NA | 2000CE | 2000 | M3 | ERS3631438 |
| Bava_0183A_BY01 | NA | NA | 2000CE | 2000 | M4 | ERS1263371 |
| CDM12_Chaidamu_DulanQinghai | NA | NA | 2000CE | 2000 | M5 | SRS4251825 |
| CDM15_Chaidamu_DulanQinghai | NA | NA | 2000CE | 2000 | M6 | SAMN28422840 |
| CuTr_0137A_CU_COL163706 | NA | NA | 2000CE | 2000 | M7 | ERS1560528 |
| CuTr_0138A_CU_COL163725 | NA | NA | 2000CE | 2000 | M8 | ERS1560529 |
| DB35_DeBa_Debao_Guangxi | NA | NA | 2000CE | 2000 | M9 | SAMN28422841 |
| DT12_DaTo_Datong_QilianQinghai | NA | NA | 2000CE | 2000 | M10 | SAMN28422842 |
| DT3_DaTo_Datong_QilianQinghai | NA | NA | 2000CE | 2000 | M11 | SAMN28422843 |
| Dutc_0308A | NA | NA | 2000CE | 2000 | M12 | ERS1246371 |
| ELC21_Erlunchun_InnerMongolia | NA | NA | 2000CE | 2000 | M13 | SRS4251811 |
| Fjor_0142A_Fjord | NA | NA | 2000CE | 2000 | M14 | SRS438157 |
| Frie_0298A_SAMEA3951220 | NA | NA | 2000CE | 2000 | M15 | ERS1138354 |
| Frie_0300A_SAMEA3951222 | NA | NA | 2000CE | 2000 | M16 | ERS1138356 |
| FrMo_0041A_FM0001 | NA | NA | 2000CE | 2000 | M17 | ERS1246356 |
| FrMo_0065A_FM1798 | NA | NA | 2000CE | 2000 | M18 | ERS1246364 |
| HafI_0309A_HF0002 | NA | NA | 2000CE | 2000 | M19 | ERS1982326 |
| HafI_0310A_HF0003 | NA | NA | 2000CE | 2000 | M20 | ERS1982327 |
| Hano_0172A_HAN01 | NA | NA | 2000CE | 2000 | M21 | ERS1263372 |
| Hano_0312A_HN001 | NA | NA | 2000CE | 2000 | M22 | ERS1982322 |
| Hols_0173A_HOL01 | NA | NA | 2000CE | 2000 | M23 | ERS1263373 |
| Icel_0144A_P5782 | NA | NA | 2000CE | 2000 | M24 | SRS309532 |
| Icel_0247A_IS074 | NA | NA | 2000CE | 2000 | M25 | ERS709890 |
| JC5_JiCh_Jianchang_SW | NA | NA | 2000CE | 2000 | M26 | SAMN28422844 |
| Jeju_0274A_SAMN01057171 | NA | NA | 2000CE | 2000 | M27 | SRS346578 |
| Jeju_0275A_SAMN01057172 | NA | NA | 2000CE | 2000 | M28 | SRS346579 |
| JZ3_JiZi_JiangziTibet | NA | NA | 2000CE | 2000 | M29 | SRS4251838 |
| JZ4_JiZi_JiangziTibet | NA | NA | 2000CE | 2000 | M30 | SRS4251838 |
| Lipi_0187A_CSess113 | NA | NA | 2000CE | 2000 | M31 | SRS1818811 |
| Lipi_0188A_FRal169 | NA | NA | 2000CE | 2000 | M32 | SRS1818795 |
| LKZ22_Langkazi_Tibet | NA | NA | 2000CE | 2000 | M33 | SAMN28422845 |
| LKZ28_Langkazi_Tibet | NA | NA | 2000CE | 2000 | M34 | SRS4251851 |
| Marw_0239A_SRR1275408 | NA | NA | 2000CE | 2000 | M35 | SRS603966 |
| Mixd_0314A_UKH4 | NA | NA | 2000CE | 2000 | M36 | ERS1076964 |
| Mong_0153A_KB7754 | NA | NA | 2000CE | 2000 | M37 | ERS805731 |
| Mong_0216A_TG1111D2629 | NA | NA | 2000CE | 2000 | M38 | SRS543625 |
| Morg_0096A_EMS595 | NA | NA | 2000CE | 2000 | M39 | ERS806987 |

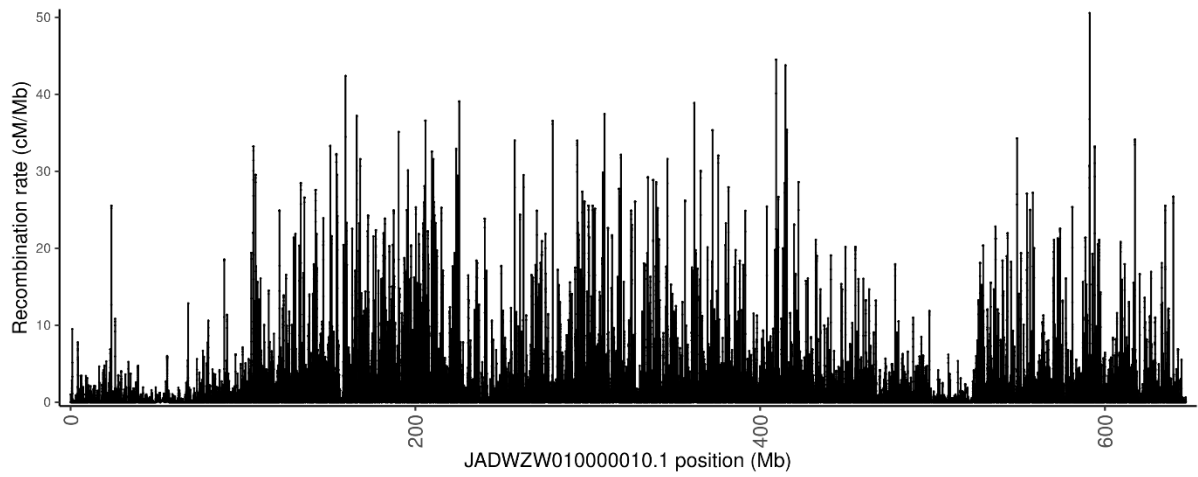
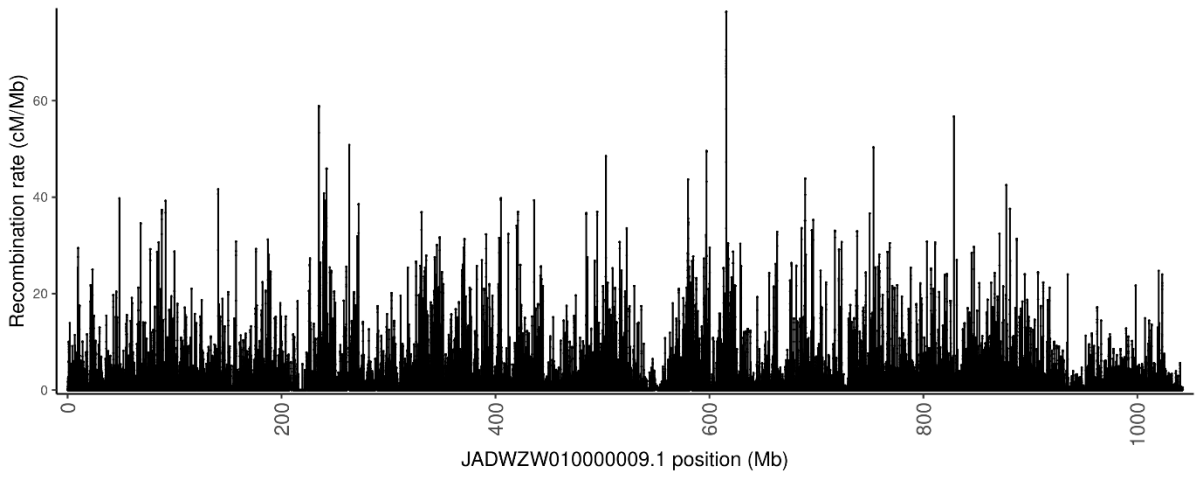
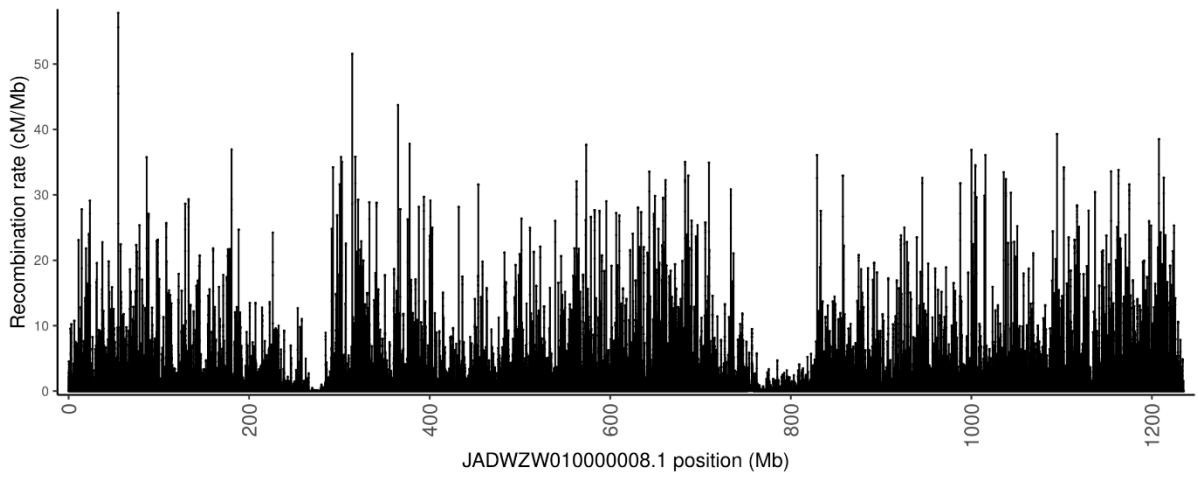
| | | | | | | |
|------------------------------------|-----------------------------------|----------------|--------|------|-----|-------------------------|
| Morg_0315A_EQ053 | NA | NA | 2000CE | 2000 | M40 | ERS1982319 |
| MZH22_Mozhu_MozhugongTibet | NA | NA | 2000CE | 2000 | M41 | SAMN28422846 |
| MZH24_Mozhu_MozhugongTibet | NA | NA | 2000CE | 2000 | M42 | SAMN28422847 |
| NM2_NiMu_Tibet | NA | NA | 2000CE | 2000 | M43 | SAMN28422848 |
| NM20_NiMu_Tibet | NA | NA | 2000CE | 2000 | M44 | SAMN28422849 |
| Nori_0316A_NO180 | NA | NA | 2000CE | 2000 | M45 | ERS1982325 |
| NQ9916_NiQi_NingqiangShaanxi | NA | NA | 2000CE | 2000 | M46 | SAMN28422850 |
| Olde_0176A_OLD01 | NA | NA | 2000CE | 2000 | M47 | ERS1263375 |
| Olde_0177A_OLD02 | NA | NA | 2000CE | 2000 | M48 | ERS1263376 |
| Pain_0319A_UKH16 | NA | NA | 2000CE | 2000 | M49 | ERS1076966 |
| Pain_0320A_UKH29 | NA | NA | 2000CE | 2000 | M50 | ERS1076967 |
| Quar_0321A_QH070 | NA | NA | 2000CE | 2000 | M51 | ERS1246372 |
| Quar_0322A_QH225 | NA | NA | 2000CE | 2000 | M52 | ERS1246374 |
| Reit_0323A_DR011 | NA | NA | 2000CE | 2000 | M53 | ERS1982318 |
| Reit_0324A_DR033 | NA | NA | 2000CE | 2000 | M54 | ERS1982315 |
| Shet_0249A_SPH020 | NA | NA | 2000CE | 2000 | M55 | ERS715262 |
| Shet_0250A_SPH041 | NA | NA | 2000CE | 2000 | M56 | ERS715261 |
| Sorr_0236A_SAMN02439778 | NA | NA | 2000CE | 2000 | M57 | SRS513153 |
| Sorr_0270A_SAMN03955413 | NA | NA | 2000CE | 2000 | M58 | SRS1022305 |
| Stan_0325A_AS002 | NA | NA | 2000CE | 2000 | M59 | ERS1230234 |
| Standardbred_UFL_CU1406_ERR3465842 | NA | NA | 2000CE | 2000 | M60 | ERS3631446 |
| Standardbred_UFL_CU2446_ERR3465843 | NA | NA | 2000CE | 2000 | M61 | ERS3631447 |
| Swis_0326A_RAO310_2 | NA | NA | 2000CE | 2000 | M62 | ERS1263382 |
| Swis_0327A_RAO441_2 | NA | NA | 2000CE | 2000 | M63 | ERS1263383 |
| Thor_0290A_SAMN01047706 | NA | NA | 2000CE | 2000 | M64 | SRS345336 |
| Thoroughbred_UFL_CU3903_ERR3465845 | NA | NA | 2000CE | 2000 | M65 | ERS3631449 |
| Trak_0178A_TRA01 | NA | NA | 2000CE | 2000 | M66 | ERS1263377 |
| Trak_0179A_TRA02 | NA | NA | 2000CE | 2000 | M67 | SRS1818810 |
| UFL_QH140147_ERR3465848 | NA | NA | 2000CE | 2000 | M68 | ERS3631452 |
| Wels_0330A_WP006 | NA | NA | 2000CE | 2000 | M69 | ERS1982316 |
| Wels_0331A_WP007 | NA | NA | 2000CE | 2000 | M70 | ERS1982323 |
| West_0180A_WF01 | NA | NA | 2000CE | 2000 | M71 | ERS1263379 |
| West_0181A_WF02 | NA | NA | 2000CE | 2000 | M72 | ERS1263380 |
| WMG8_Mongolian_Mongolia | NA | NA | 2000CE | 2000 | M73 | SAMN28422851 |
| Wurt_0182A_BW01 | NA | NA | 2000CE | 2000 | M74 | ERS1263370 |
| WZ6_MoGo_InnerMongolia | NA | NA | 2000CE | 2000 | M75 | SRS4251803 |
| Yaku_0164A_Yak2 | NA | NA | 2000CE | 2000 | M76 | ERS849387 |
| Yaku_0169A_Yak7 | NA | NA | 2000CE | 2000 | M77 | ERS849392 |
| YL2_YiLi_Zhaosu_Pair | NA | NA | 2000CE | 2000 | M78 | SAMN28422852 |
| YQ29_YaQi_Yanqi_Xinjiang | NA | NA | 2000CE | 2000 | M79 | SAMN28422853 |
| ARUS_0222A_CGG101397 | Tumeski | Russia | 1825CE | 1825 | A1 | SRS497178, SRS497177 |
| WitterPlace_UK17_267 | Witter Place | United Kingdom | 1750CE | 1750 | A2 | ERS3213633 |
| Beauvais_GVA375_467 | Beauvais, Villiers-de-l'Isle Adam | France | 1550CE | 1550 | A3 | ERS3213470 |
| TavanTolgoi_GEP13_730 | Tavan Tolgoi | Mongolia | 1287CE | 1287 | A4 | ERS3213603 |
| TavanTolgoi_GEP14_730 | Tavan Tolgoi | Mongolia | 1287CE | 1287 | A5 | ERS3213604 |

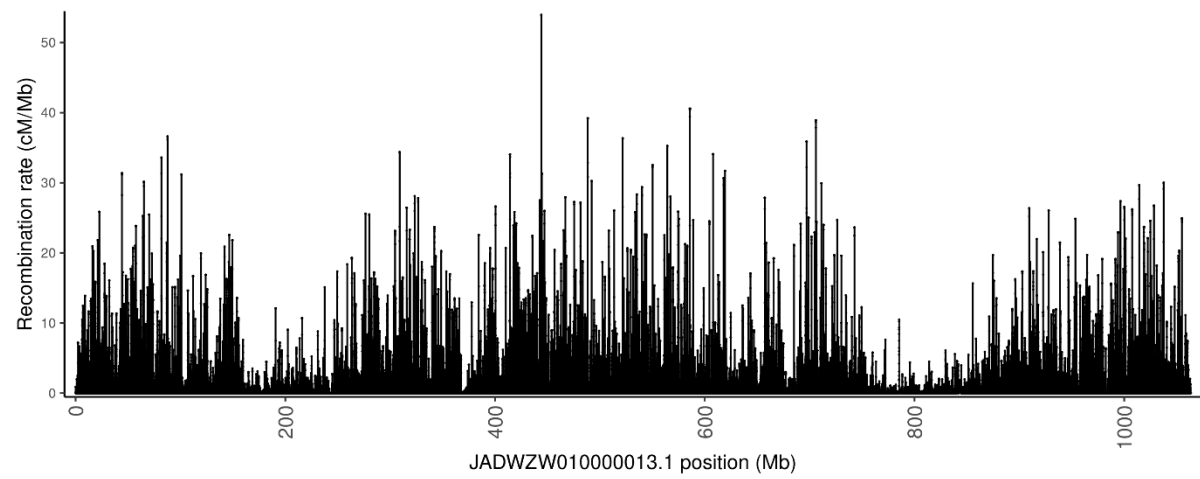
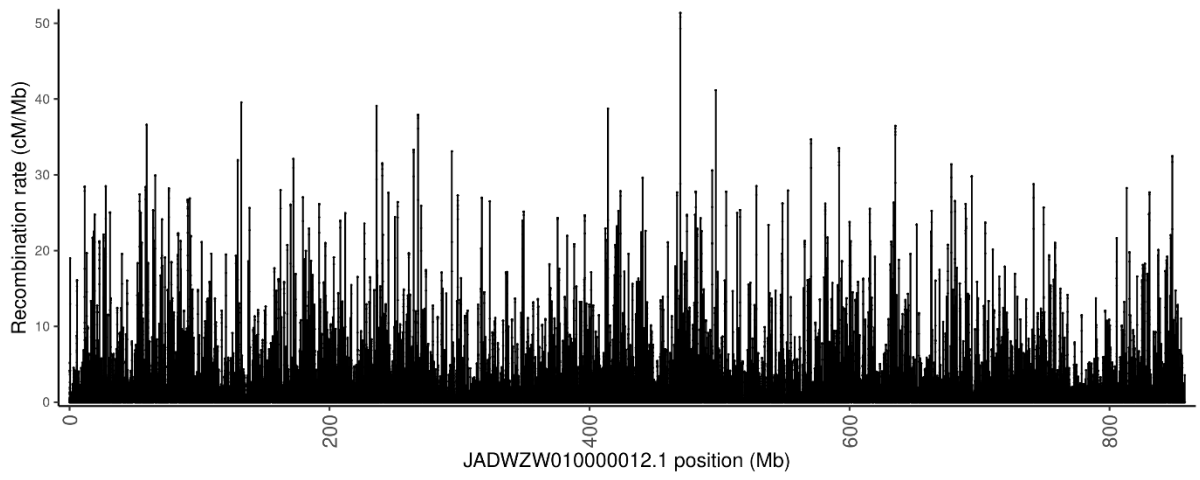
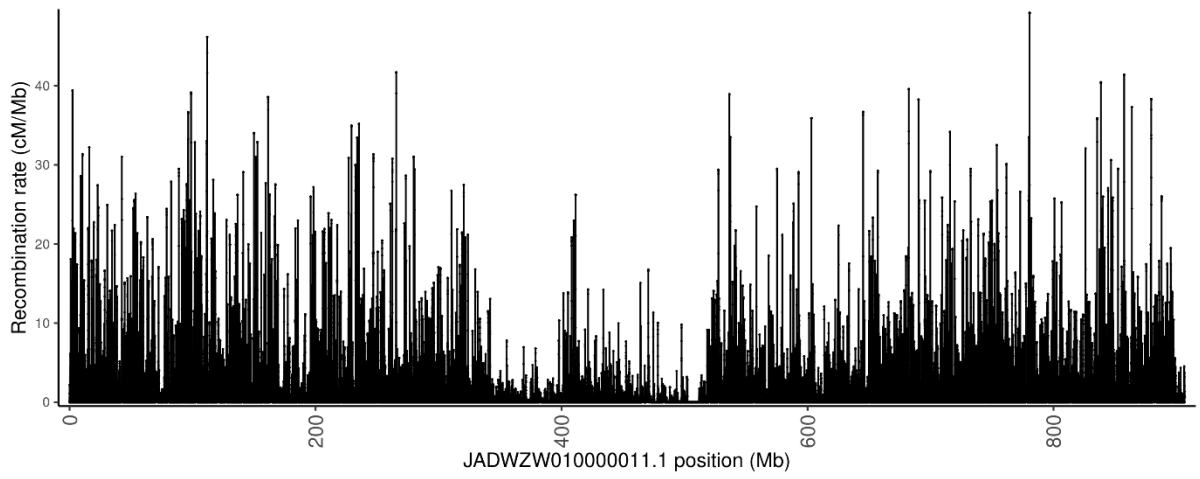
| | | | | | | |
|-------------------------------------|-------------------------------------|------------|--------|------|-----|------------|
| TavanTolgoi_GEP21_730 | Tavan Tolgoi | Mongolia | 1287CE | 1287 | A6 | ERS3213605 |
| Yenikapi_Tur150_1443 | Yenikapi | Turkey | 961CE | 961 | A7 | ERS3213646 |
| Yenikapi_Tur145_1156 | Yenikapi | Turkey | 951CE | 951 | A8 | ERS3213642 |
| Saadjarve_Saa1_1117 | Saadjärve | Estonia | 900CE | 900 | A9 | ERS3213583 |
| Nustar_5_1187 | Nuštar | Croatia | 830CE | 830 | A10 | ERS3213573 |
| Marvele_18_1189 | Marvele cemetery | Lithuania | 829CE | 829 | A11 | ERS3213561 |
| Marvele_32_1144 | Marvele cemetery | Lithuania | 829CE | 829 | A12 | ERS3213565 |
| Yenikapi_Tur229_1443 | Yenikapi | Turkey | 827CE | 827 | A13 | ERS3213660 |
| Grigorevka4_PAVH2_1192 | Gregorevka | Kazakhstan | 825CE | 825 | A14 | ERS1892698 |
| Yenikapi_Tur193_1443 | Yenikapi | Turkey | 792CE | 792 | A15 | ERS3213657 |
| Yenikapi_Tur140_1289 | Yenikapi | Turkey | 777CE | 777 | A16 | ERS3213638 |
| Khotont_UCIE2012x85_1291 | Khotont | Mongolia | 725CE | 725 | A17 | ERS3213547 |
| BozAdyr_KYRH10_1267 | Boz-Adyr | Kyrgyzstan | 700CE | 700 | A18 | ERS3213485 |
| BozAdyr_KYRH8_1267 | Boz-Adyr | Kyrgyzstan | 700CE | 700 | A19 | ERS3213486 |
| Yenikapi_Tur172_1695 | Yenikapi | Turkey | 674CE | 674 | A20 | ERS1892707 |
| Yenikapi_Tur194_1360 | Yenikapi | Turkey | 657CE | 657 | A21 | ERS3213658 |
| Yenikapi_Tur142_1396 | Yenikapi | Turkey | 648CE | 648 | A22 | ERS3213640 |
| Yenikapi_Tur141_1430 | Yenikapi | Turkey | 640CE | 640 | A23 | ERS3213639 |
| Yenikapi_Tur170_1443 | Yenikapi | Turkey | 601CE | 601 | A24 | ERS3213649 |
| SharIQumis_AM115_1557 | Shar-I-Qumis | Iran | 472CE | 472 | A25 | ERS3213596 |
| Yenikapi_Tur146_1730 | Yenikapi | Turkey | 350CE | 350 | A26 | ERS3213643 |
| Yenikapi_Tur171_1689 | Yenikapi | Turkey | 336CE | 336 | A27 | ERS3213650 |
| FrankfurtHeddenheim_Fr1_1863 | Frankfurt-Heddenheim | Germany | 180CE | 180 | A28 | ERS3213533 |
| Chartres_GVA26_1917 | Chartres, boulevard de la Courtille | France | 110CE | 110 | A29 | ERS3213502 |
| Chartres_GVA4_1917 | Chartres, boulevard de la Courtille | France | 110CE | 110 | A30 | ERS3213506 |
| Chartres_GVA43_1917 | Chartres, boulevard de la Courtille | France | 110CE | 110 | A31 | ERS3213507 |
| Chartres_GVA81_1917 | Chartres, boulevard de la Courtille | France | 110CE | 110 | A32 | ERS3213518 |
| GolModII_Mon24_1993 | Gol Mod II | Mongolia | 40CE | 40 | A33 | ERS3213535 |
| GolModII_Mon23_2007 | Gol Mod II | Mongolia | 35CE | 35 | A34 | ERS3213534 |
| GolModII_Mon26_1999 | Gol Mod II | Mongolia | 27CE | 27 | A35 | ERS3213537 |
| GolModII_Mon28_1988 | Gol Mod II | Mongolia | 27CE | 27 | A36 | ERS1892697 |
| GolModII_Mon25_2011 | Gol Mod II | Mongolia | 17CE | 17 | A37 | ERS3213536 |
| GolModII_Mon27_2011 | Gol Mod II | Mongolia | 17CE | 17 | A38 | ERS3213538 |
| SaintJust_GVA242_2250 | Saint-Just-en-Chaussée | France | 75BCE | -75 | A39 | ERS3213589 |
| Actiparc_GVA308_2312 | Actiparc | France | 210BCE | -210 | A40 | ERS3213454 |
| AC7970_AMIS-1-00131_Tur_m290 | Acemhoyuk | Turkey | 290BCE | -290 | A41 | ERS7255955 |
| OlonKurinGol_OKG2_2367 | Olon Kurin Gol | Mongolia | 350BCE | -350 | A42 | ERS3213577 |
| Fetusx9m_CGG-1-022147_Spa_m475 | Els Vilars | Spain | 475BCE | -475 | A43 | ERS7256018 |
| SV2019x18_AMIS-1-02382_Tun_m581 | Althiburos | Tunisia | 581BCE | -581 | A44 | ERS7256181 |
| 18ELTu18_AMIS-1-01102_Spa_m588 | El Turuñuelo | Spain | 588BCE | -588 | A45 | ERS7255954 |
| SV2019x19_AMIS-1-02383_Tun_m643 | Althiburos | Tunisia | 643BCE | -643 | A46 | ERS7256182 |
| UE4618_CGG_1_020962 | Els Vilars | Spain | 655BCE | -655 | A47 | ERS3213526 |
| Hasanlu1140_CGG-1-019998_Ira_m663 | Tepe Hasanlu | Iran | 663BCE | -663 | A48 | ERS7256042 |
| UE11080x11082_CGG-1-020973_Spa_m664 | Els Vilars | Spain | 664BCE | -664 | A49 | ERS7256188 |
| Rid1_CGG_1_018468 | Ridala | Estonia | 700BCE | -700 | A50 | ERS7256148 |

| | | | | | | |
|-----------------------------------|---------------|----------|---------|-------|-----|------------|
| Rid2_CGG_1_018469 | Ridala | Estonia | 700BCE | -700 | A51 | ERS7256149 |
| Hasanlu2327_CGG-1-019995_Ira_m768 | Tepe Hasanlu | Iran | 768BCE | -768 | A52 | ERS7256043 |
| Hasanlu3398_CGG-1-019986_Ira_m768 | Tepe Hasanlu | Iran | 768BCE | -768 | A53 | ERS7256046 |
| HasanluV31E_CGG-1-021461_Ira_m768 | Tepe Hasanlu | Iran | 768BCE | -768 | A54 | ERS7256049 |
| Hasanlu3394_CGG-1-019997_Ira_m790 | Tepe Hasanlu | Iran | 790BCE | -790 | A55 | ERS7256045 |
| Fen4_CGG-1-018396_Chi_m800 | Fengtai | China | 800BCE | -800 | A56 | ERS7256017 |
| Hasanlu2405_CGG-1-019992_Ira_m868 | Tepe Hasanlu | Iran | 868BCE | -868 | A57 | ERS7256044 |
| Hasanlu368_CGG-1-019994_Ira_m878 | Tepe Hasanlu | Iran | 878BCE | -878 | A58 | ERS7256048 |
| Hasanlu3461_CGG-1-020003_Ira_m913 | Tepe Hasanlu | Iran | 913BCE | -913 | A59 | ERS7256047 |
| CD5203_AMIS-1-00107_Tur_m985 | Çadır Höyük | Turkey | 985BCE | -985 | A60 | ERS7255998 |
| UushgiinUvur_Mon45_3080 | Uushgiin Uvur | Mongolia | 1065BCE | -1065 | A61 | ERS3213624 |
| UushgiinUvur_Mon37_3085 | Uushgiin Uvur | Mongolia | 1075BCE | -1075 | A62 | ERS3213617 |
| UushgiinUvur_Mon39_3085 | Uushgiin Uvur | Mongolia | 1075BCE | -1075 | A63 | ERS3213618 |
| UushgiinUvur_Mon84_3123 | Uushgiin Uvur | Mongolia | 1075BCE | -1075 | A64 | ERS1892705 |
| UushgiinUvur_Mon86_3039 | Uushgiin Uvur | Mongolia | 1075BCE | -1075 | A65 | ERS1892706 |
| SAGxS27_CGG-1-019559_Ira_m1102 | Sagzabad | Iran | 1102BCE | -1102 | A66 | ERS7256175 |
| UushgiinUvur_Mon87_3117 | Uushgiin Uvur | Mongolia | 1103BCE | -1103 | A67 | ERS3213626 |
| Mon43_CGG_1_018079 | Uushgiin Uvur | Mongolia | 1106BCE | -1106 | A68 | ERS3213622 |
| UushgiinUvur_Mon42_3130 | Uushgiin Uvur | Mongolia | 1110BCE | -1110 | A69 | ERS3213621 |
| CD1819_AMIS-1-00115_Tur_m1299 | Çadır Höyük | Turkey | 1299BCE | -1299 | A70 | ERS7255996 |
| Bateni_Rus16_3350 | Bateni | Russia | 1336BCE | -1336 | A71 | ERS3213468 |
| TP4_CGG-1-018394_Geo_m1578 | Tachtı Perda | Georgia | 1578BCE | -1578 | A72 | ERS7256186 |
| AC9016_AMIS-1-00134_Tur_m1900 | Acemhoyuk | Turkey | 1900BCE | -1900 | A73 | ERS7255957 |
| Sintashta_NB46_4023 | Sintashta | Russia | 2009BCE | -2009 | A74 | ERS821436 |
| AC8811_AMIS-1-00133_Tur_m2125 | Acemhoyuk | Turkey | 2125BCE | -2125 | A75 | ERS7255956 |

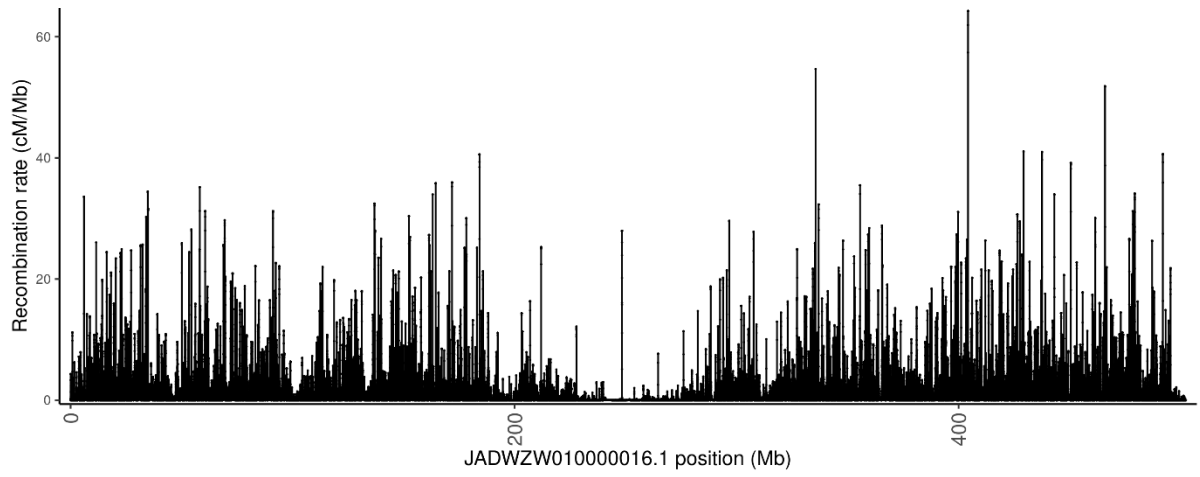
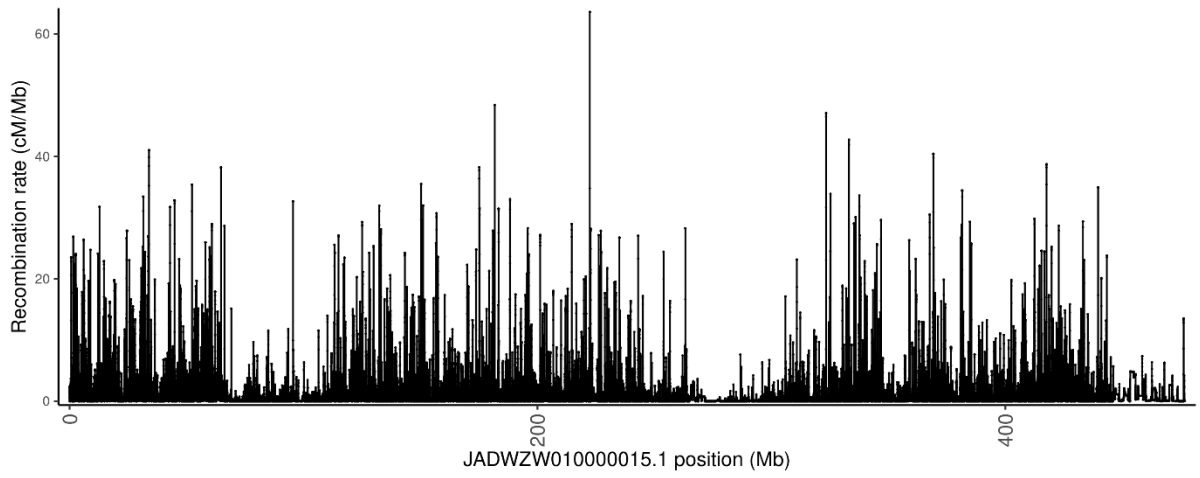
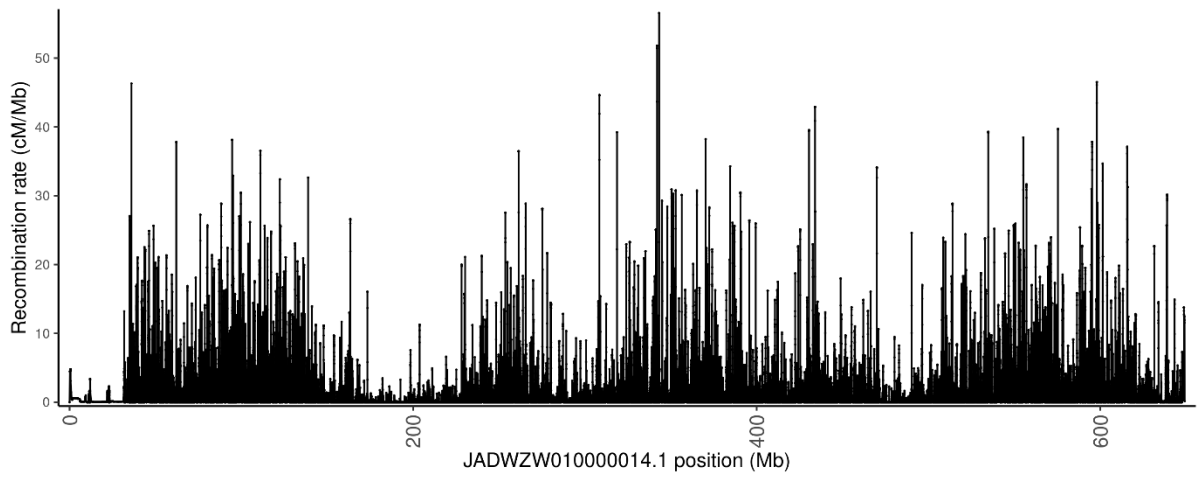


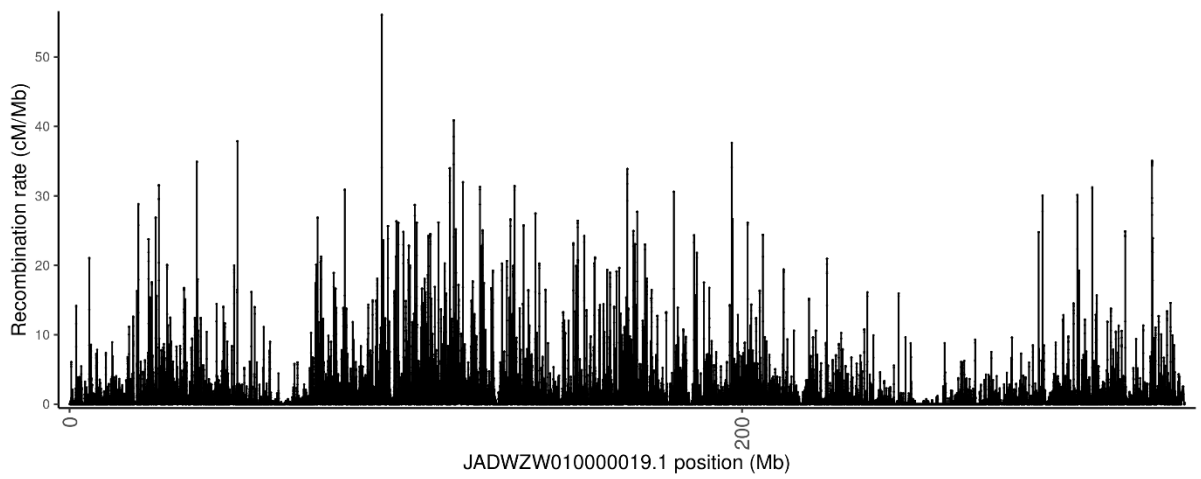
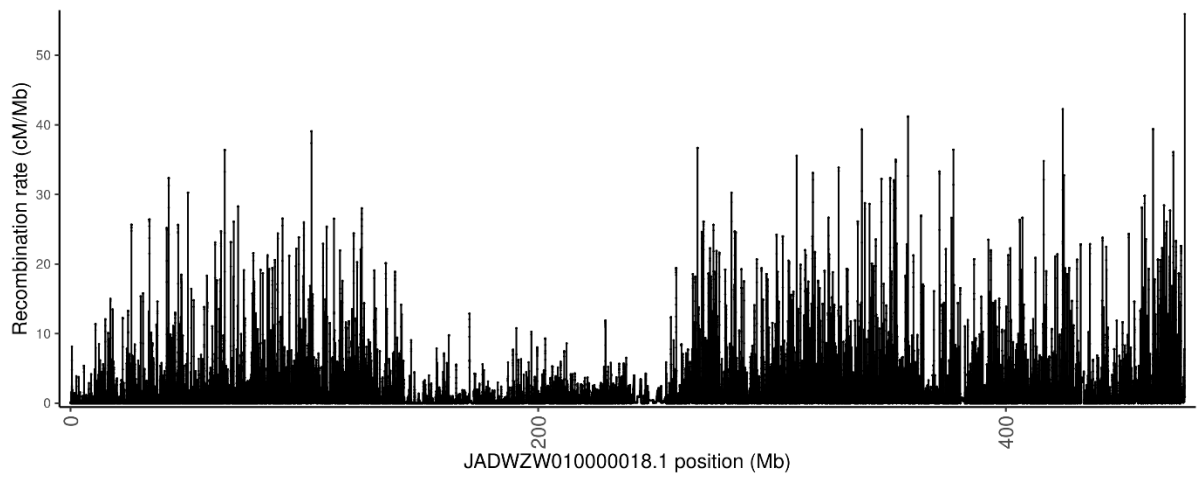
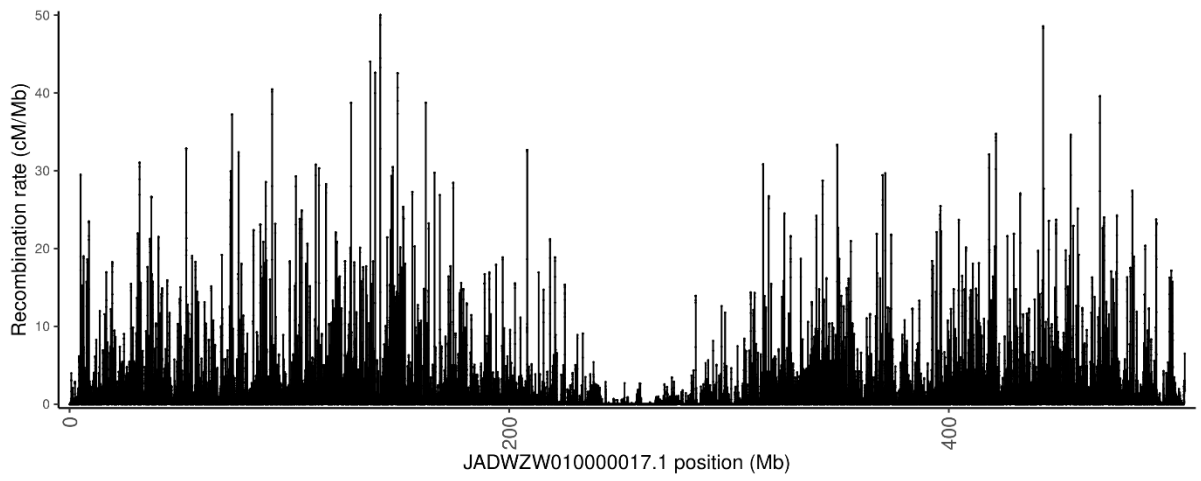


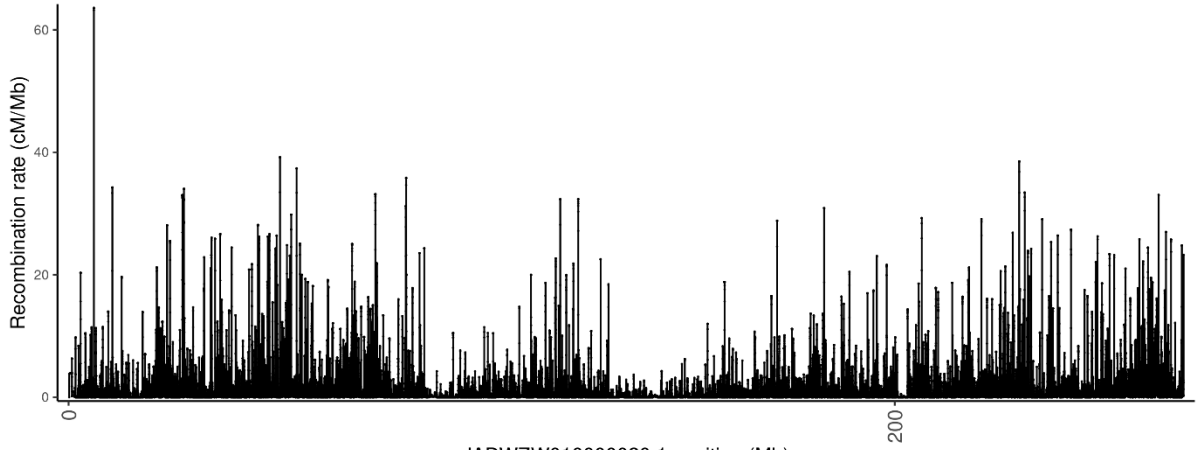




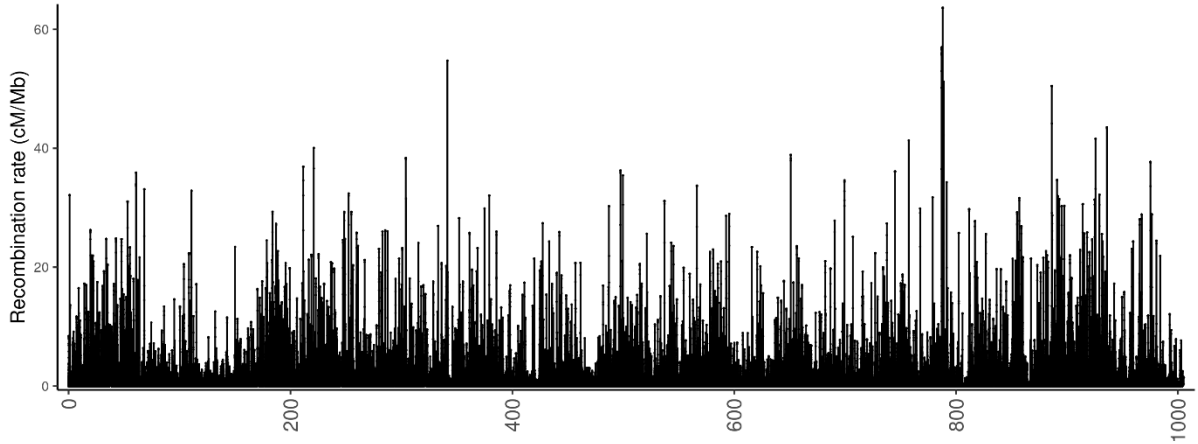
887



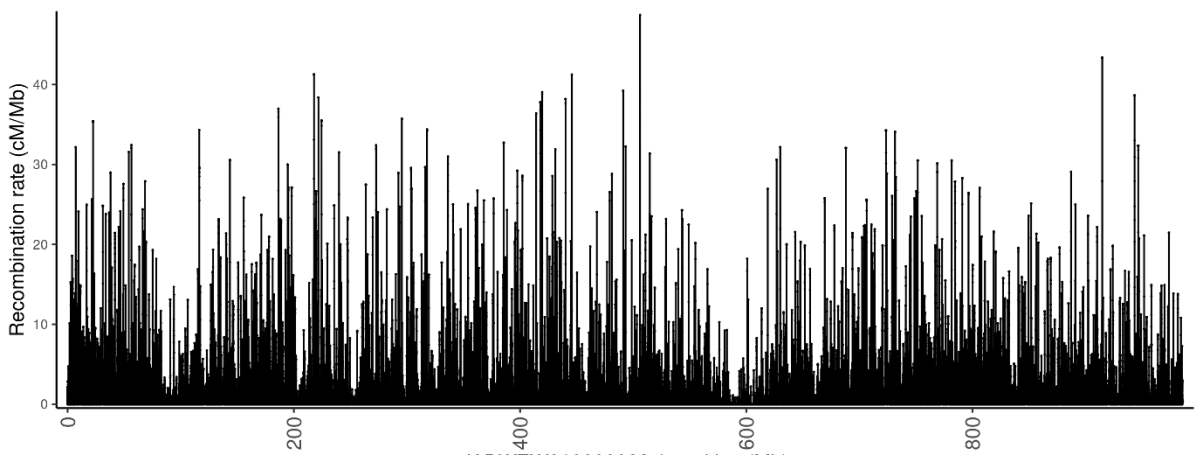




JADWZW010000020.1 position (Mb)

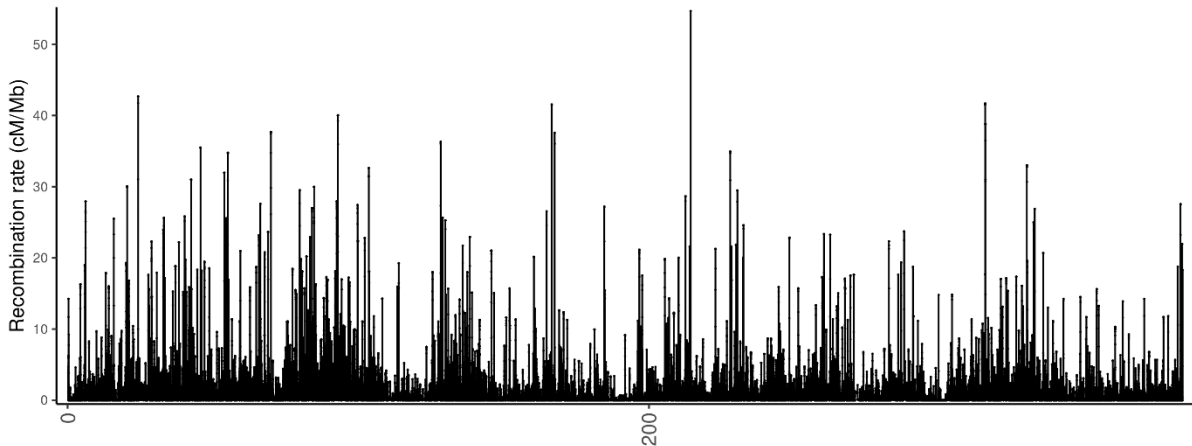


JADWZW010000021.1 position (Mb)

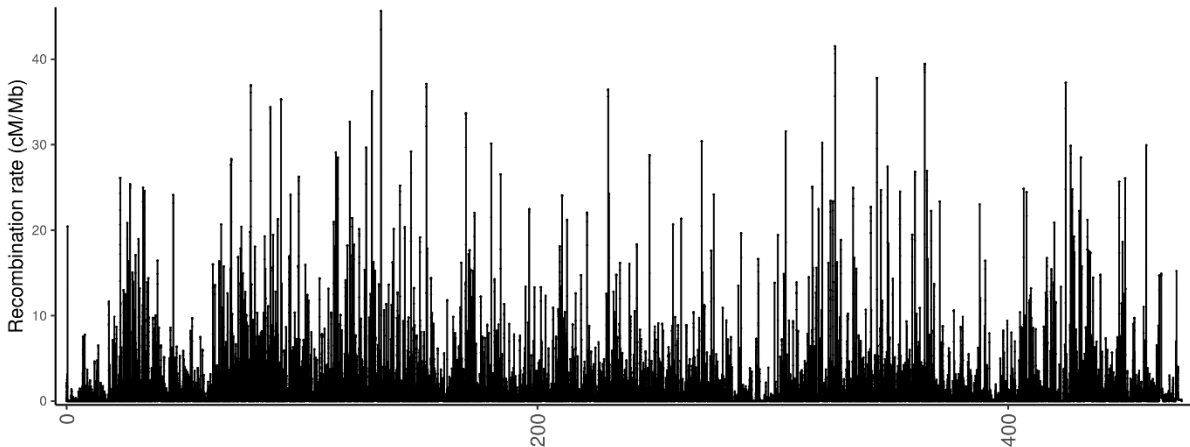


JADWZW010000022.1 position (Mb)

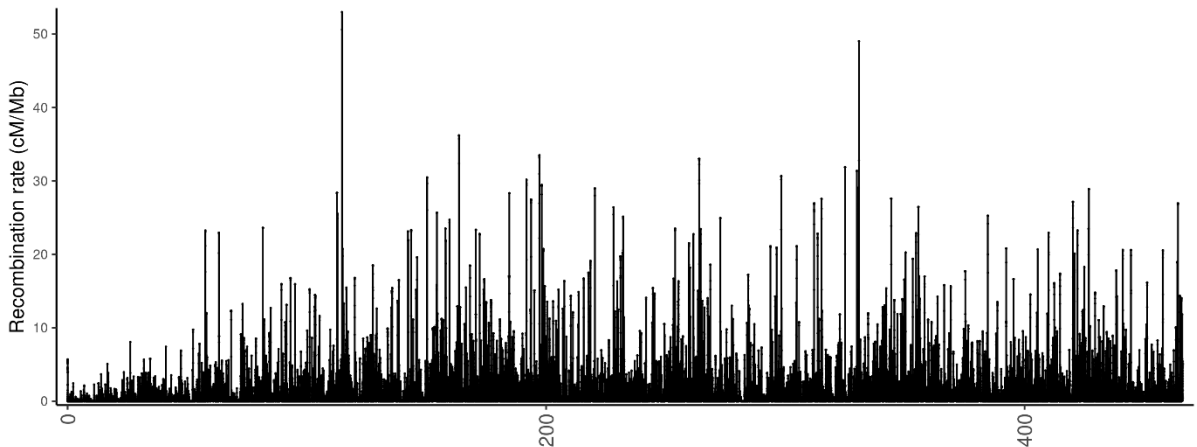
890



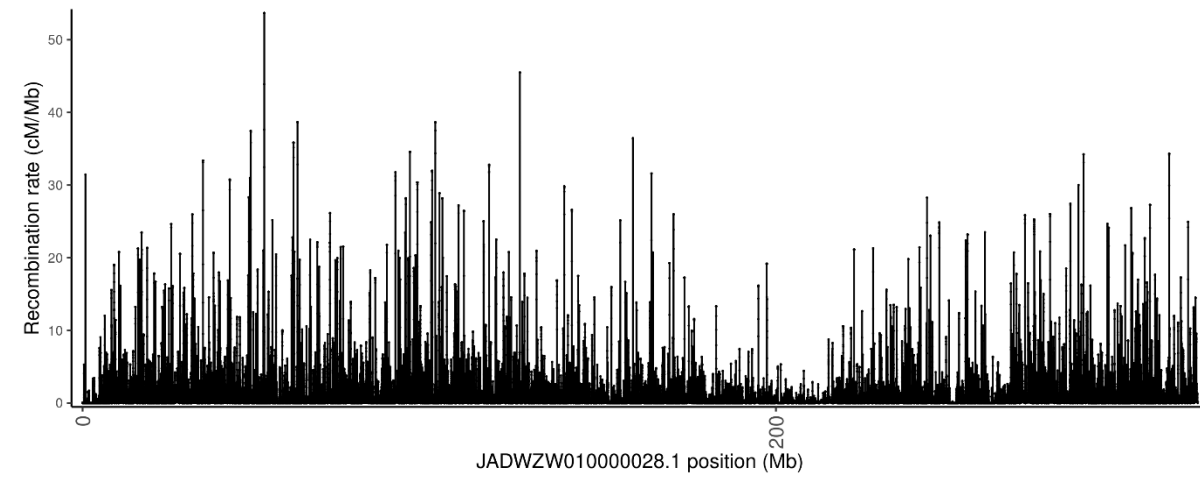
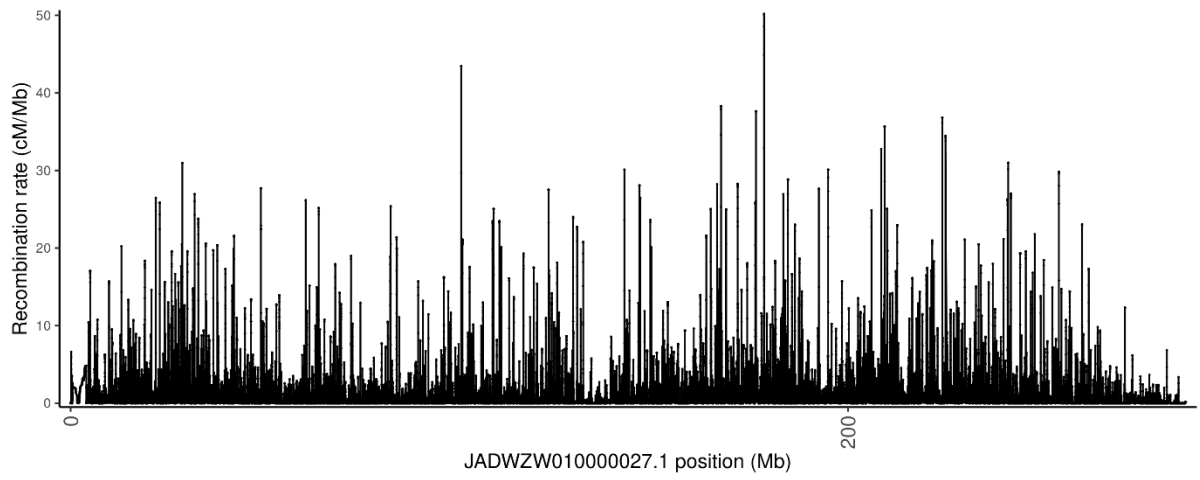
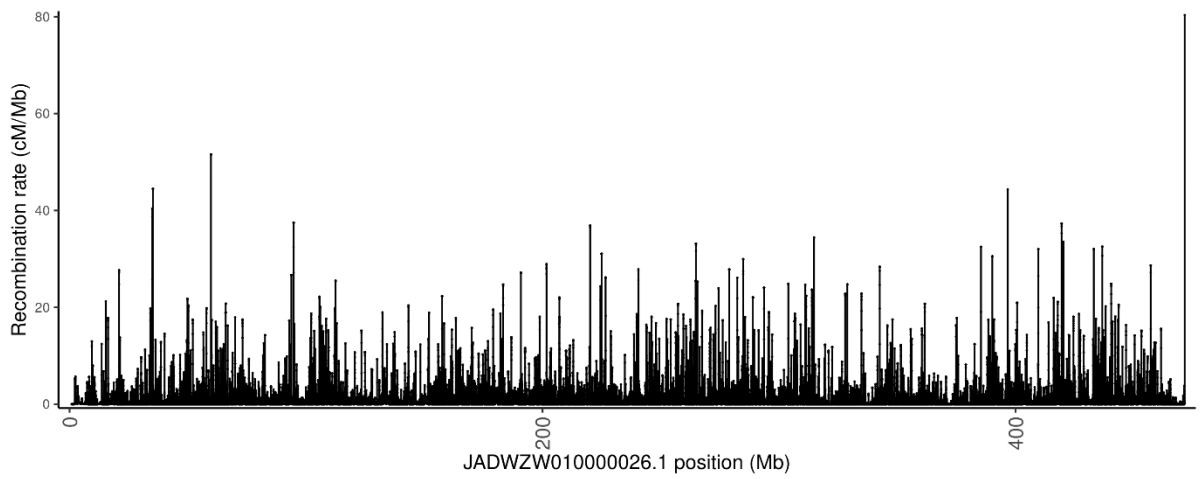
JADWZW01000023.1 position (Mb)



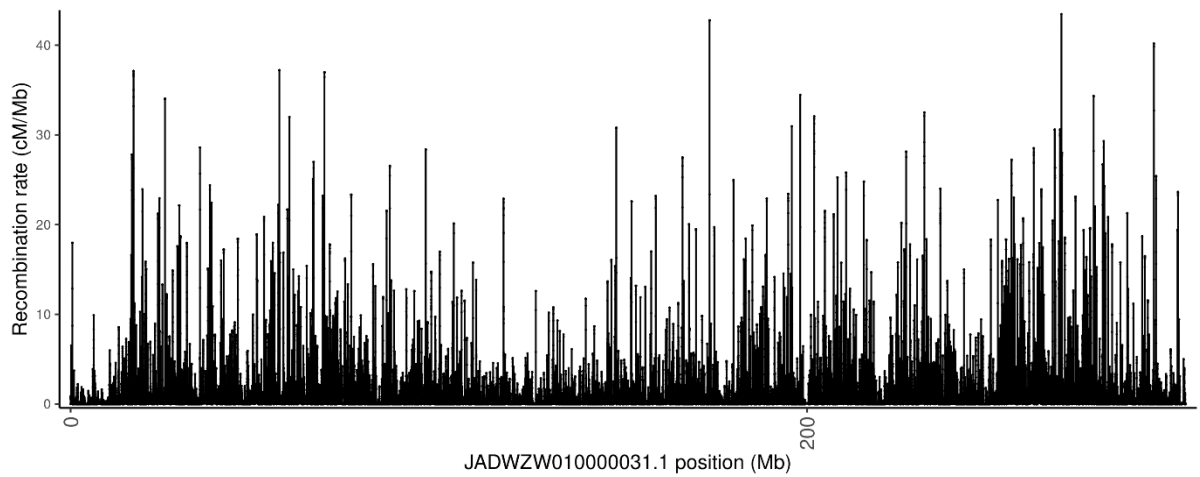
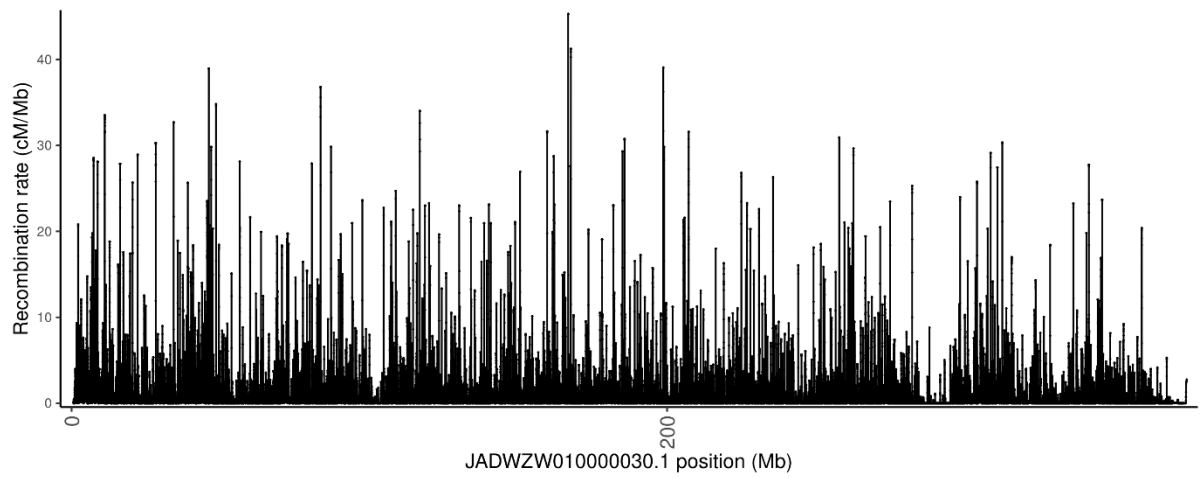
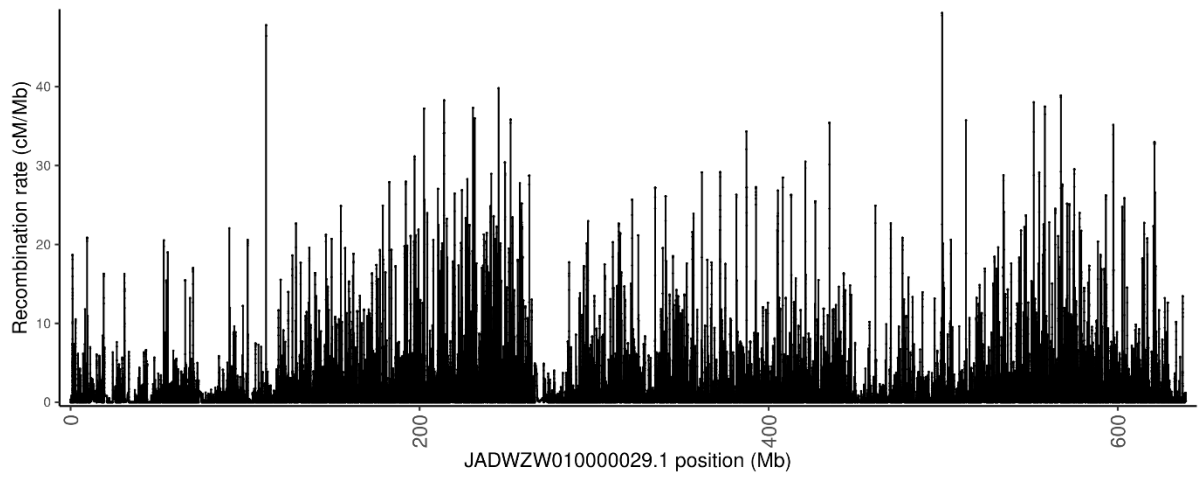
JADWZW01000024.1 position (Mb)



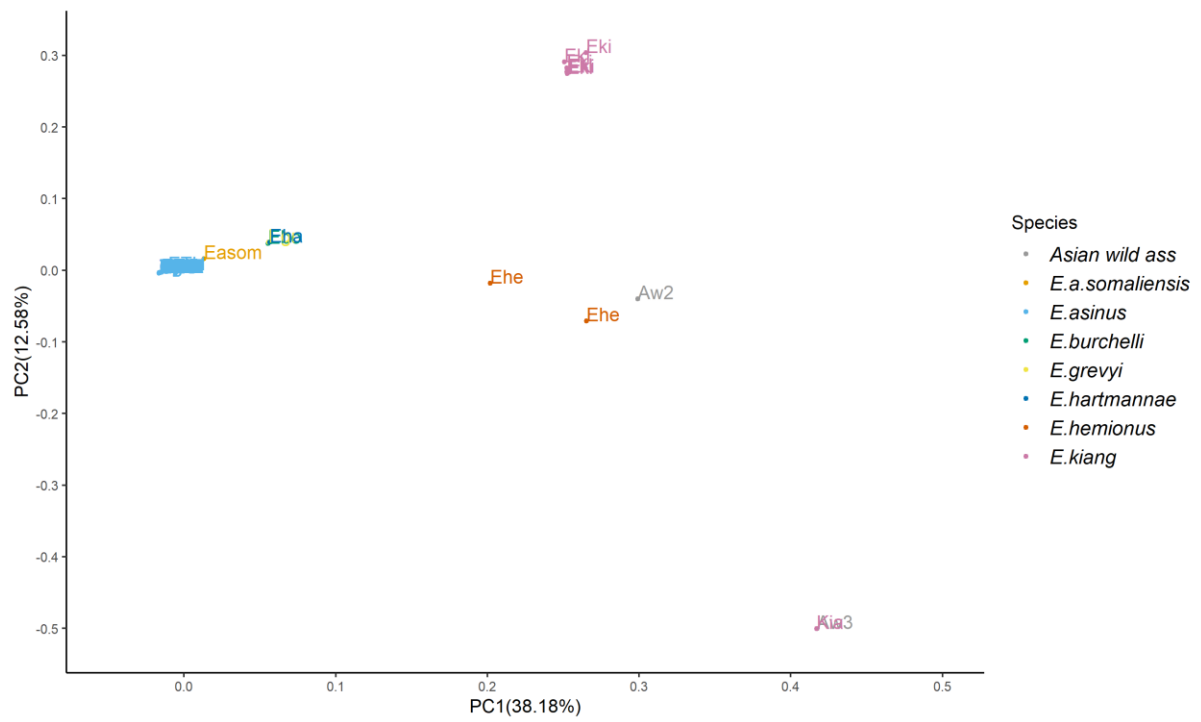
JADWZW01000025.1 position (Mb)



892

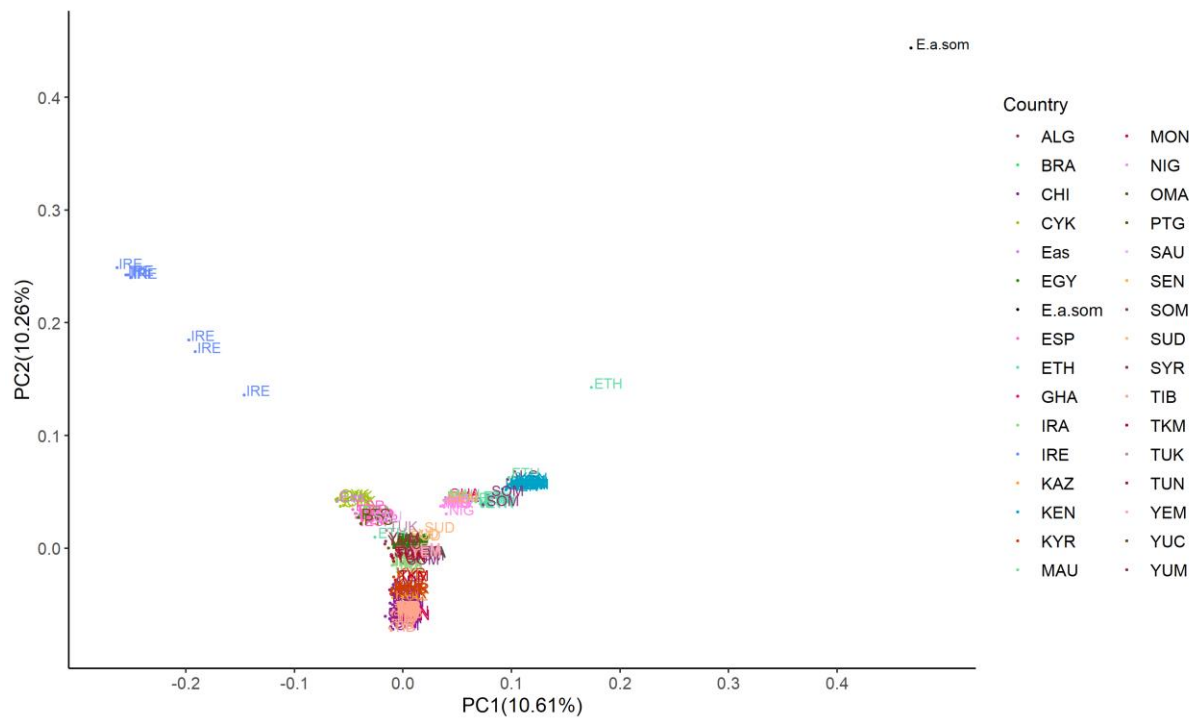


893 **Fig. S1:** Recombination rates across all 30 donkey autosomes as estimated using LDHat
 894 (version 2.2) (62).



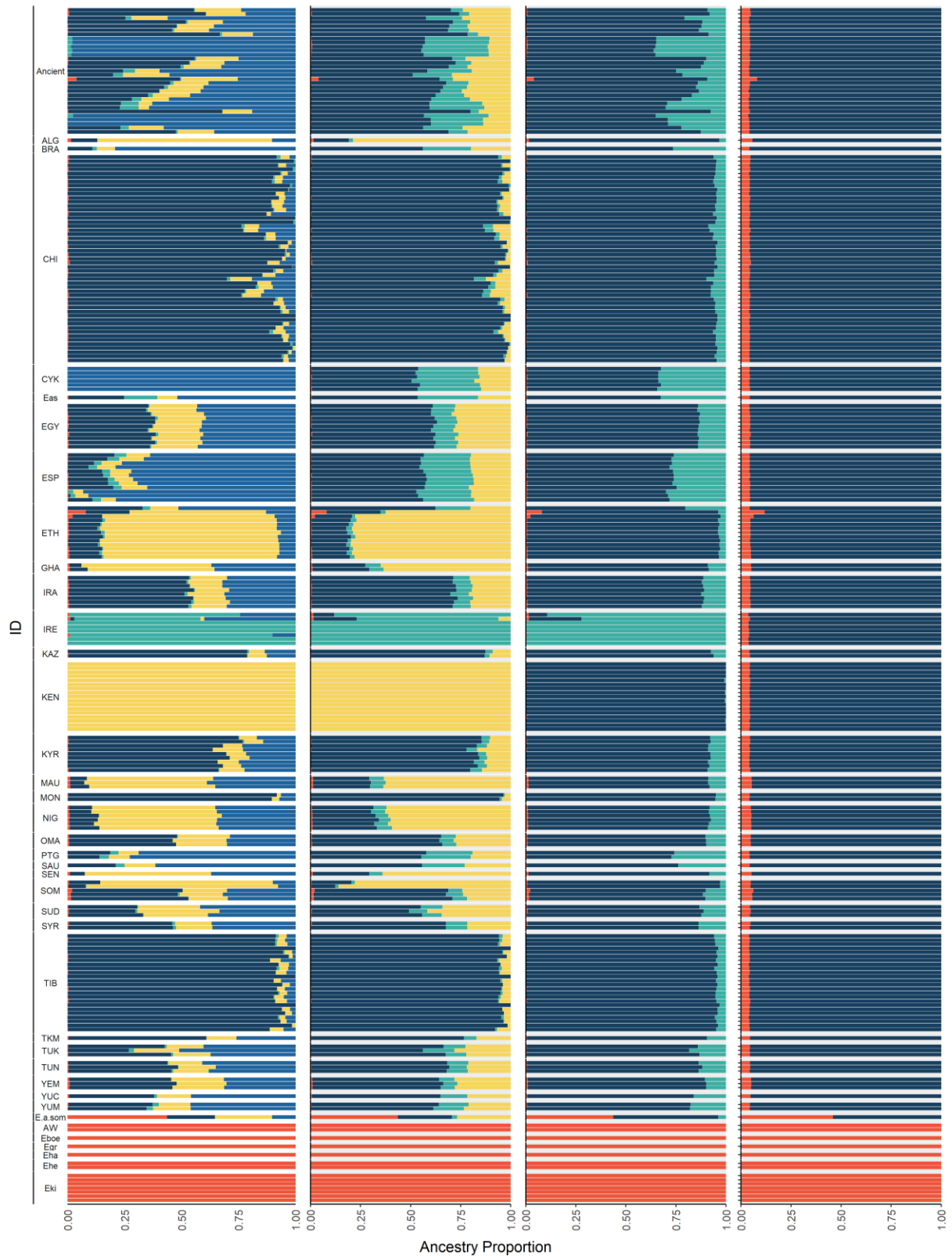
895
896
897

Fig. S2: PCA of domestic donkeys and wild ass species using the phased variant panel ($n=222$ individuals, $n=13,013,551$ variants, $TI/TV=2.18$) using PLINK (version 1.9) (63).

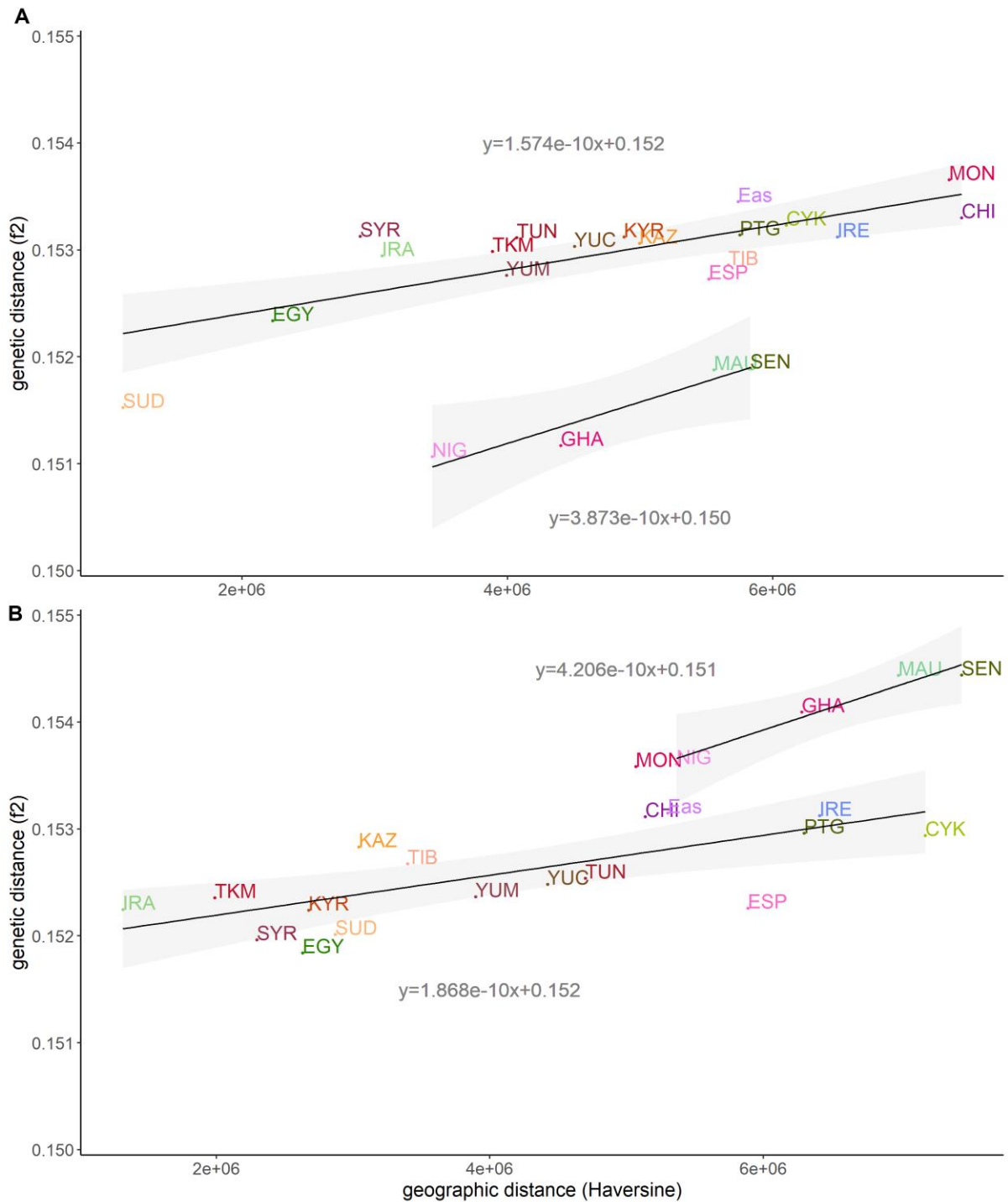


898
 899
 900
 901

Fig. S3: PCA of domestic donkeys and wild ass species (*E.a.som*) using the phased variant panel ($n=208$ individuals, $n=13,013,551$ variants, $TS/TV=2.18$) using PLINK (version 1.9) (63).

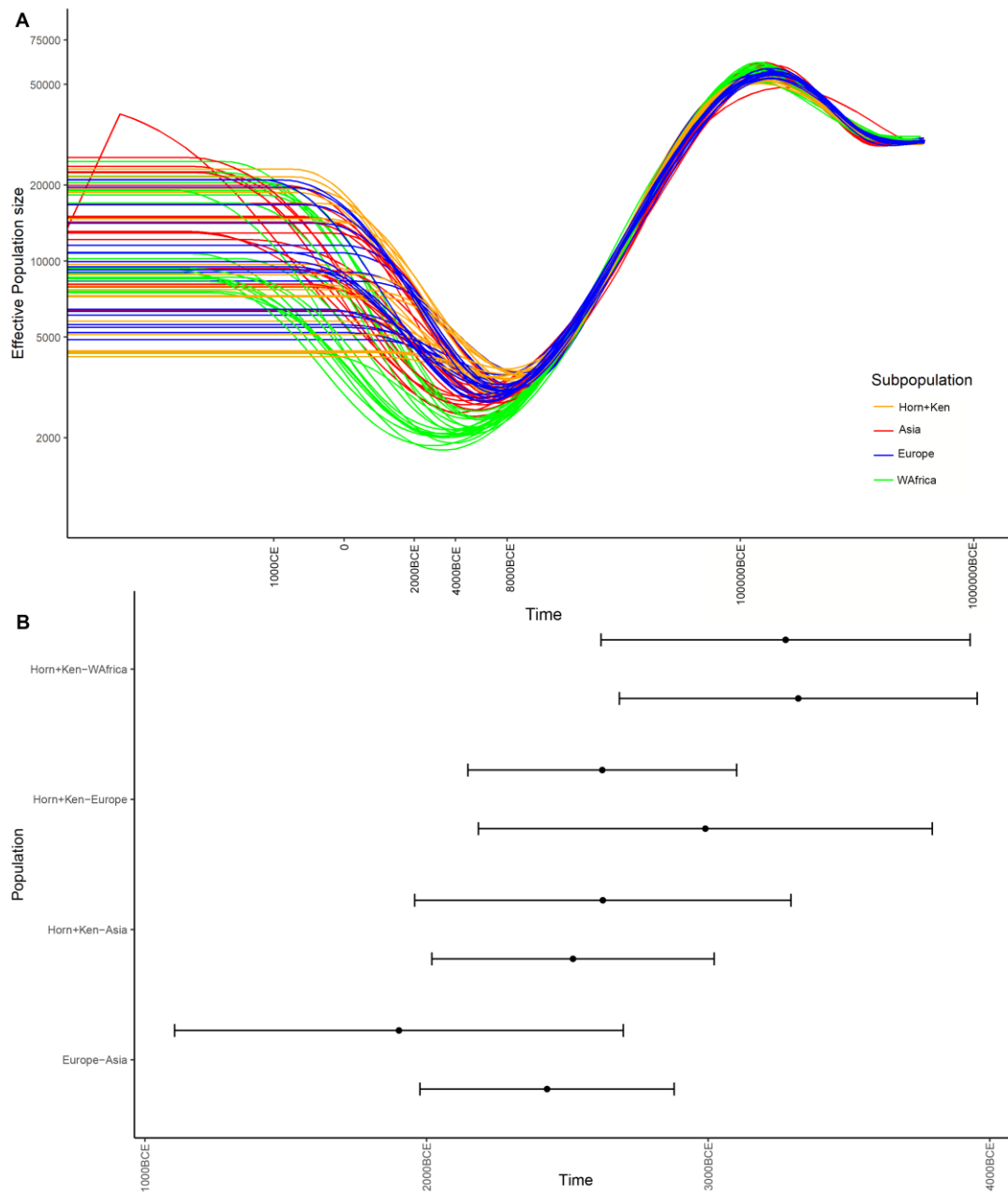


902 **Fig. S4:** ADMIXTURE (version 1.3.0) (56) analysis for all modern equids (donkeys and wild
 903 asses) and ancient donkeys using the imputed variant panel for K values of 2-5 ($n=222$
 904 modern equids, $n=31$ ancient donkeys, $n=494,050$ variants, $TI/TV= 2.18$, optimal $K=4$).

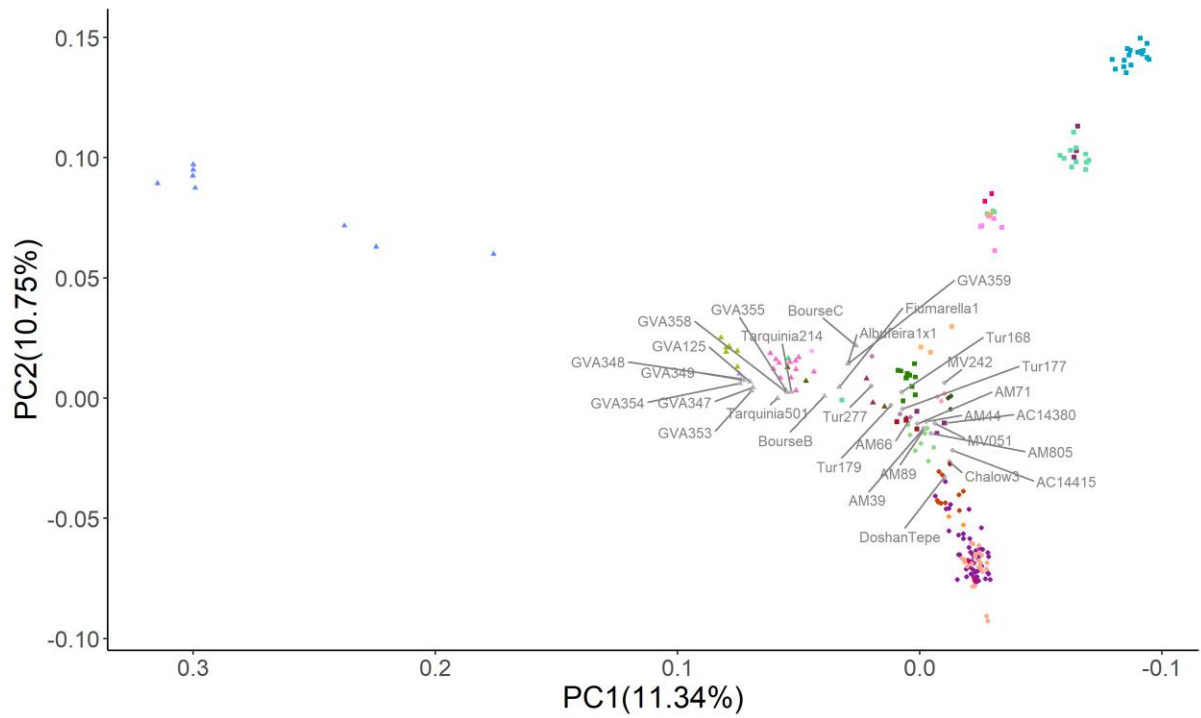


905
 906
 907
 908
 909
 910
 911
 912

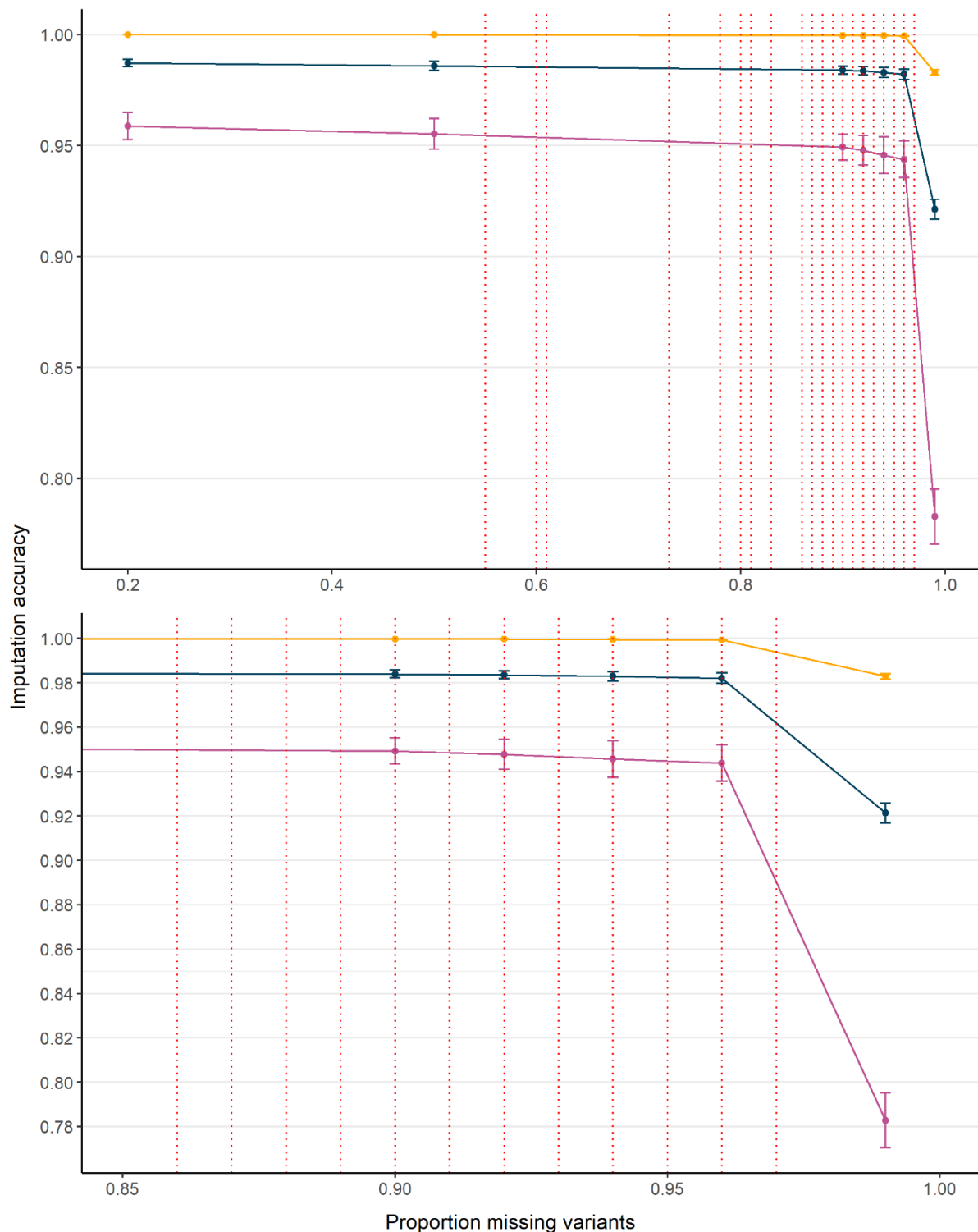
Fig. S5: Genetic distance (f2, estimated using ADMIXTOOLS2) (124, 125) verses geographical distance (estimated as haversine distance) from: A) donkeys from Ethiopia, and B) donkeys from Yemen. Two separate linear regressions were fitted for each dataset: one for subpopulations from western Africa only, and another for all other subpopulations. F2 statistics were estimated for all phased SNPs, but masking regions that were attributed to wild ancestry as estimated using PCAdmix ($n=11,577,531$ variants, $TI/TV=2.18$).



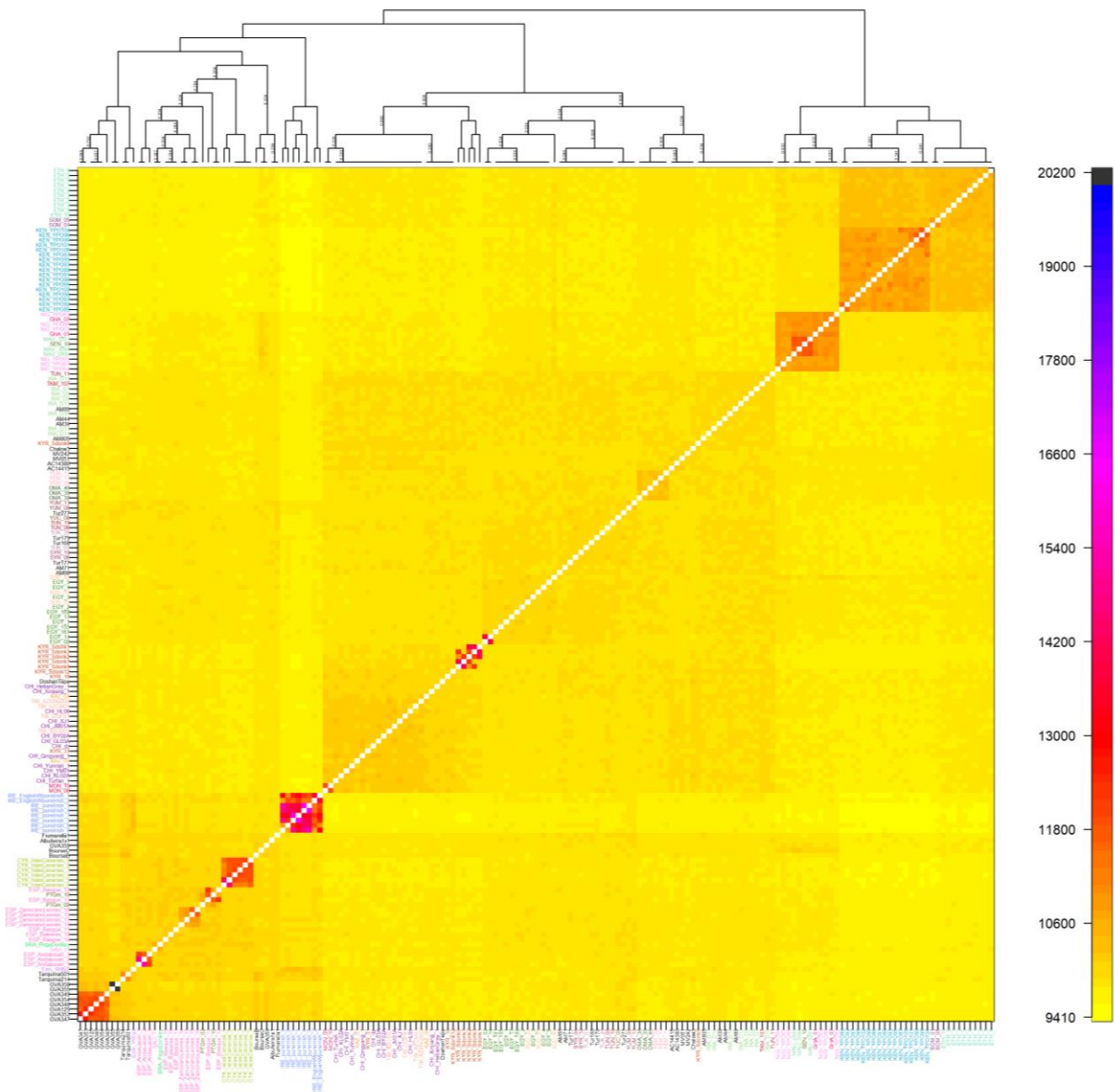
913 **Fig. S6:** SMC++ (version 1.15.4) (28) population models dating splits from Horn of Africa +
 914 Kenya (Horn+Ken), western Africa (WAfrica), Asia (Asia) and Europe (Europe) with an
 915 assumed generational time interval of 8 years. Three donkeys from each subpopulation were
 916 used, with 10 bootstrap pseudo-replicates (resampling 90% of each chromosome) for two
 917 different datasets. Samples used for the first dataset were Horn+Ken: KEN_YPO90, ETH_4,
 918 SOM_01, WAfrica: SEN_10, GHA_01, NIG_YPO62, Asia: CHI_KL02A, CHI_GL04A,
 919 TIB_DQFS1, Europe: PTGm10, ESP_Andalusian_1, CYK_IslasCanarias_4. The samples
 920 used for the second dataset were Horn+Ken: KEN_YPO89, SOM_05, ETH_5, WAfrica:
 921 NIG_YPO63, NIG_YPO65, NIG_YPO66, Asia: CHI_JM05A, CHI_XJ6, TIB_XZSNQS07,
 922 Europe: PTGm02, ESP_Andalusian_3, ESP_Basque_10. A) Estimated effective population
 923 sizes over time (the second dataset is shown in semi transparency). B) Estimated population
 924 split times between the subpopulations for the two datasets with standard deviation bars.



925
 926 **Fig. S7:** PCA of ancient imputed donkeys (black, n=31) and modern donkeys (coloured,
 927 n=206) using the smartpca program from the EIGENSOFT package (version 6.1.4) (75, 76).
 928 The pseudo-haploidized genomes of the ancient donkeys (n=31) were projected onto the PCA
 929 and labelled and colored in grey.

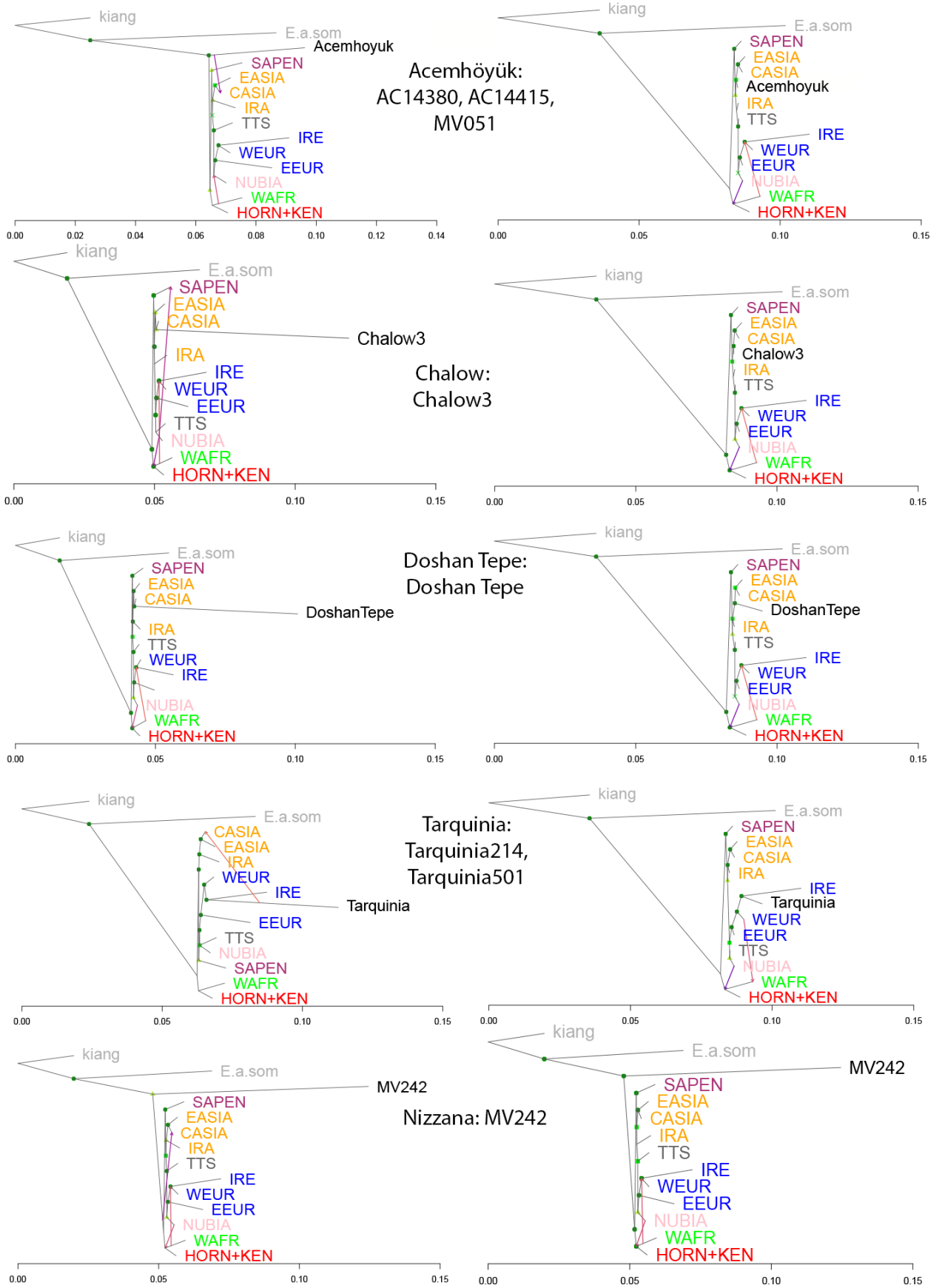


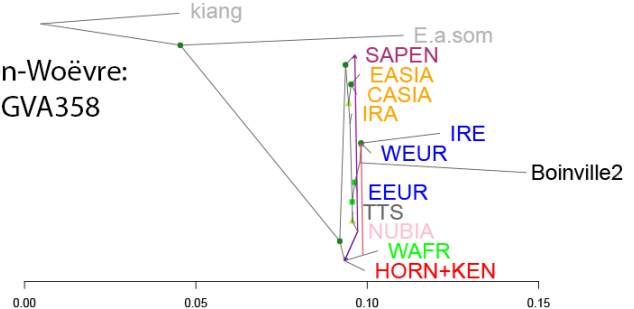
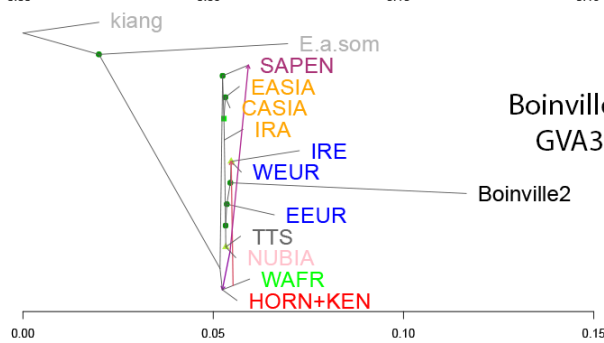
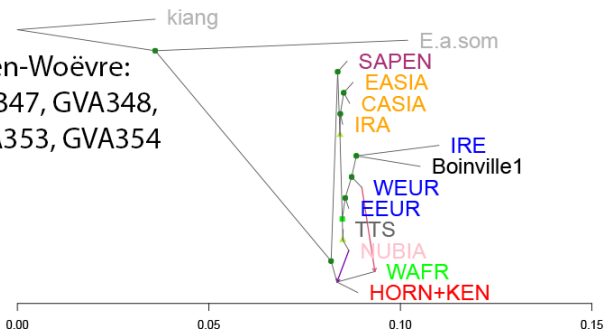
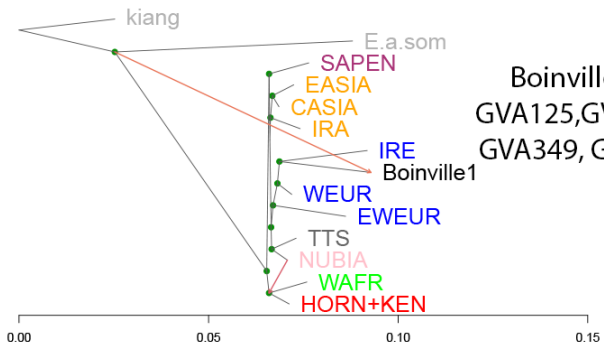
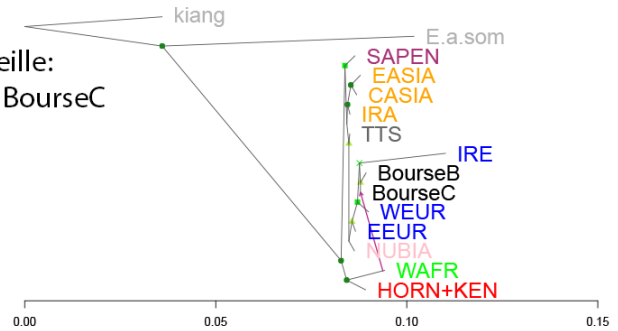
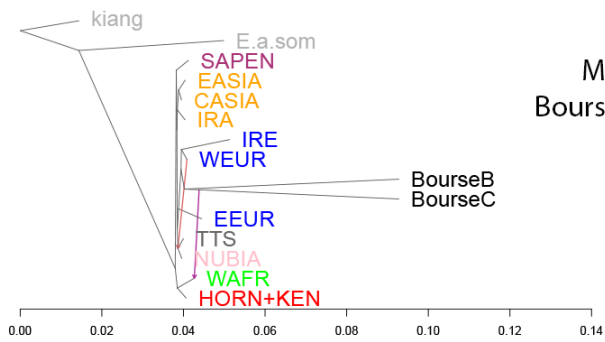
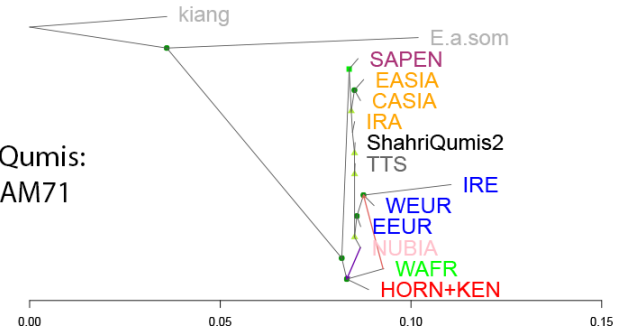
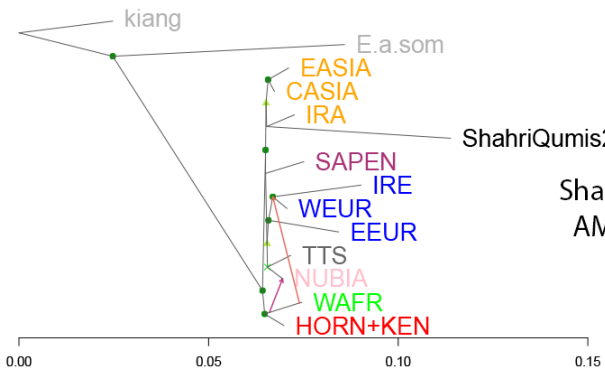
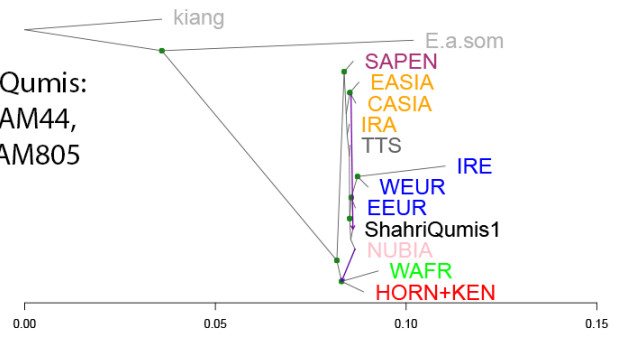
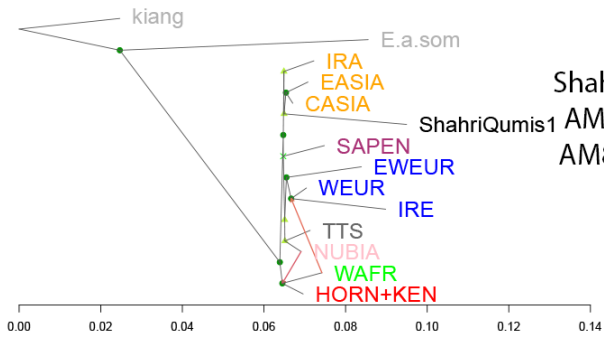
930 **Fig. S8:** The imputation accuracy versus the proportion of missing variants before imputation
 931 as estimated by downscaling modern donkey variants ($n=10$ individuals). Accuracy of all
 932 variants (blue), homozygotes only (yellow) and heterozygotes only (purple) and plotted
 933 separately. The same imputation pipeline was used as that to impute the ancient donkey
 934 genomes. The proportion of missing variants for each ancient sample ($n=31$) are shown as red
 935 dotted lines.

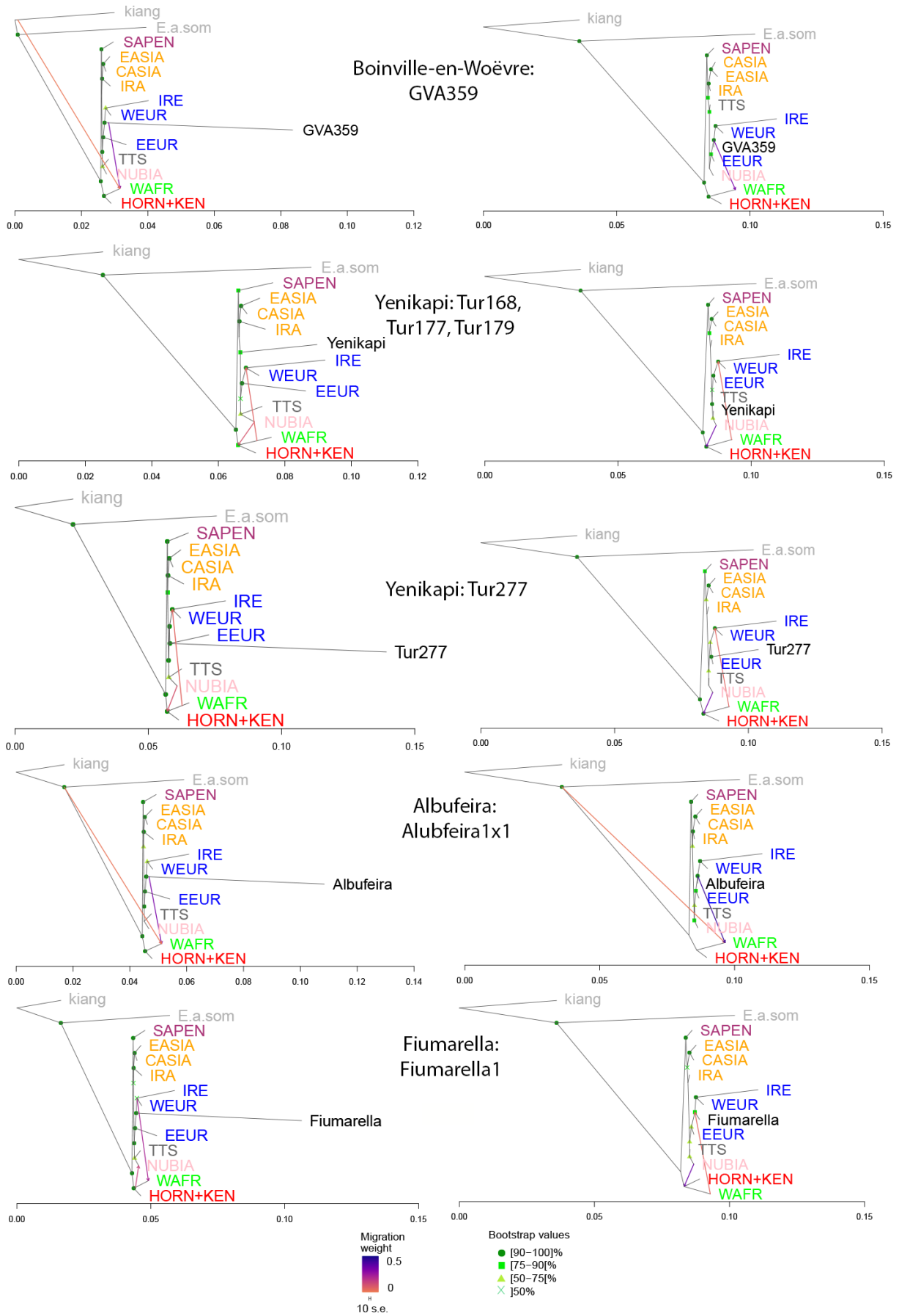


936

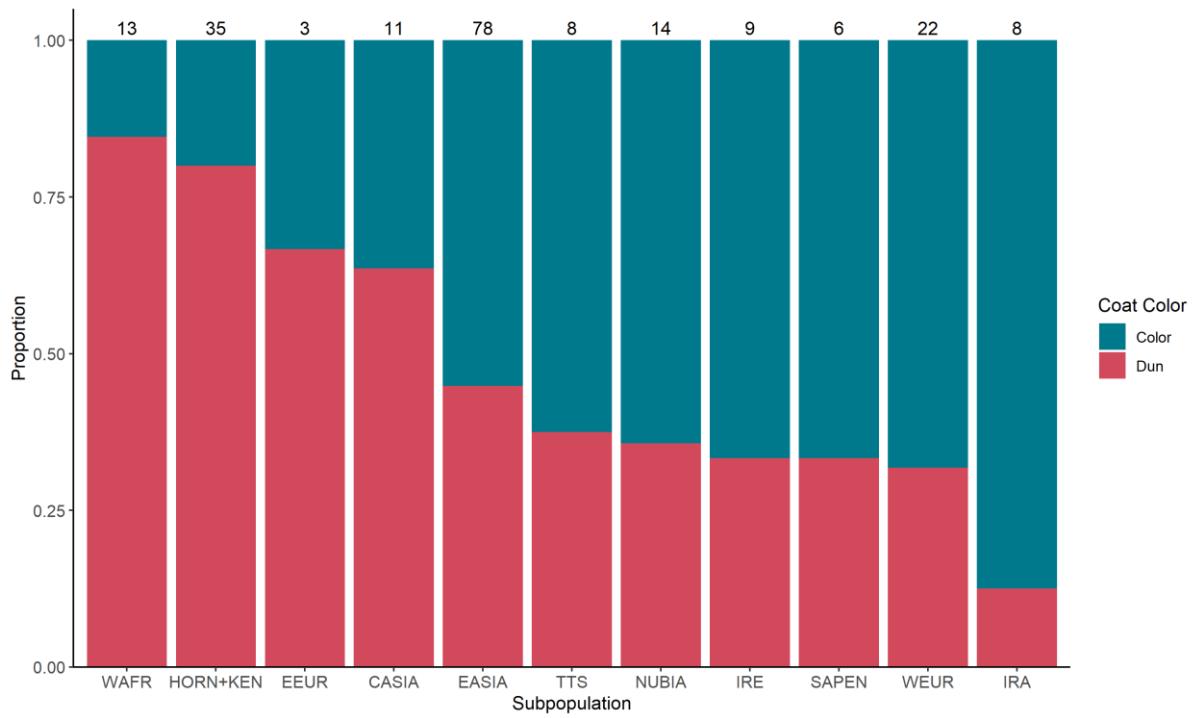
937 **Fig. S9:** Maximum likelihood tree and heatmap generated from haplotype sharedness
 938 estimated using fineSTRUCTURE (version 4.1.1) for donkeys ($n=141$ modern and 31 ancient
 939 individuals) using imputed variants ($n=2,245,992$, $TI/TV=2.21$) (35). Only node support
 940 values less than 1 are shown on the tree. The heatmap is colour coded according to the
 941 number of shared haplotype chunks in the genome.



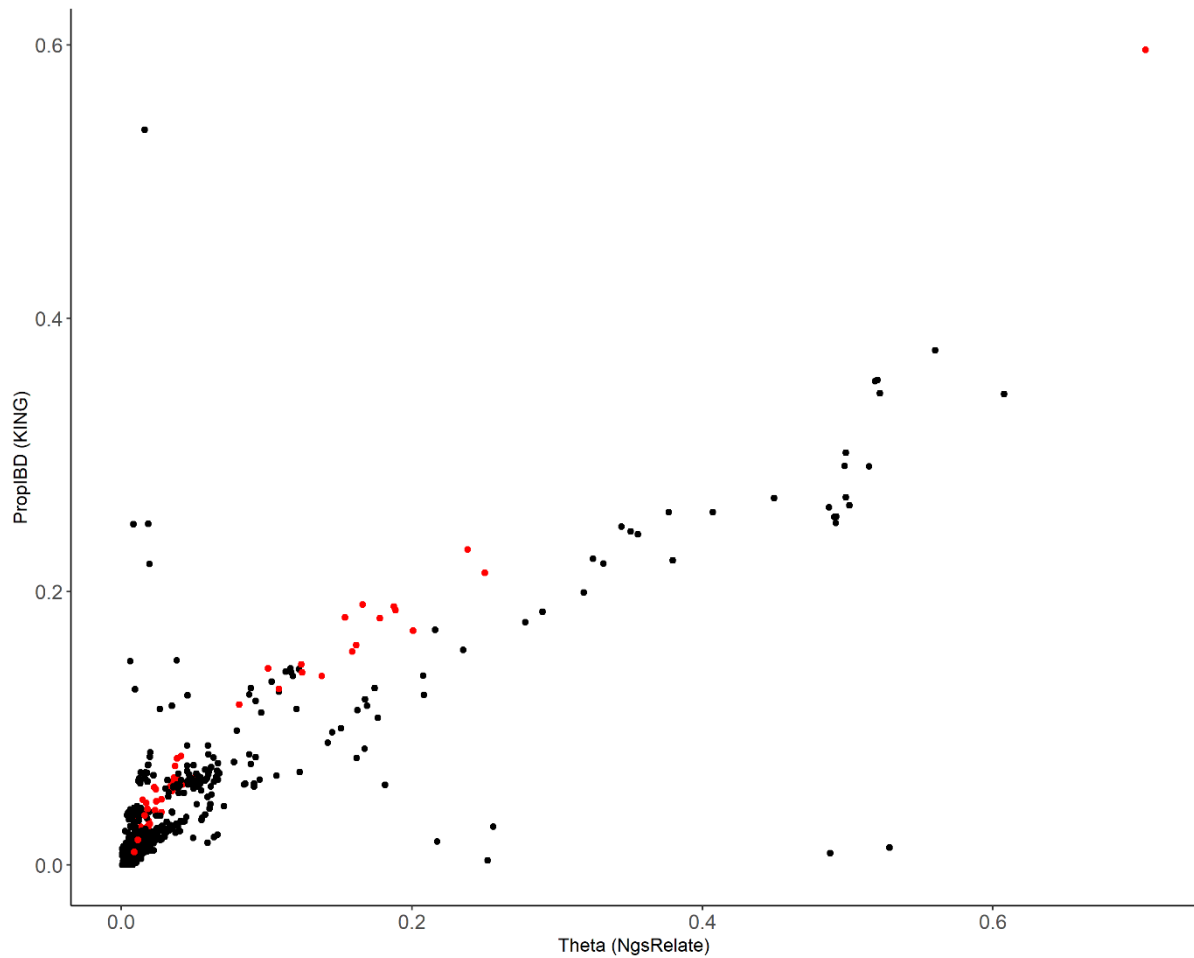




945 **Fig. S10:** Treemix (version 1.13)(27) phylogenies for modern donkeys grouped into
946 populations according to Fig. 1C, with kiang as an outgroup. The left column shows the
947 Treemix inferred from pseudo-haploidized variants ($n=496,697$) and the right from imputed
948 variants ($n=175,093$ variants). The trees on each row are from the same site of ancient
949 donkeys, with the site and individuals labelled in the centre of the row. The optimal number
950 of migration edges are shown for each tree, and nodes coloured according to support values
951 from 100 bootstrap replicates.

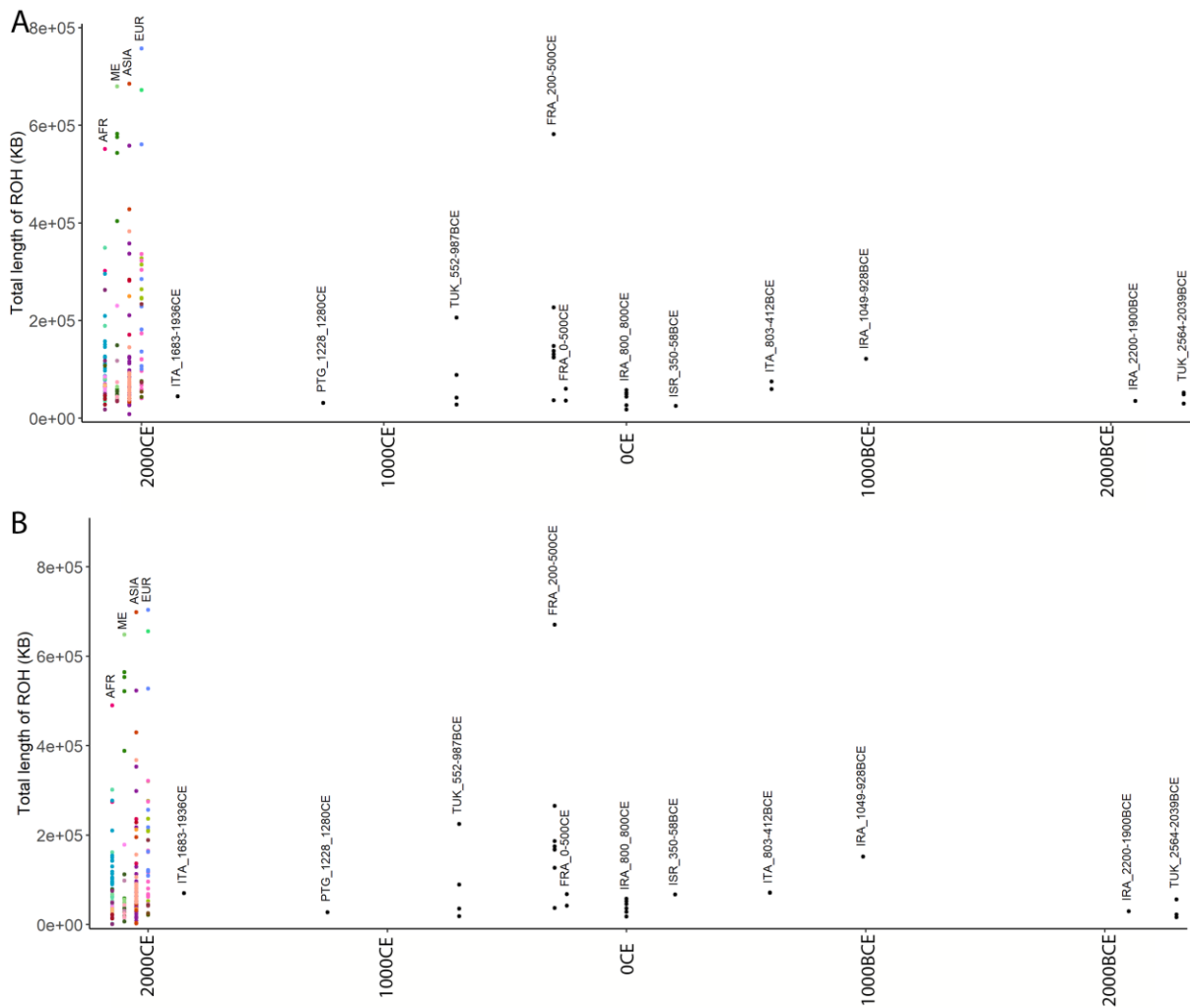


952 **Fig. S11:** The proportion of modern donkeys with dun and derived coat colors from each
 953 subpopulation ($n=207$). The total number of donkeys from each subpopulation is shown
 954 above each bar.

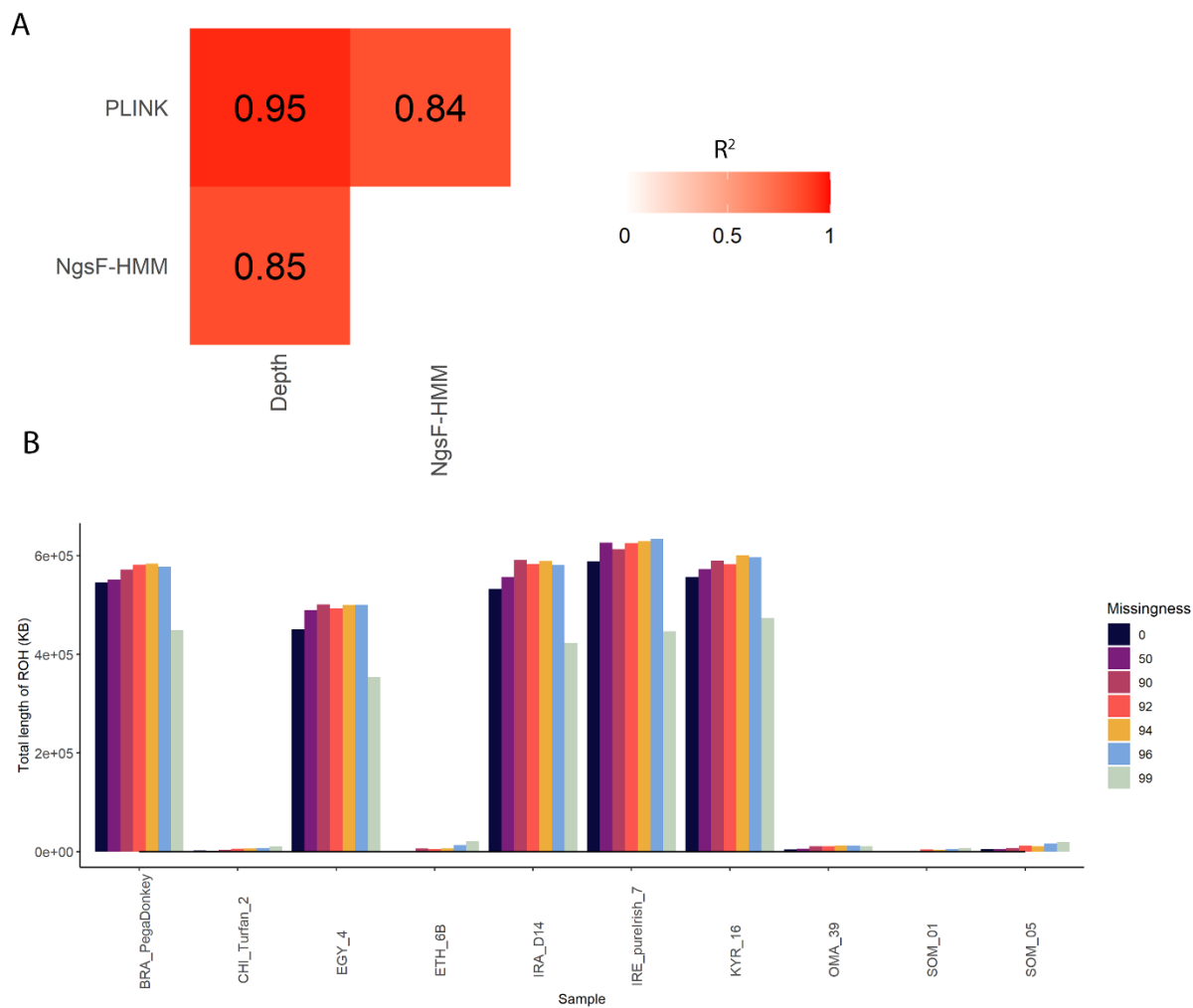


955 **Fig. S12:** The relationship between relatedness coefficients calculated using phased and
 956 imputed variants in KING (version 2.2.7) ($n=2,245,992$ variants) (66) and unimputed variants
 957 using NgsRelate (version 2) ($n=473,263$, variants, transversions only) (67). Only pairs
 958 modern donkey from the same country and ancient donkeys from the same site were included
 959 in the analysis ($n=2096$ pairs). Pairs of ancient donkeys were coloured in red and modern
 960 donkeys in black ($r=0.871$, $r^2=0.759$).

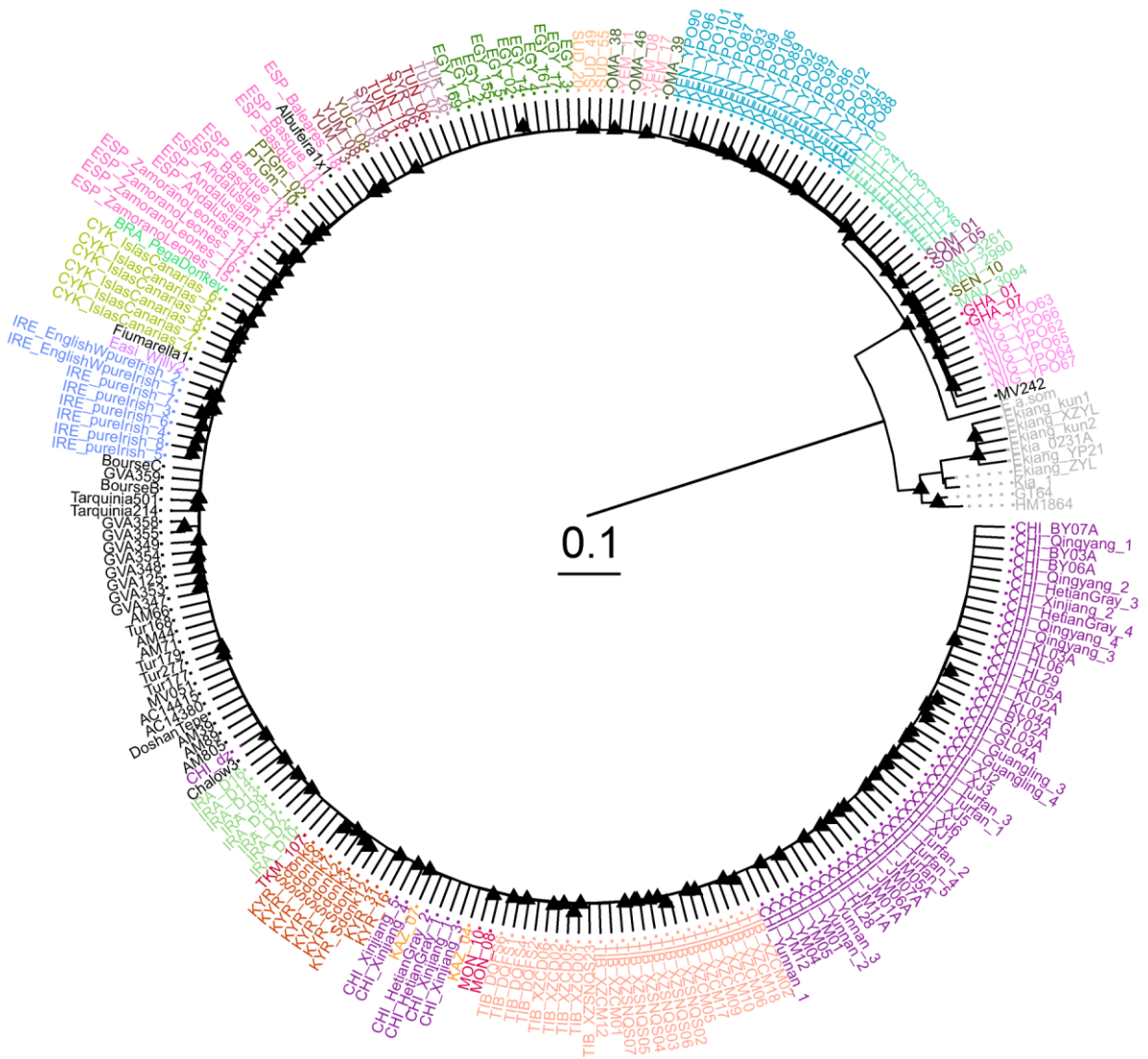
961



962
 963 **Fig. S13:** A) Total length of runs of homozygosity in kilobases, estimated using PLINK
 964 (version 1.9) (63) plotted as a function of time for all modern and ancient donkeys ($n=238$
 965 individuals), conditioning on transversions only ($n=1,949,850$ variants). B) Total length of
 966 runs of homozygosity in kilobases, from depth-based estimated using variants called by
 967 ANGSD (version 0.930) (114) counts plotted as a function of time for all modern and ancient
 968 donkeys ($n=238$ individuals).



969 **Fig. S14:** A) Semi-matrix of squared correlation coefficients between three measures of ROH
 970 (PLINK (version 1.9) (63), ngsF-HMM (version 1) (59) and from depth-based estimated
 971 using variants called by ANGSD (version 0.930) (114)). B) The total length of ROH
 972 estimated in PLINK for 10 modern donkeys after down-sampling and re-imputing variants



973
 974 **Fig. S15:** Neighbour joining tree constructed using FastME (version 2.1.4) (129) with 100
 975 bootstrap pseudo-replicates of modern donkeys, ancient donkeys and kiangs which were
 976 included in the Treemix analysis. Two ancient hemippes with coverage over 1X were also
 977 included. Bootstrap support values over 90% are labelled with a black triangle.

978 References

979

- 980 61. H. P. Eggertsson, H. Jonsson, S. Kristmundsdottir, E. Hjartarson, B. Kehr, G. Masson
 981 *et al.*, GraphTyper enables population-scale genotyping using pangenome graphs. *Nat.*
 982 *Genet.* **49**, 1654-1660 (2017).
- 983 62. A. Auton, G. McVean, Recombination rate estimation in the presence of hotspots.
 984 *Gen. Res.* **17**, 1219-1227 (2007).
- 985 63. S. Purcell, B. Neale, K. Todd-Brown, L. Thomas, M. A. Ferreira, D. Bender *et al.*,
 986 PLINK: a tool set for whole-genome association and population-based linkage
 987 analyses. *Am. J. Hum. Genet.* **81**, 559-575 (2007).
- 988 64. W. Haak, I. Lazaridis, N. Patterson, N. Rohland, S. Mallick, B. Llamas *et al.*, Massive
 989 migration from the steppe was a source for Indo-European languages in Europe.
 990 *Nature* **522**, 207-211 (2015).
- 991 65. B. M. Peter, Admixture, population structure, and f-statistics. *Genetics* **202**, 1485
 992 (2016).
- 993 66. A. Manichaikul, J. C. Mychaleckyj, S. S. Rich, K. Daly, M. Sale, W. M. Chen,
 994 Robust relationship inference in genome-wide association studies. *Bioinformatics* **26**,
 995 2867-2873 (2010).
- 996 67. K. Hanghøj, I. Moltke, P. A. Andersen, A. Manica, T. S. Korneliussen, Fast and
 997 accurate relatedness estimation from high-throughput sequencing data in the presence
 998 of inbreeding. *GigaScience* **8**, (2019).
- 999 68. R. Bouckaert, T. G. Vaughan, J. Barido-Sottani, S. Duchêne, M. Fourment, A.
 1000 Gavryushkina *et al.*, BEAST 2.5: An advanced software platform for Bayesian
 1001 evolutionary analysis. *PLoS Comput. Biol.* **15**, e1006650 (2019).
- 1002 69. A. J. Drummond, S. Y. W. Ho, M. J. Phillips, A. Rambaut, Relaxed phylogenetics
 1003 and dating with confidence. *PLoS Biol.* **4**, e88 (2006).
- 1004 70. A. J. Drummond, A. Rambaut, B. Shapiro, O. G. Pybus, Bayesian coalescent
 1005 inference of past population dynamics from molecular sequences. *Mol. Biol. Evol.* **22**,
 1006 1185-1192 (2005).
- 1007 71. S. Rosenbom, V. Costa, N. Al-Araimi, E. Kefena, A. S. Abdel-Moneim, M. A.
 1008 Abdalla *et al.*, Genetic diversity of donkey populations from the putative centers of
 1009 domestication. *Anim. Genet.* **46**, 30-36 (2015).
- 1010 72. D. Cook, S. Brooks, R. Bellone, E. Bailey, Missense mutation in exon 2 of SLC36A1
 1011 responsible for champagne dilution in horses. *PLoS Genet.* **4**, e1000195 (2008).
- 1012 73. L. Zeng, H. Q. Liu, X. L. Tu, C. M. Ji, X. Gou, A. Esmailizadeh *et al.*, Genomes
 1013 reveal selective sweeps in kiang and donkey for high-altitude adaptation. *Zool Res* **42**,
 1014 450-460 (2021).
- 1015 74. S. W. Manning, L. Wacker, U. Büntgen, C. Bronk Ramsey, M. W. Dee, B. Kromer *et*
 1016 *al.*, Radiocarbon offsets and old world chronology as relevant to Mesopotamia, Egypt,
 1017 Anatolia and Thera (Santorini). *Sci. Rep.* **10**, 13785 (2020).
- 1018 75. N. Özgüç, "Seal impressions from the palaces at Acemhöyük" in *Ancient Art in Seals*,
 1019 E. Porada, Ed. (Princeton University Press, Princeton, 1980), pp. 61-99.
- 1020 76. Y. Kamis, "Acemhöyük Buluntuları Işığında Erken Tunç Çağı'nda Orta Anadolu'nun
 1021 Güneyinde Çark Yapımı Seramiğin Ortaya Çıkışı" in *Adalya* (Umran Savaş İnan,
 1022 Istanbul, 2018), vol. 21, pp. 59-84.
- 1023 77. A. Öztan, 2010 Yılı Acemhöyük Kazıları. *Kazı Sonuçları Toplantısı* 393-412 (2012).
- 1024 78. A. Öztan, 2013 Yılı Acemhöyük Kazıları ve Sonuçları. *Kazı Sonuçları Toplantısı* **36**,
 1025 61-72 (2014).
- 1026 79. Y. S. Erdal, K. Özdemir, Ö. D. Erdal, "Acemhöyük'ten Bir İnsan İskeletinde
 1027 Saptanan Yaralanmaların Adli Antropolojik Açından İncelenmesi." in *Samsat'tan*

- 1028 *Acemhöyük'e Eski Uygarlıkların Izinde: Prof. Dr Aliye Öztan'a Armağan*, S. Özkan,
 1029 H. Hüryılmaz, A. Türker, Eds. (Ege Üniversitesi Basımevi, İzmir, 2017), pp. 105-119.
- 1030 80. Y. Kamış, A. Öztan, 2018 Yılı Acemhöyük Kazıları. Kazı Sonuçları Toplantısı *Kazı*
 1031 *Sonuçları Toplantısı* **41**, 147-160 (2020).
- 1032 81. A. Vahdati, R. Biscione, R. Le Farina, M. Mashkour, M. Tengberg, H. Fathi *et al.*,
 1033 "Preliminary report on the first season of excavations at Tepe Chalow: New GKC
 1034 (BMAC) finds in the plain of Jajarm, NE Iran." in *The Iranian Plateau during the*
 1035 *Bronze Age. Development of Urbanisation, Production and Trade*, J. W. Meyer, E.
 1036 Vila, M. Mashkour, M. Casanova, R. Vallet, Eds. (MOM Éditions, 2019), pp. 179-
 1037 200.
- 1038 82. M. Mashkour, A. F. Mohaseb, "Hunting and husbandry in the Ozbaki archaeological
 1039 Zone (Savojbolagh plain) from the 6th millennium until the Iron Age:
 1040 Archaeozoological study of Jeiran Tepe, Maral Tepe, Doshan Tepe and Tepe Ozbaki"
 1041 in *The Archaeological Excavation of Ozbaki. Vol. 1. Art and Architecture* (ICHTO
 1042 Editions, 2011), pp. 273–302, 597–601.
- 1043 83. Bagnasco Gianni G., A. Garzulino, M. Marzullo, "The last ten years of research at
 1044 Tarquinia" in *Knowledge, Analysis and Innovative Methods for the Study and the*
 1045 *Sissemination of Ancient Urban Areas, Proceedings of the KAINUA 2017*
 1046 *International Conference in Honour of Professor Giuseppe Sassatelli's 70th Birthday*
 1047 *(Bologna, 18-21 Aprile 2017)*, S. Garagnani, A. Gaucci, Eds. (CNR - Istituto di
 1048 Scienze del Patrimonio Culturale, 2017), vol. Archeologia e Calcolatori 28.2, pp. 211-
 1049 221.
- 1050 84. A. Negev, "Nessana" in *The New Encyclopaedia of Archaeological Excavations in the*
 1051 *Holy Land*, E. Stern, Ed. (Israel Exploration Society Jerusalem, 1993), pp. 1145–
 1052 1149.
- 1053 85. D. Urman, *Nessana: Excavations and Studies* (Ben Gurion University, Beer Sheva,
 1054 2004), vol. 7.
- 1055 86. G. Avni, *The Byzantine–Islamic transition in Palestine* (Oxford University Press,
 1056 Oxford, 2014).
- 1057 87. J. Hansman, D. Stronach, Excavations at Shahr-i Qūmis, 1967. *J. R. Asiat. Soc.* **102**,
 1058 29-62 (1970).
- 1059 88. J. Hansman, D. Stronach, A Sasanian Repository at Shahr-i Qūmis. *J. R. Asiat. Soc.*,
 1060 142-155 (1970).
- 1061 89. M. Mashkour, H. Davoudi, F. A. Mohaseb, D. S. Beizae, R. Khazaeli, S. Amiri *et*
 1062 *al.*, "Human and animal interactions in the Iranian Plateau. Research conducted by the
 1063 Osteology Department of Iran National Museum. " in *Iran National Museum*
 1064 *publications and Institut Français de Recherche en Iran, Bibliothèque iranienne N°85*
 1065 (2021), pp. 86-99.
- 1066 90. L. Jourdan, *La faune du site gallo-romain et paléo-chrétien de la Bourse (Marseille)*
 1067 (Editions du CNRS, France, 1976), vol. 1.
- 1068 91. V. Onar, H. Alpak, G. Pazvant, A. Armutak, A. Chrószcz, Byzantine horse skeletons
 1069 of Theodosius harbour: 1. Paleopathology. *Rev. Med. Vet.* **163**, 139-146 (2012).
- 1070 92. V. Onar, G. Pazvant, H. Alpak, N. G. Ince, A. Armutak, Z. Kiziltan, Animal skeletal
 1071 remains of the Theodosius harbor: general overview. *Turkish J. Vet. Anim. Sci.* **37**,
 1072 81-85 (2013).
- 1073 93. V. Onar, G. Pazvant, E. Pasicka, A. Armutak, H. Alpak, Byzantine horse skeletons of
 1074 Theodosius Harbour: 2. Withers height estimation. *Rev. Med. Vet.* **166**, (2015).
- 1075 94. M. T. Antunes, A. C. Balbino, P. M. Callapez, E. Crespo, P. Legoinha, P. R. Mein *et*
 1076 *al.*, *Silo Islâmico de Albufeira (Rua Henrique Calado). Estudos Arqueozoológicos e*

- 1077 *Arqueobotânicos*. (Instituto de Arqueologia e Paleociências (IAP). Universidade Nova
1078 de Lisboa, Lisbon, Portugal, 2012).
- 1079 95. V. Tinè, "Gli scavi nel Riparo della Fiumarella di Tortora (Cosenza)" in *Proceedings*
1080 *of the XXXVII Scientific Meeting "Prehistory and Protohistory of Calabria" (Scalea,*
1081 *Papasidero, Praia a Mare, Tortora, 29 September - 4 October 2002)* (IIPP - Italian
1082 Institute of Prehistory and Protohistory, Florence, 2004), pp. 781-789.
- 1083 96. A. Curci, I resti faunistici dell'insediamento dell'età del Bronzo di Madonna del Petto,
1084 scavi 1977. *Taras* **XV**, 204-215 (1995).
- 1085 97. P. Farello, I reperti faunistici. *Primi Insediamenti sul Monte Titano. Scavi e Ricerche*
1086 *(1997-2004)*, 87-95 and 135-140 (2009).
- 1087 98. A. Riedel, Notizie preliminari sullo studio della fauna di Spina. *Atti dell'Accademia*
1088 *delle Scienze di Ferrara* **55**, 1-7 (1978).
- 1089 99. G. Siracusano, La fauna del Bronzo tardo del sito stratificato di Coppa Nevigata: una
1090 visione d'insieme. *Origini* **XV**, 201-217 (1992).
- 1091 100. A. Seguin-Orlando, R. Donat, C. Der Sarkissian, J. Southon, C. Thèves, C. Manen *et*
1092 *al.*, Heterogeneous hunter-gatherer and steppe-related ancestries in late Neolithic and
1093 bell beaker genomes from present-day France. *Curr. Biol.* **31**, 1072-1083.e1010
1094 (2021).
- 1095 101. C. Gamba, K. Hanghøj, C. Gaunitz, A. H. Alfarhan, S. A. Alquraishi, K. A. Al-
1096 Rasheid *et al.*, Comparing the performance of three ancient DNA extraction methods
1097 for high-throughput sequencing. *Mol. Ecol. Resour.* **16**, 459-469 (2016).
- 1098 102. N. Rohland, E. Harney, S. Mallick, S. Nordenfelt, D. Reich, Partial uracil-DNA-
1099 glycosylase treatment for screening of ancient DNA. *Philos. Trans. R. Soc. Lond., B,*
1100 *Biol. Sci.* **370**, 20130624 (2015).
- 1101 103. P. J. Reimer, W. E. N. Austin, E. Bard, A. Bayliss, P. G. Blackwell, C. Bronk Ramsey
1102 *et al.*, The IntCal20 northern hemisphere radiocarbon age calibration curve (0–55 cal
1103 kBP). *Radiocarbon* **62**, 725-757 (2020).
- 1104 104. C. Bronk Ramsey, Bayesian analysis of radiocarbon dates. *Radiocarbon* **51**, 337-360
1105 (2016).
- 1106 105. M. Schubert, S. Lindgreen, L. Orlando, AdapterRemoval v2: rapid adapter trimming,
1107 identification, and read merging. *BMC Res. Notes* **9**, 88 (2016).
- 1108 106. M. Schubert, H. Jónsson, D. Chang, C. Der Sarkissian, L. Ermini, A. Ginolhac *et al.*,
1109 Prehistoric genomes reveal the genetic foundation and cost of horse domestication.
1110 *Proc. Natl. Acad. Sci. U.S.A.* **111**, E5661-5669 (2014).
- 1111 107. M. Poulet, L. Orlando, Assessing DNA sequence alignment methods for
1112 characterizing ancient genomes and methylomes. *Front. Ecol. Evol.* **8**, (2020).
- 1113 108. P. Skoglund, B. H. Northoff, M. V. Shunkov, A. P. Derevianko, S. Pääbo, J. Krause *et*
1114 *al.*, Separating endogenous ancient DNA from modern day contamination in a
1115 Siberian Neandertal. *Proc. Natl. Acad. Sci. U.S.A.* **111**, 2229-2234 (2014).
- 1116 109. H. Jónsson, A. Ginolhac, M. Schubert, P. L. Johnson, L. Orlando, mapDamage2.0:
1117 fast approximate Bayesian estimates of ancient DNA damage parameters.
1118 *Bioinformatics* **29**, 1682-1684 (2013).
- 1119 110. H. Li, B. Handsaker, A. Wysoker, T. Fennell, J. Ruan, N. Homer *et al.*, The sequence
1120 alignment/map format and SAMtools. *Bioinformatics* **25**, 2078-2079 (2009).
- 1121 111. E. Garrison, Z. N. Kronenberg, E. T. Dawson, B. S. Pedersen, P. Prins, Vcflib and
1122 tools for processing the VCF variant call format. *bioRxiv*, 2021.2005.2021.445151
1123 (2021).
- 1124 112. A. McKenna, M. Hanna, E. Banks, A. Sivachenko, K. Cibulskis, A. Kernytsky *et al.*,
1125 The Genome Analysis Toolkit: a MapReduce framework for analyzing next-
1126 generation DNA sequencing data. *Gen. Res.* **20**, 1297-1303 (2010).

- 1127 113. L. Orlando, A. Ginolhac, G. Zhang, D. Froese, A. Albrechtsen, M. Stiller *et al.*,
1128 Recalibrating Equus evolution using the genome sequence of an early Middle
1129 Pleistocene horse. *Nature* **499**, 74-78 (2013).
- 1130 114. T. S. Korneliussen, A. Albrechtsen, R. Nielsen, ANGSD: analysis of next generation
1131 sequencing data. *BMC Bioinform.* **15**, 356 (2014).
- 1132 115. S. K. Beeson, J. R. Mickelson, M. E. McCue, Equine recombination map updated to
1133 EquCab3.0. *Anim Genet* **51**, 341-342 (2020).
- 1134 116. F. Alhaique, F. Marshall, Preliminary report on the Jebel Gharbi fauna from site SJ-
1135 00-56 (2000 and 2002 excavations). *Africa* **54**, 498-507 (2009).
- 1136 117. F. Marshall, L. Weissbrod, Domestication processes and morphological change:
1137 through the lens of the donkey and African pastoralism. *Curr. Anthropol.* **52**, S397-
1138 S413 (2011).
- 1139 118. L. Shackelford, F. Marshall, J. Peters, Identifying donkey domestication through
1140 changes in cross-sectional geometry of long bones. *J. Archaeol. Sci.* **40**, 4170-4179
1141 (2013).
- 1142 119. Y. X. Zhao, J. Yang, F. H. Lv, X. J. Hu, X. L. Xie, M. Zhang *et al.*, Genomic
1143 reconstruction of the history of native sheep reveals the peopling patterns of nomads
1144 and the expansion of early pastoralism in East Asia. *Mol. Biol. Evol.* **34**, 2380-2395
1145 (2017).
- 1146 120. J. E. Decker, S. D. McKay, M. M. Rolf, J. Kim, A. Molina Alcalá, T. S. Sonstegard *et al.*,
1147 Worldwide patterns of ancestry, divergence, and admixture in domesticated cattle.
1148 *PLoS Genet.* **10**, e1004254 (2014).
- 1149 121. M. P. Verdugo, V. E. Mullin, A. Scheu, V. Mattiangeli, K. G. Daly, P. Maisano
1150 Delser *et al.*, Ancient cattle genomics, origins, and rapid turnover in the Fertile
1151 Crescent. *Science* **365**, 173-176 (2019).
- 1152 122. M. Milanese, S. Capomaccio, E. Vajana, L. Bomba, J. F. Garcia, P. Ajmone-Marsan *et al.*,
1153 BITE: an R package for biodiversity analyses. *bioRxiv*, 181610 (2017).
- 1154 123. A. Brisbin, K. Bryc, J. Byrnes, F. Zakharia, L. Omberg, J. Degenhardt *et al.*,
1155 PCAdmix: principal components-based assignment of ancestry along each
1156 chromosome in individuals with admixed ancestry from two or more populations.
1157 *Hum. Biol.* **84**, 343-364 (2012).
- 1158 124. D. Reich, K. Thangaraj, N. Patterson, A. L. Price, L. Singh, Reconstructing Indian
1159 population history. *Nature* **461**, 489-494 (2009).
- 1160 125. G. Bhatia, N. Patterson, S. Sankararaman, A. L. Price, Estimating and interpreting
1161 Fst: the impact of rare variants. *Gen. Res.* **23**, 1514-1521 (2013).
- 1162 126. S. Schiffels, K. Wang, MSMC and MSMC2: The multiple sequentially markovian
1163 coalescent. *Methods Mol. Biol.* **2090**, 147-166 (2020).
- 1164 127. Z. Zheng, X. Wang, M. Li, Y. Li, Z. Yang, X. Wang *et al.*, The origin of
1165 domestication genes in goats. *Sci. Adv.* **6**, eaaz5216 (2020).
- 1166 128. C. Michel, The Old Assyrian trade in the light of Recent Kültepe Archives. *Journal of*
1167 *the Canadian Society for Mesopotamian Studies* **3**, 71-82 (2008).
- 1168 129. V. Lefort, R. Desper, O. Gascuel, FastME 2.0: a comprehensive, accurate, and fast
1169 distance-based phylogeny inference program. *Mol. Biol. Evol.* **32**, 2798-2800 (2015).
- 1170 130. A. Rambaut, A. J. Drummond, D. Xie, G. Baele, M. A. Suchard, Posterior
1171 summarization in Bayesian phylogenetics using Tracer 1.7. *Syst. Biol.* **67**, 901-904
1172 (2018).
- 1173 131. P. Librado, C. Gamba, C. Gaunitz, C. Der Sarkissian, M. Pruvost, A. Albrechtsen *et al.*,
1174 Ancient genomic changes associated with domestication of the horse. *Science*
1175 **356**, 442-445 (2017).

- 1176 132. X. Liu, Y. Zhang, Y. Li, J. Pan, D. Wang, W. Chen *et al.*, EPAS1 gain-of-function
1177 mutation contributes to high-altitude adaptation in Tibetan horses. *Mol. Biol. Evol.* **36**,
1178 2591-2603 (2019).
- 1179 133. V. Jagannathan, V. Gerber, S. Rieder, J. Tetens, G. Thaller, C. Drögemüller *et al.*,
1180 Comprehensive characterization of horse genome variation by whole-genome
1181 sequencing of 88 horses. *Anim. Genet.* **50**, 74-77 (2019).
- 1182 134. L. S. Andersson, M. Larhammar, F. Memic, H. Wootz, D. Schwochow, C.-J. Rubin *et*
1183 *al.*, Mutations in DMRT3 affect locomotion in horses and spinal circuit function in
1184 mice. *Nature* **488**, 642-646 (2012).
- 1185 135. B. Wallner, N. Palmieri, C. Vogl, D. Rigler, E. Bozlak, T. Druml *et al.*, Y
1186 Chromosome Uncovers the Recent Oriental Origin of Modern Stallions. *Curr. Biol.*
1187 **27**, 2029-2035.e2025 (2017).
- 1188 136. C. Der Sarkissian, L. Ermini, M. Schubert, M. A. Yang, P. Librado, M. Fumagalli *et*
1189 *al.*, Evolutionary genomics and conservation of the endangered Przewalski's horse.
1190 *Curr. Biol.* **25**, 2577-2583 (2015).
- 1191 137. J. Metzger, M. Karwath, R. Tonda, S. Beltran, L. Águeda, M. Gut *et al.*, Runs of
1192 homozygosity reveal signatures of positive selection for reproduction traits in breed
1193 and non-breed horses. *BMC Genom.* **16**, 764 (2015).

1194